NTNU – Trondheim
Norwegian University of
Science and Technology

Guidance and control of iceberg towing operation in open water, with experimental testing

Mika Nikolai Sundland

Marine Technology
Submission date: June 2013
Supervisor: Roger Skjetne, IMT

Norwegian University of Science and Technology
Department of Marine Technology

NTNU Trondheim
Norwegian University of Science and Technology
Department of Marine Technology

PROJECT DESCRIPTION SHEET

Name of the candidate: Mika Sundland

Field of study: Marine control engineering.

Thesis title (Norwegian): Automatisk baneplanlegging og styring av slepefartøy for tauing av isfjell i åpne farvann.

Thesis title (English): Guidance and control of iceberg towing vessel for towing of icebergs in open water.

Background
Icebergs pose serious threats to existing and planned offshore structures, vessels, and operations in Arctic waters such as the East Coast of Canada, East and West Greenland, the Barents Sea, and the Kara Sea. The intrusion of icebergs into an operational area must be detected within safety time limits, continuously tracked, and their future motion must be forecasted in order to assess the threat of structures and operations. This is typically done by an *iceberg management system*. If an iceberg is evaluated as a threat, then *physical iceberg management* must be mobilized to mitigate the threat. For open water, this is typically done by single vessel towing of the iceberg using a synthetic floating tow line.

In this project, a model shall be developed for open water iceberg towing using a single towing vessel and a synthetic towline. The student should study several towing configuration choices, such as

- towline connection to the vessel by a single or double connection point,
- fixed connection or active tension-controlled winch connection(s),
- floating towline or submerged towline, and
- passive towline hawser or active fin-controlled hawser.

The model should be verified in simulation, and a discussion should be provided on all physical and operational constraints in such a towing operation, practical aspects, and important requirements. This discussion shall include a suggestion for how to actively use the tension measurements of the towline in the towing control system. The proposed model, proposed towline configuration and tension measurement, and the discussion on constraints and practical issues should be concluded in a control objective and problem statement for an iceberg towing operation.

Thereby, guidance and control laws for the towing vessel shall be designed, taking into account:

- the towing path of the vessel and iceberg, and a guidance system for generating the desired path,
- motion and actual path of the towed iceberg under influence by wind and current,
- tension in the towing line(s) to be within maximum limits, and
- avoidance of towline rupture, towline slippage, and iceberg rolling and overturning.

The design should be concluded by assessment of stability and verification of performance through simulations.

Finally, the proposed guidance and control system for iceberg towing should be implemented and tested in the MC Lab using the model ship CS Enterprise I towing an object that emulates an iceberg in wind/current.

Guidelines
The scope of work may prove to be larger than initially anticipated. By the approval from the supervisor, described topics may be deleted or reduced in extent without consequences with regard to grading.

The candidate shall present his personal contribution to the resolution of problems within the scope of work. Theories and conclusions should be based on mathematical derivations and logic reasoning identifying the various steps in the deduction.

The report shall be organized in a rational manner to give a clear exposition of results, assessments, and conclusions. The text should be brief and to the point, with a clear language. The report shall be written in English (preferably US) and contain the following elements: Abstract, acknowledgements, table of contents, main body, conclusions with recommendations for further work, list of symbols and acronyms, references and (optional) appendices. All figures, tables, and equations shall be numerated. The original contribution of the candidate and material taken from other sources shall be clearly identified. Work from other sources shall be properly acknowledged using quotations and a Harvard citation style (e.g. *natbib* Latex package). The work is expected to be conducted in an honest and ethical manner, without any sort of plagiarism and misconduct. Such practice is taken very seriously by the university and will have consequences. NTNU can use the results freely in research and teaching by proper referencing, unless otherwise agreed upon.

The thesis shall be submitted in 3 printed copies, each signed by the candidate. The final revised version of this project description must be included. The report must appear in a bound volume or a binder according to the NTNU standard template. Computer code and a PDF version of the report should be included electronically.

A 15 min. presentation (conference style) on your status, intermediate results, and plan for completion is expected to be delivered at a scheduled time midway into the project period.

Start date: January, 2013 **Due date:** As specified by the administration.

Supervisor: Prof. Roger Skjetne, IMT, NTNU
Co-advisor(s): Prof. Aleksey Marchenko, UNIS

Trondheim,

_____
Roger Skjetne
Supervisor

Abstract

Icebergs pose serious threats to existing and planned offshore structures, vessels, and operations in Arctic waters such as the East Coast of Canada, East and West Greenland, the Barents Sea, and the Kara Sea. A collision between an offshore installation and an iceberg could cause serious damage to the installation, and in a worst case scenario take life. Therefore, if an iceberg is evaluated as a threat, physical iceberg management must be mobilized to mitigate the threat. For open water, this is typically done by single vessel towing of the iceberg using steel hawser and synthetic floating tow lines.

This work describes a model for open water iceberg towing using a single towing vessel. This includes a mathematical model of the towing vessel, the iceberg and the towline between them. It also looks into certain towline configuration choices, estimation of damping and mass, and other things that can affect the towing model. The mathematical model was based on the work of Marchenko and Eik [2008] and then generalized to the Fossen-style of notation [Fossen, 2011].

A maneuvering controller was designed for use in the towing operation. The controller was designed using maneuvering theory as described by Skjetne [2005]. The controller is responsible for guiding the ship along a path, with the iceberg trailing behind it. Another controller has been designed for controlling the tension in the towline.

In addition to the controllers, several observers had to be designed. These observers are responsible for estimating position, velocity, bias, and tension in the system.

Finally, an experiment with the *CS Enterprise I* model vessel, and an emulated iceberg, was conducted in a towing tank. The experiment gave important qualitative data regarding the iceberg towing system, and confirmed that the controller worked in a real-life scenario.

Sammendrag

Isfjell utgjør en seriøs trussel for eksisterende og planlagte offshore-strukturer, fartøy og operasjoner i arktiske farvann, slik som Canadas østkyst, Øst- og Vest-Grønland, Barentshavet og Karahavet. En kollisjon mellom en offshore-installasjon og et isfjell kan forårsake seriøse skader på installasjonen, og i verste fall ta liv. Derfor, hvis et isfjell er ansett for å være en trussel, så må fysisk isfjellhådtering (eng: physical iceberg management) mobiliseres for å redusere trusselen. For åpne farvann er dette typisk gjort med tauing med enkeltfartøy, ved bruk av ståltrosser og syntetiske og flytende tau.

Dette arbeidet beskriver en modell for isfjelltauing i åpne farvann, ved bruk av ett enkelt tauefartøy. Dette inkluderer en matematisk modell av tauefartøyet, isfjellet og tauekabelen mellom dem. Det ser også nærmere på et par tauekonfigurasjoner, estimerer demping og masse, og ser på andre ting som kan påvirke tauemodellen. Den matematiske modellen var basert på arbeidet til Marchenko and Eik [2008], og videre generalisert til Fossen-notasjon [Fossen, 2011].

En manøvreringsregulator ble designet for bruk i taueoperasjonen. Denne regulatoren ble designet med manøvreringsteori som beskrevet i avhandlingen til Skjetne [2005]. Regulatoren er ansvarlig for å veilede skipet langs en bane, med isfjellet slepende bak det. En annen regulator ble designet for å regulere kraften i tauekabelen.

I tillegg til regulatorene måtte flere observere designes. Disse observerne er ansvarlig for å estimere posisjon, hastighet, bias og tauekraft i systemet.

Til slutt ble et eksperiment med modellfartøyet *CS Enterprise I* og et emulert isfjell utført i en tauetank. Eksperimentet ga viktig kvalitative data med tanke på reguleringssystemet, og bekreftet at regulatoren virker i den virkelige verden.

Preface

This master thesis was written at the Department of Marine Technology at the Norwegian University of Science and Technology, during the spring of 2013.

First and foremost, I would like to thank my thesis advisor, Roger Skjetne, for advising me during the work on the thesis, and valuable input and guidance in general.

I would also like to thank PhD student Øivind Kåre Kjerstad for helping me in the lab, and for the help in the modeling process. I am grateful for the help Staff Engineer Torgeir Wahl gave me in the MC Lab. He has been invaluable in the practical aspects of the implementation of CS Enterprise I. I would like to thank Nam Dinh Tran, a fellow master student, for all the help he gave me in the towing tank.

In the end I would like to thank my office mates, Raimon and Paal, for keeping me entertained during the two last semesters at NTNU.

Trondheim, June 10, 2013

Mika Nikolai Sundland

List of symbols

$\boldsymbol{\eta}_s = [x_s, y_s, \psi_s]^\top$	vector of positions and orientations for the vessel in NED
$\boldsymbol{\nu}_s = [u_s, v_s, r_s]^\top$	vector of velocities and orentation rates for the vessel in BODY
$\boldsymbol{M}_{RB,s}$	rigid-body system inertia matrix for the vessel
$\boldsymbol{M}_{A,s}$	added mass matrix for the vessel
$\boldsymbol{M}_s$	total mass matrix for the vessel
$\boldsymbol{\tau}_s = [\tau_x, \tau_y, \tau_N]^\top$	control forces vector
$\boldsymbol{T} = [X_{tow}, Y_{tow}, N_{tow}]^\top$	towline forces
$\boldsymbol{D}_s$	damping matrix for the vessel
$\boldsymbol{\eta}_i = [x_i, y_i, \psi_i]^\top$	vector of positions and orientations for the iceberg in NED
$\boldsymbol{\nu}_i = [u_i, v_i, r_i]^\top$	vector of velocities and orentation rates for the iceberg in BODY
$\boldsymbol{M}_{RB,i}$	rigid-body system inertia matrix for the iceberg
$\boldsymbol{M}_{A,i}$	added mass matrix for the iceberg
$\boldsymbol{M}_i$	total mass matrix for the iceberg
$\boldsymbol{D}_i$	damping matrix for the iceberg
$\boldsymbol{R}(\psi)$	rotation matrix
ψ_s	yaw angle for the vessel
ψ_i	yaw angle for the iceberg

θ	path variable in the guidance system
$\dot{\theta}$	time derivative of the path variable in the guidance system
$\boldsymbol{\eta}_d = [x_d, y_d, \psi_d]^\top$	desired path in the guidance system
$\boldsymbol{\eta}_d^\theta = [x_d^\theta, y_d^\theta, \psi_d^\theta]^\top$	θ derivative of the desired path in the guidance system
$\boldsymbol{\eta}_d^{\theta^2} = [x_d^{\theta^2}, y_d^{\theta^2}, \psi_d^{\theta^2}]^\top$	θ^2 derivative of the desired path in the guidance system
$U_d(t)$	desired speed in the guidance system
$v_s(\theta, t)$	desired speed function in the guidance system
$v_s^\theta(\theta, t)$	theta derivative of the desired speed function in the guidance system
$v_s^t(\theta, t)$	time derivative of the desired speed function in the guidance system
$\boldsymbol{z}_1$	error variable in the guidance system
$\dot{\boldsymbol{z}}_1$	time derivative of an error variable in the guidance system
$\boldsymbol{z}_2$	error variable in the guidance system
$\dot{\boldsymbol{z}}_2$	time derivative of an error variable in the guidance system
ω_s	error variable in the guidance system
r_s	yaw rate of the ship
$\boldsymbol{S}$	a skew-symmetric matrix used in the guidance system
V_1	first control Lyapunov function (CLF) used in the guidance system
$\dot{V}_1$	time derivatice of the first control Lyapunov function (CLF) used in the guidance system
V_2	second control Lyapunov function (CLF) used in the guidance system
$\dot{V}_2$	time derivative of the sec-

$\dot{\boldsymbol{\alpha}}_1$	time derivative of the virtual control function used in the guidance system
$\boldsymbol{\alpha}_1^\theta$	θ derivative of the virtual control function used in the guidance system
$\boldsymbol{\sigma}_1$	part of $\dot{\boldsymbol{\alpha}}_1$ used in the guidance system
$\boldsymbol{K}_p$	tuning matrix used in the maneuvering controller
$\boldsymbol{K}_d$	tuning matrix used in the maneuvering controller
λ	tuning constant used by the update law in the guidance system
μ	tuning constant used by the update law in the guidance system
T_d	desired tension in the tension controller
$\dot{T}_d$	time derivative of the desired tension in the tension controller
$\dot{T}$	time derivative of the tension in the tension controller
K_{scale}	scaling factor between force and velocity
K_p	tuning gain in the tension controller
K_i	tuning gain in the tension controller
K_d	tuning gain in the tension controller

$\boldsymbol{\xi}$	wave elevation in the observer
$\boldsymbol{A}_w$	system matrix for the waves in the observer
$\boldsymbol{y}$	measuring vector in the observer
$\tau_w = [X_{wind}, Y_{wind}, N_{wind}]^\top$	Wind forces acting on the vessel and iceberg
q	apparent dynamic pressure from wind
C_X, C_Y, C_N	wind coefficients
γ_w	wind angle of attack
A_{Fw}	projected frontal area
A_{Lw}	projected lateral area
L_{oa}	length over all for vessel or iceberg
β_w	wind direction
ρ_a	density of wind
V_w	wind velocity

Contents

List of Figures

List of Tables

Chapter 1

Introduction

1.1 Background

Icebergs pose serious threats to existing and planned offshore structures, vessels, and operations in Arctic waters such as the East Coast of Canada, East and West Greenland, the Barents Sea, and the Kara Sea. The intrusion of icebergs in to an operational area must be detected within safety time limits, continuously tracked, and their future motion must be forecasted in order to assess the threat of structures and operations. This is typically done by an ice intelligence system. If an iceberg is evaluated as a threat, then physical iceberg management must be mobilized to mitigate the threat. For open water, this is typically done by single vessel towing of the iceberg using a synthetic floating tow line.

In this project the aim is to present a model for open water iceberg towing using a single towing vessel and a synthetic floating tow line. Thereby a control strategy should be proposed, taking into account:

- the towing path of the vessel and a guidance system for generating the desired path,
- motion and actual path of the towed iceberg,
- tension in the towing line(s) to be within maximum limits, and

- avoidance of towline rupture, towline slippage, or iceberg overturning.

This project will study several towing configuration choices, such as

- towline connection to the vessel by a single or double connection point,
- fixed connection (with tension measurement) or active tension-controlled winch connection(s),
- floating towline or submerged towline, and
- passive towline hawser or active fin-controlled hawser.

The final goal of the project is to design a guidance and control strategy for a towing vessel, based on a chosen towing configuration. This includes creating a system that can be tested in the MC Lab using a model ship together with an emulated iceberg.

1.1.1 Former literature on the subject

Iceberg towing is a very narrow subject without much research behind it, but a few papers have been published on it before. The main author behind most of the papers is Aleksey Marchenko, who is a professor in ice mechanics at The University Center in Svalbard (UNIS). The most up-to-date papers at the moment are *Iceberg towing in open water: Mathematical modeling and analysis of model tests* by Marchenko and Eik [2011] and *Model tests of iceberg towing* by Eik and Marchenko [2009]. The initial scalar model were taken from these papers.

Another important paper in this project was *Grand Banks Iceberg Management* by Timco [2007]. This report reveals a lot of information on how icebergs are actually towed in real life scenarios, and also gives data for various iceberg types. Another report that supplements

the report by Timco [2007] is *Greenland Iceberg Management: Implications for Grand Banks Management Systems* by John McClintock and Brown [2002]. This report goes deeper into the subject of practical iceberg towing, and was maybe the most interesting of the mentioned papers.

Some of the control aspects are based on the work of Skjetne [2005]. However, this has nothing to do with iceberg towing, only the maneuvering aspects in the control system. Towing and anchor handling has been covered before in the master thesis of Wennersberg [2009]. The tension observer in this thesis was based on the work of Wennersberg [2009].

1.2 The concept of towing

The following situation can be imagined: An offshore platform is at risk due to icebergs drifting towards it. The offshore platform can only be moved in emergency situations, but this is extremely expensive, both in terms of operation costs and downtime costs. A better solution is therefore to tow the iceberg in such a way that it is no longer a threat to the offshore platform. Figure 1.1 illustrates the concept of towing an iceberg on a collision course with an offshore installation.

At the moment the towing is done manually using a vessel capable of towing large objects. This means a ship with a large bollard pull, such as a tug or an anchor handling tug supply vessel (AHTS), is required. Moreover, the crew of the vessel do most of the navigation themselves, without the help of autopilot or dynamic positioning systems [John McClintock and Brown, 2002].

The towing process can also be looked at more analytically. Figure 1.2 illustrates a towing vessel and an iceberg, together in a North-East coordinate system. The vessel and iceberg are connected together with a tow rope. The blue line illustrates the a vessel trajectory, while the red line illustrates the iceberg trailing behind the vessel.

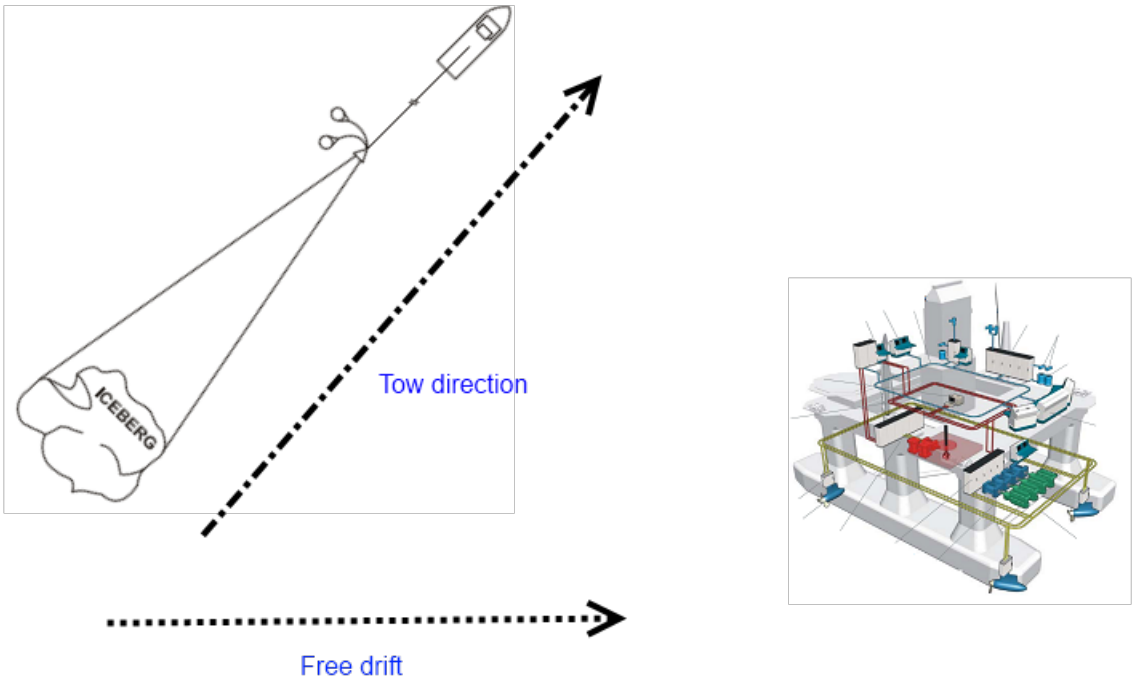

Figure 1.1: An iceberg drifting towards a semi-submersible. Courtesy of Timco [2007] and Sørensen [2011].

The tow rope can be considered a spring, mathematically. Due to environmental forces and towline dynamics, the iceberg will most likely not follow the same trajectory as the ship.

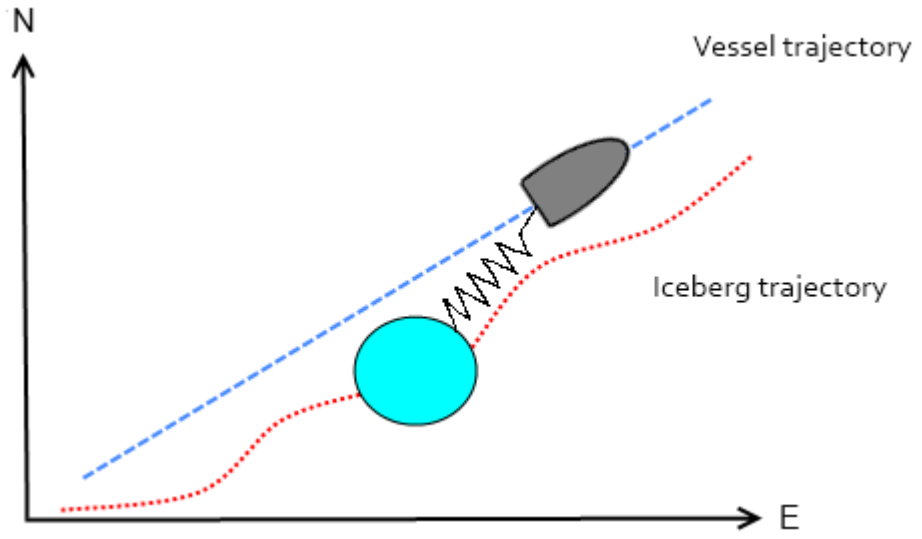

Figure 1.2: The concept of towing.

1.2.1 Towing procedure

The towing procedure involves trapping the iceberg using a floating synthetic rope that is looped around the iceberg [Marchenko and Eik, 2011]. Depending on the connection configuration, the rope ends are either connected directly to the boat stern, or to a heavy steel hawser that is fastened to the boat stern. This is illustrated in Figure 1.3.

According to Marchenko and Eik [2011], the first method has only been used in experiments in the Barents Sea. The method involving a hawser is used on the Canadian Shelf. The hawser method will therefore be used further on in this thesis.

Furthermore, the connection between towline and the vessel can be performed in several different ways:

Single connection point

In the single connection points configuration, the towline is connected to the vessel at only one point at the stern. The rope is twined around the iceberg and then connected to a hawser,

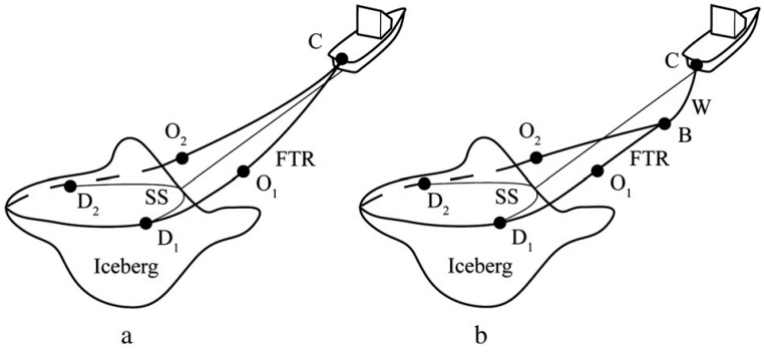

Figure 1.3: Schematics of towing icebergs. Courtesy of Marchenko and Eik [2011].

which again is connected to the towing vessel. The rope is submerged at the connection with the hawser. The hawser is usually shorter than the rope. This method is illustrated in Figure (1.3) b).

Double connection points

In the dual connection points configuration the rope is fastened to the boat at two different points at the stern. The iceberg is towed using only the rope, and the rope is floating or hanging during the towing operation. This method is illustrated in Figure (1.3) a).

According to Marchenko and Eik [2011] the dual connection point method can damage the ship if the rope breaks. If the single connection method is used, the hawser will be submerged and act as a buffer if the towline breaks. Another advantage of the single connection point method is that the hawser depresses the line of the tow force. This brings it closer to the iceberg's center of hydrodynamic drag, and therefore reduces the risk of overturning [Eik, 2010]. The double connection point method has only been used in experiments before, and the singe point connection method will therefore be used

further on. This also assumes that the towline is submerged around the junction between hawser and rope.

1.2.2 Towline choice

The towlines used during towing can vary in material choice and length, both for the hawser and the tow rope.

Type

The material type is usually a choice between various wires and synthetic fiber towlines; materials that behave very differently. A wire is stiff and heavy which results in a larger catenary [Desroches, 1997].

Moreover, a synthetic fiber rope is light and flexible. This results in a smaller catenary and a reduced dependence on mean tension.

During a towing operation there will usually be two types of materials in use: one material type for the hawser and one for the rope. According to Timco [2007] the hawser are usually made of steel and the rope usually of braided polypropylene.

Length

Another important factor is the choice of towline length. Longer towlines will decrease the geometrical stiffness of the catenary and thus lower the dynamic tension in the towline [Desroches, 1997]. According to Timco [2007] the length of the hawser is usually in the range of $100\ m - 400\ m$ and the rope about $1200\ m$. Although the length of the rope is much larger than the hawser, the rope will be looped around the iceberg and therefore not contribute that much to the total length between vessel and iceberg. The rope is often divided into two or three sections of $400\ m$ to $500\ m$ in length. The diameter is about $11\ cm - 12\ cm$.

1.2.3 Fixed connection or active tension-controlled winch connection

The towline between the vessel and the iceberg will have a certain tension, depending on the bollard pull of the vessel. An important aspect in towing is how this tension is controlled, in order to keep it below the rupture limit of the towline. The two different methods are

Fixed connection: the vessel itself has no tension-control mechanism. The towline is directly to the vessel, and the towline length is constant if the strain in the towline is constant. The tension can be controlled by adjusting the velocity of the vessel.

Active tension-controlled winch connection: a vessel with active tension control will actively control the tension of the towline, using the winch as an actuator. If the tension is too large, more towline is released by the winch. If the tension is too small, the towline is tightened by drawing in the towline until the desired tension is acquired.

The vessel used in the towing experiment in this thesis does not have an active tension-controlled winch, which means the tension control will be based on the fixed-connection method.

Chapter 2

Mathematical model

This chapter introduces the mathematical models that are used in the thesis. The goal is to find a *control plant model* as defined by Sørensen [2011, p 175]:

> *Control plant model is a simplified mathematical description containing only the main physical properties of the process or plant. This model may constitute a part of the controller. The control plant model is also used in analytical stability analysis based on e.g. Lyapunov stability and passivity.*

The goal with the control plant model is to create a controller for use in the iceberg towing system. The modeling process will therefore exclude or simplify several aspects compared to a *process plant model/simulation model*.

2.1 The model by Marchenko and Eik

Marchenko and Eik [2011] proposes a model that balance the momentum between the boat and the iceberg connected by a towline:

$$M_s \frac{dv_s}{dt} + M_{add,s} \frac{d(v_s - u)}{dt} = -R_s - T + P \tag{2.1}$$

$$M_i \frac{dv_i}{dt} + M_{add,i} \frac{d(v_i - u)}{dt} = -R_i + T, \tag{2.2}$$

where M_s and M_i are the masses of the boat and the iceberg, respectively. $M_{add,s}$ and $M_{add,i}$ are the added masses of the boat and the iceberg. v_s and v_i are the velocities of ship and iceberg, respectively. u is the velocity of the current in surge. P is the propulsion of the vessel and T is the rope tension.

The resistances of the water on the ship and iceberg are described by the following equation:

$$\begin{aligned} R_s &= \rho_w C_{ws} S_s |v_s - u|(v_s - u) \\ R_i &= \rho_w C_{wi} S_i |v_i - u|(v_i - u), \end{aligned} \tag{2.3}$$

where S_s is the wetted surface of the ship and S_i is the representative vertical cross-sectional area of the submerged surface of the iceberg that is perpendicular to the tow direction. u is the water velocity. C_{ws} and C_{wi} are the shear drag coefficient and form drag coefficient of the ship and iceberg, respectively. Marchenko and Eik used estimates found by Voitkunsky and Robe. They are as follows: $C_{ws} = 0.003$ and $C_{wi} \in (0.5, 1)$. This is basically the nonlinear damping in the model, usually denoted $\boldsymbol{D}(\boldsymbol{\nu})\boldsymbol{\nu}$ in Fossen-notation.

The Marchenko and Eik model is complete when the definition of the boat velocity relative to the iceberg velocity is included:

$$\frac{dX}{dt} = v_s - v_i. \tag{2.4}$$

Where X is the distance between vessel and iceberg in surge.

In this model the forces from wind and waves are considered negligible. Current is modeled through the relative velocity $v_s - u$. This approach is also explained in Fossen [2011, p 220], but not used further on.

2.2 The model in Fossen notation

Although the model in (2.1) and (2.2) works, it is too simple to use for anything but a towing tank experiment. The system is only modeled in surge, and we need a system modeled in at least three degrees-of-freedom. A new notation based on matrices are therefore used further on.

2.2.1 6 degrees of freedom

The dynamics of a ship are often described by 6-degrees-of-freedom differential equations. According to Fossen [2011, p 222] the equation of motions of a marine craft (not towing) can be written as

$$\begin{aligned} \dot{\boldsymbol{\eta}} &= \boldsymbol{J}_{\Theta}(\boldsymbol{\eta})\boldsymbol{\nu} \\ \boldsymbol{M}_{RB}\dot{\boldsymbol{\nu}} + \boldsymbol{M}_{A}\dot{\boldsymbol{\nu}}_r + \boldsymbol{C}_{RB}(\boldsymbol{\nu})\boldsymbol{\nu} + \boldsymbol{C}_{A}(\boldsymbol{\nu}_r)\boldsymbol{\nu}_r + \boldsymbol{D}(\boldsymbol{\nu})\boldsymbol{\nu} + \boldsymbol{g}(\boldsymbol{\eta}) \\ + \boldsymbol{g}_0 &= \boldsymbol{\tau} + \boldsymbol{\tau}_{wind} + \boldsymbol{\tau}_{wave}, \end{aligned} \tag{2.5}$$

where $\boldsymbol{\eta} = [x, y, z, \phi, \theta, \psi]^\top$ is a vector of position and orientation of the the floating body. $\boldsymbol{\nu} = [u, v, w, p, q, r]^\top$ is a vector of velocities and time derivatives of the orientation of the body. $\boldsymbol{\nu}_r = [u, v, w, p, q, r]^\top$ is a vector of relative velocities: $\boldsymbol{\nu}_r = \boldsymbol{\nu} - \boldsymbol{\nu}_c$. $\boldsymbol{\nu}_c = [u_c, v_c, w_c, 0, 0, 0]^\top$ is the generalized ocean current velocity of an irrotational fluid. $\boldsymbol{M}$, $\boldsymbol{C}(\boldsymbol{\nu})$, and $\boldsymbol{D}(\boldsymbol{\nu})$ are model matrices that denote inertia, Coriolis and damping, respectively. $\boldsymbol{g}(\boldsymbol{\eta})$ is a vector of generalized gravitational and buoyancy forces. The $\boldsymbol{g}_0$ term collects static restoring forces and moments due to ballast systems and water tanks. $\boldsymbol{\tau}$ is a vector of forces and moments acting on the vessel. The forces due to wind and waves are given in their own terms.

2.2.2 3 degrees of freedom

For maneuvering purposes a simplified version of the model is used and can be found by eliminating some of the degrees of freedom

(DOFs). A frequent simplification is to use 3 DOFs (surge, sway and yaw). This is a good approximation as long as ϕ and θ are small. The rotation matrix can then be written as $\boldsymbol{R}(\boldsymbol{\psi}) := \boldsymbol{R}_{z,\psi}$, that is

$$\boldsymbol{J}_\Theta(\boldsymbol{\eta}) \overset{3 \text{ DOF}}{=} \boldsymbol{R}(\psi) = \begin{bmatrix} \cos(\psi) & -\sin(\psi) & 0 \\ \sin(\psi) & \cos(\psi) & 0 \\ 0 & 0 & 1 \end{bmatrix}, \tag{2.6}$$

where ψ is the yaw angle. $\boldsymbol{\eta} = [x, y, \psi]^\top$ and $\boldsymbol{\nu} = [u, v, r]^\top$. Furthermore, wind, wave, gravitational, buoyancy, and restoring forces are neglected. The new simplified model can then be written as

$$\begin{aligned} \dot{\boldsymbol{\eta}} &= \boldsymbol{R}(\psi)\boldsymbol{\nu} \\ \boldsymbol{M}\dot{\boldsymbol{\nu}}_r + \boldsymbol{C}(\boldsymbol{\nu}_r)\boldsymbol{\nu}_r + \boldsymbol{D}(\boldsymbol{\nu}_r)\boldsymbol{\nu}_r &= \boldsymbol{\tau} \end{aligned} \tag{2.7}$$

The inertia matrix consists of two parts: $\boldsymbol{M} = \boldsymbol{M}_{RB} + \boldsymbol{M}_A$. It is positive definite and symmetric, $\boldsymbol{M} = \boldsymbol{M}^\top > 0$, and constant, $\dot{\boldsymbol{M}} = 0$. $\boldsymbol{M}_{RB}$ is the rigid-body system inertia matrix. For a starboard-port symmetric ship with origin in the center of gravity this can be written as

$$\boldsymbol{M}_{RB} = \begin{bmatrix} m & 0 & 0 \\ 0 & m & mx_g \\ 0 & mx_g & I_z \end{bmatrix}, \tag{2.8}$$

where m is the mass of the body, I_z the moment of inertia about the z_b-axis and x_g the distance between the center of gravity and the body axis. The added mass matrix is computed in the origin of the coordinate system (CO). Using SNAME notation this can be written as

$$\boldsymbol{M}_A = \begin{bmatrix} -X_{\dot{u}} & 0 & 0 \\ 0 & -Y_{\dot{v}} & -Y_{\dot{r}} \\ 0 & -Y_{\dot{r}} & -N_{\dot{r}} \end{bmatrix}, \tag{2.9}$$

where $X_{\dot{u}}$ is the added mass force X along the x axis due to an acceleration $\dot{u}$ in the x direction. The other elements of the matrix

follow similar notation. The added mass matrix has to be positive semi-definite and symmetric: $\boldsymbol{M}_A = \boldsymbol{M}_A^\top \geq 0$.

The damping matrix can also be decomposed into two different matrices:
$\boldsymbol{D}(\boldsymbol{\nu}_r) = \boldsymbol{D}_p + \boldsymbol{D}_n(\boldsymbol{\nu}_r)$. $\boldsymbol{D}_p$ is the linear damping matrix due to potential damping. $\boldsymbol{D}_n(\boldsymbol{\nu}_r)$ is the nonlinear damping matrix due to quadratic damping and higher-order terms [Fossen, 2011, p 123].

2.2.3 Slowly-varying environmental forces

A model is needed to describe the slowly varying environmental forces and moments. According to Fossen [2011] a *first-order Markov* model can be used to describe:

- second-order wave drift forces
- ocean currents
- wind forces

The first-order Markov process can be described by

$$\dot{\boldsymbol{b}} = -\boldsymbol{T}_b^{-1}\boldsymbol{b} + \boldsymbol{w}, \tag{2.10}$$

where $\boldsymbol{w}$ is a zero-mean Gaussian noise vector and $\boldsymbol{T}_b = \text{diag}\{T_1, T_2, T_3\} \in \mathbb{R}^{3x3}$. $\boldsymbol{T}_b$ is a user-specified diagonal matrix of positive bias constants [Fossen, 2011]. The bias, $\boldsymbol{b}$, is given in the NED frame, and have to be converted to the body frame when used in the motion equation.

The Marchenko model used relative velocity to describe a current acting on the ship. The relative velocity model is based on first principles, and therefore gives a mathematically precise result. However, this thesis will use the bias model instead. Although the relative-velocity model gives a more physically correct result, the quantitative values for the current velocities are needed. Because the current velocities are considered unknown, the bias model has to be used.

2.2.4 Thrust allocation

It is necessary to distribute the generalized control forces $\boldsymbol{\tau}_s \in \mathbb{R}^n$ to input values the actuators actually use. The input to the actuators can be described by $\boldsymbol{u} \in \mathbb{R}^r$. n and r are the dimension of the configuration space and number of actuators, respectively.

A model for thrust allocation with azimuth propellers is taken from Fossen [2011]. The control forces and moments $\boldsymbol{f} = [u_1, \ldots, u_n]^\top$ can be expressed as

$$\boldsymbol{f} = \boldsymbol{K}\boldsymbol{u}, \tag{2.11}$$

where $\boldsymbol{u} = [u_1, \ldots, u_r]^\top$ is a control input vector and $\boldsymbol{K}$ can be expressed by

$$\boldsymbol{K} = \text{diag}\{K_1, \ldots, K_r\}. \tag{2.12}$$

The relation between the control forces and the actuator input can then be expressed with

$$\boldsymbol{\tau}_s = \boldsymbol{T}_c(\boldsymbol{\alpha})\boldsymbol{f} = \boldsymbol{T}_c(\boldsymbol{\alpha})\boldsymbol{K}\boldsymbol{u}, \tag{2.13}$$

where $\boldsymbol{\alpha} = [\alpha_1, \ldots, \alpha_p]^\top \in \mathbb{R}^p$ is a vector of azimuth angles and $\boldsymbol{T}_c(\boldsymbol{\alpha}) \in \mathbb{R}^{nxr}$ is the thrust configuration matrix. $\boldsymbol{T}_c(\boldsymbol{\alpha})$ and $\boldsymbol{K}$ varies with each vessel.

The inverse relationship is also needed in the thrust allocation:

$$\boldsymbol{u} = \boldsymbol{K}^{-1}\boldsymbol{T}_c^\dagger(\boldsymbol{\alpha})\boldsymbol{\tau}_s \tag{2.14}$$

which is the generalized inverse [Fossen, 2011]. $\boldsymbol{T}_c^\dagger$ is the pseudo-invserse of $\boldsymbol{T}_c$ and can be found by with

$$\boldsymbol{T}_c^\dagger(\boldsymbol{\alpha}) = \boldsymbol{W}^{-1}\boldsymbol{T}_c^\top(\boldsymbol{\alpha})[\boldsymbol{T}_c(\boldsymbol{\alpha})\boldsymbol{W}^{-1}\boldsymbol{T}_c^\top(\boldsymbol{\alpha})]^{-1}, \tag{2.15}$$

where the weighting matrix $\boldsymbol{W} = \boldsymbol{W}^\top > 0$, is usually chosen as diagonal. Because both $\boldsymbol{\alpha}$ and $\boldsymbol{u}$ can be used to change the thrust, an optimization problem has to be set up to distribute the control

forces. A simplification is to keep either the thruster angles $\boldsymbol{\alpha}$ or the input $\boldsymbol{u}$ constant. Optimization in thrust allocation is outside the scope of this thesis and will not be treated here.

2.3 Final vessel model

In the final model the bias model is added. In addition, the velocity is considered small and therefore the Coriolis matrices can be neglected. The towing vessel can now be described in the Fossen notation with

$$\begin{aligned} \dot{\boldsymbol{\eta}}_s &= \boldsymbol{R}(\psi_s)\boldsymbol{\nu}_s \\ \dot{\boldsymbol{b}}_s &= -\boldsymbol{T}_{b,s}^{-1}\boldsymbol{b}_s + \boldsymbol{w} \\ \boldsymbol{M}_s\dot{\boldsymbol{\nu}}_s + \boldsymbol{D}_s(\boldsymbol{\nu}_s)\boldsymbol{\nu}_s &= \boldsymbol{\tau}_s - \boldsymbol{R}^\top(\psi_s)\boldsymbol{T} + \boldsymbol{R}(\psi_s)^\top\boldsymbol{b} \end{aligned} \tag{2.16}$$

where $\boldsymbol{\eta}_s = [x_s, y_s, \psi_s]^\top$, $\boldsymbol{\nu}_s = [u_s, v_s, r_s]^\top$, $\boldsymbol{b} = [b_1, b_2, b_3]^\top$, $\boldsymbol{\tau}_s = [\tau_x, \tau_y, \tau_N]^\top$, and $\boldsymbol{T} = [X_{tow}, Y_{tow}, N_{tow}]^\top$. τ_x, τ_y, and τ_N are the control forces, and X_{tow}, Y_{tow} and N_{tow} are the tension forces in the towline.

2.4 Final iceberg model

$$\begin{aligned} \dot{\boldsymbol{\eta}}_i &= \boldsymbol{R}(\psi_i)\boldsymbol{\nu}_i \\ \dot{\boldsymbol{b}}_i &= -\boldsymbol{T}_{b,i}^{-1}\boldsymbol{b}_i + \boldsymbol{w} \\ \boldsymbol{M}_i\dot{\boldsymbol{\nu}}_i + \boldsymbol{D}_i(\boldsymbol{\nu}_i)\boldsymbol{\nu}_i &= \boldsymbol{R}^\top(\psi_i)\boldsymbol{T} + \boldsymbol{R}(\psi_i)^\top\boldsymbol{b} \end{aligned} \tag{2.17}$$

where $\boldsymbol{\eta}_i = [x_i, y_i, \psi_i]^\top$, $\boldsymbol{\nu}_i = [u_i, v_i, r_i]^\top$, $\boldsymbol{b} = [b_1, b_2, b_3]^\top$, and $\boldsymbol{T} = [X_{tow}, Y_{tow}, N_{tow}]^\top$. N_{tow}, Y_{tow}, and N_{tow} are the towline forces. The towline forces are the same as in the vessel model.

Chapter 3

Hydrodynamic properties of ships and icebergs

The motion and behavior of the iceberg depends greatly on the hydrodynamic properties of them. This involves the $\boldsymbol{M}_{RB}$, $\boldsymbol{M}_A$, and $\boldsymbol{D}$ matrices, that captures the geometry and mass properties of the floating body. This chapter deals with these hydrodynamic properties.

3.1 Hydrodynamic properties of ships

This thesis is mainly using the model ship *CS Enterprise I* as a testing platform. The hydrodynamic properties will therefore be found for this vessel. The relevant data was found in the master thesis of Håkon Skåtun [Skåtun, 2011] and the PhD thesis of Roger Skjetne [Skjetne, 2005].

3.1.1 Mass and added mass

Skåtun [2011] tried to find the added mass of CS Enterprise I using system identification in Matlab. This involved setting up a state-space model of the vessel with the parameters unknown. Data series

of the vessel was then recorded and the parameters were found using least-square curve fitting. The parameters that were found are presented in Table 3.1.

As one can see, the order of magnitude of the standard deviation makes these data unusuable. Skåtun [2011] solved this problem by using data from *Cybership II*, which is a vessel with similar geometry and size as *CS Enterprise I*. These parameters were found by Skjetne [2005] and are presented in Table 3.3.

Parameter	**Value**	**Standard deviation**
m	14.1	0
$X_{\dot{u}}$	-2.67748	0.239336
$Y_{\dot{v}}$	-19.9938	2.31892
$Y_{\dot{r}}$	0.48225	3734.23
$N_{\dot{v}}$	-6.77422	3733.9
$N_{\dot{r}}$	$-7.38588 \cdot 10^{-5}$	526.339

Table 3.1: Estimated added mass of CS Enterprise I, found by Skåtun [2011].

3.1.2 Damping

The damping was also found by Skåtun [2011] using system identification. The values found are presented in Table 3.2.

The estimation of the damping had the same standard deviation problem as the added mass, although not as large. The values given in Table 3.3 are therefore used further on.

Parameter	Value	Standard deviation
X_u	-0.55	0
Y_v	-3.94	0
Y_r	1.47519	0.0804179
N_v	0.887797	0.0735087
N_r	-0.653684	0.029075

Table 3.2: Estimated damping of CS Enterprise I, found by Skåtun [2011].

Parameter	Value
m	23.8
I_z	1.760
$X_{\dot{u}}$	-2.0
$Y_{\dot{v}}$	-10.0
$Y_{\dot{r}}$	0
$N_{\dot{v}}$	0
$N_{\dot{r}}$	-1.0
X_u	-2.0
Y_v	-7.0
Y_r	-0.1
N_v	-0.1
N_r	-0.5

Table 3.3: Estimated added mass and damping for Cybership II, found by Skjetne [2005].

3.2 Hydrodynamic properties of icebergs

Icebergs vary greatly in size and shape. They can be everything from small growlers about the size of a big boat, to gigantic icebergs with a waterline length of several hundred meters. Icebergs with masses up to 4 million tonnes have been towed successfully, although towing

is most effective for masses between 1000 and 100,000 tonnes [Timco, 2007].

The *International Ice Patrol* uses the following (Table 3.4) size categories to identify icebergs.

Iceberg type	**Mass (T)**	**Height (m)**	**Length (m)**
Growler	500	< 1	< 5
Bergy bit	1,400	1 - 5	5 - 15
Small berg	100,000	5 - 15	15 - 50
Medium berg	750,000	15 - 50	50 - 100
Large berg	5,000,000	50 - 100	100 - 200
Very large berg	$> 5,000,000$	> 100	> 200

Table 3.4: International Ice Patrol Iceberg Size Classifications

3.2.1 Mass and added mass

As Table 3.4 shows, the mass of an iceberg vary between 500 tonnes to more than 5 million tonnes. This thesis is mostly concerned with iceberg towing in a towing tank. The mass and added mass calculations can then be made of a iceberg model. If the scaling ratio is $\lambda = 50$, like the model vessel used further on, Table 3.4 can be scaled down and written as Table 3.5.
This means we will deal with icebergs between 4 kg and 40 tonnes in the towing tank. However, anything above a few tonnes are unable to fit in the towing tank, which means we will only deal with icebergs classified as *small bergs* or smaller.

3.2.2 Damping

It is very hard to estimate the damping of an iceberg. First of all, it varies a lot depending on the iceberg size. Second of all, the damping is very hard to measure due to the size of the iceberg. Thus, in order

Iceberg type	**Mass (kg)**	**Height (m)**	**Length (m)**
Growler	4	< 0.02	< 0.1
Bergy bit	11.2	0.02 - 0.1	0.1 - 0.3
Small berg	800	0.1 - 0.3	0.3 - 1
Medium berg	6,000	0.3 - 1	1 - 2
Large berg	40,000	1 - 2	2 - 4
Very large berg	$> 40,000$	> 2	> 4

Table 3.5: International Ice Patrol Iceberg Size Classifications scaled down to model size using $\lambda = 50$

to find linear damping, an analysis have to performed in software such as Wamit [2012]. The nonlinear damping in surge, described by (2.3), can be estimated by finding an approximate underwater surface area.

The underwater surface area can be approximated by assuming the iceberg has a conic shape under water. If the length of the iceberg is $L_i = 50\ m$, an empirical formula can be used to find the draft of the iceberg:

$$D_i = 3.781 \cdot L_i^{0.63} = 3.781 \cdot 50^{0.63} \approx 44.5\ m. \tag{3.1}$$

The surface area of the cone is then

$$S_i = \frac{\pi}{2} L_i \left(\sqrt{\left(\frac{L_i}{2}\right)^2 + D^2} \right) \approx 4000\ m^2, \tag{3.2}$$

which makes the damping coefficient in surge

$$D_{nl,surge} = \rho_w C_{wi} S_i \approx 3,075 \cdot 10^6\ kg/m, \tag{3.3}$$

when $C_{wi} = 0.75$ and $\rho_w = 1025\ kg/m^3$.

If the underwater shape can be approximated as cylindrical, the surface area becomes

$$S_i = \pi LD \approx 7000\ m^2, \tag{3.4}$$

and the damping is:

$$D_{nl,surge} = \rho_w C_{wi} S_i \approx 5,38 \cdot 10^6\ kg/m. \tag{3.5}$$

As one can see, the damping varies greatly depending on shape, size and empirical coefficients. Therefore the damping might be treated as a tuning parameter unless one can perform numerical simulations to find it. In the simulations, scaled versions of the damping on the model ship *Cybership II* were used.

Chapter 4

Iceberg controllability

This chapter deals with the ability of a vessel to control an iceberg. This includes a view of which the freedom-of-degrees the iceberg can be controlled in, what sensors are needed for the controller to work, the disturbances that will affect the controller, and which states that have to be estimated. In the end, a few different problems with iceberg towing will be explained.

4.1 Detailed look on iceberg control

Figure 4.1 shows an iceberg modeled as a cylinder, connected to a towing rope.

The following list describes the degrees-of-freedom the iceberg can be controlled in.

- The iceberg will move in positive surge direction (arrow marked with 2) when the tow rope is pulled in this direction. However, when the vessel is moving in negative surge direction (arrow marked with 1), with the iceberg towed behind it, the iceberg will not move at all.
- The tow rope will slide along the iceberg in the heave direction (arrow marked 3 and 4). The friction is neither large enough

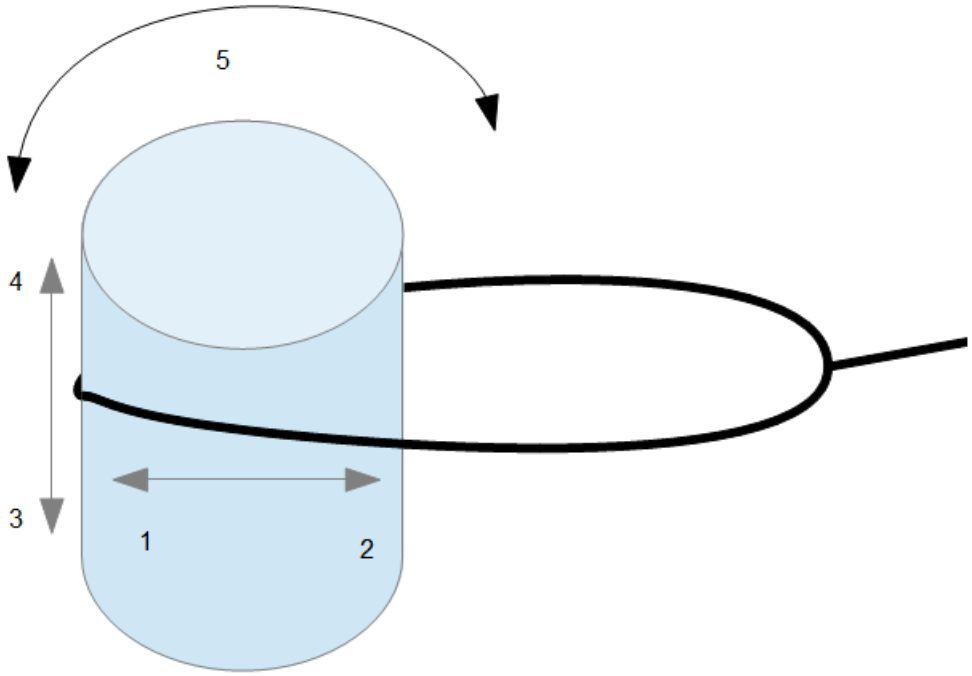

Figure 4.1: Figure of an iceberg with a towing rope.

to actually move the iceberg in the heave direction, nor is the force large enough compared to the gravitational force.

- The friction between tow rope and iceberg is not large enough to rotate the iceberg (arrow marked with 5). While there is some friction, the moment that is created is very small compared to the gigantic mass and inertia of the iceberg. The tow rope will slide along the iceberg when it is rotated.

The conclusion is that the iceberg only can be moved in the plane, without any real ability to control the heading. The vessel is only an actuator on the iceberg in the surge direction (the way the towline is pointing). Figure 4.2 represents these degrees-of-freedom.

Moreover, the geometry of the vessel will also cause limitations on its motion. A deck plan of the vessel can be seen in Figure 4.3. The

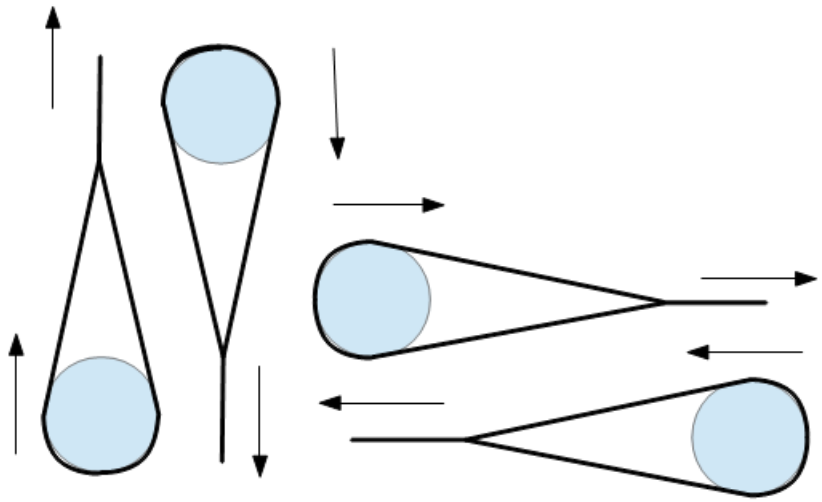

Figure 4.2: Figure of the different degrees-of-freedom of an iceberg.

towing configuration consists of a winch system that is responsible for controlling the towline length and tension, the towline itself, and two or more guide pins to keep the tow line in the middle of the vessel.

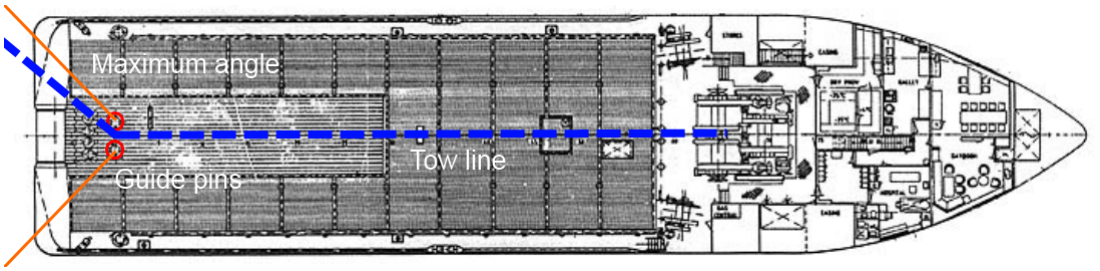

Figure 4.3: Figure of a deck plan of an AHTS (Normand Jarl). Courtesy of John McClintock and Brown [2002].

The guide pins will restrict the movement of the towline in the aft end of the vessel. In theory the towline is able to move 90° to both starboard and port side, aft of the guide pins. However, if the angle exceeds about 60° the towline will start scraping against the

hull, which can damage the vessel. That means the yaw angle of the vessel is restricted to 60° compared to the towline, and that the vessel is unable to do any hard turns. If a change in course is needed, the vessel should stop completely to remove tension in the towline. It should then get the new course while not having tension in the towline, and while keeping the towline behind the vessel at all times. When the new course is set, the vessel can start towing again. This maneuver should make the vessel able to keep the towline away from the port and starboard side at all times.

4.2 Sensors, measurements and disturbances

The system is not assumed to have full-state feedback due to noise and unmeasurable states. We therefore have to take a deeper look at the various sensors available, what disturbances that affect the system and how we can estimate the unmeasurable states.

4.2.1 Sensors and measurements

It can be assumed that the vessel has the following sensors available for use by the DP system:

Differential Global Positioning System (DGPS)	The DGPS allows the user to find his position using ground-based reference stations, in addition to the satellites provided by the GPS. The position (x_e, y_e, z_e) is given in the Earth-centered Earth-fixed (ECEF) reference frame [Fossen, 2011]. The error is usually in the range of 1-3 meters. [Center, 2012].
Compass	All vessels will have a compass that measures the yaw angle, ψ. A gyrocompass is usually the type of compass used on a offshore vessel [Fossen, 2011, p 305]. A gyrocompass is not affected by the ship's hull and will not be affected by deviation like a magnetic compass.
Wind sensor	A wind sensor will measure the velocity and direction of the wind.
Tension sensor	The tension in the towing hawser is available for measurement in modern anchor-handling vessels.

The iceberg does not have any sensors or available measurements by itself. This is a problem because the model described by (2.17) is dependent on the measured or estimated velocities. Without the distance between the vessel and the iceberg, the towline forces cannot

be estimated, unless the tension can be measured with a tension sensor.

An iceberg that is going to be controlled with a model-based controller needs a GPS unit, which will have to be placed on the iceberg. This will make it possible to estimate position and velocity of the iceberg, and thus the tension in the towing wire if a tension observer is used.

4.2.2 Disturbances

Both the vessel and iceberg will be affected by various disturbances. According to Morris [2001] the measurements will have errors due to:

- error in the output of the measuring instrument due to factors inherent in the manufacture of the instrument arising out of tolerances in the components of the instrument. They can also arise due to wear in instrument components over a period of time.

- corruption of the measurement signal by induced noise during transfer of the signal from one point of the measurement to some other point.

This noise is called measurement noise and can be considered to be zero-mean Gaussian white noise. Second of all, the process itself will be polluted by noise due to environmental disturbances.

The environmental disturbances usually comes from three different sources: wind, waves, and current. In addition, the vessel can be affected by ice disturbances. These environmental disturbances will produce pressure changes on the vessel hull, which in turn induces forces [Fossen, 2011, p 285]. The pressure-induced forces causes two distinct kind of motions: a slowly-varying motion, and a high-frequency motion that linearly depends on the wave elevation.

The slowly-varying motion is due to current, wind and wave-drift forces. The high-frequency motion is due to 1st order wave-induced loads.

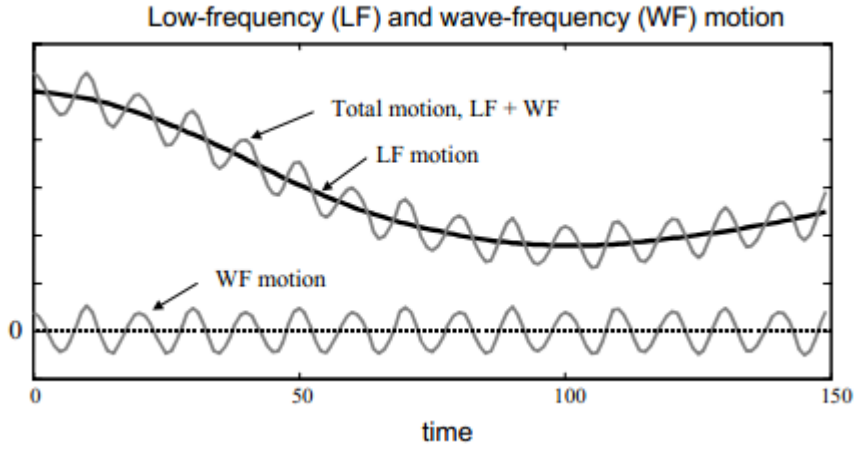

Figure 4.4: Separation of the total motion of a marine craft into LF and WF motion components. Courtesy of Fossen [2011].

The dynamic positioning system must suppress the low-frequency motion, and keep the mean position of the vessel as close as possible to the desired set-point [Tannuri et al., 2003]. However, we do not want the high-frequency motion to enter the feedback loop, because it can cause higher power consumptions and potential wear on the actuators [Fossen, 2011, p 286]. Moreover, with a high wave effect the thruster's power would not be able to correct the whole effect. The removal of high-frequency motion from the measurement is done by wave-filtering techniques.

The wave filter is usually implemented as a model-based observer, such as a Kalman filter or a nonlinear observer.

Disturbances in the tension measurements

The tension measurements will also be influenced by measurement and process noise. This noise has a high frequency, similar to the noise that affects the positioning measurement system. Noise damp-

ing can be done using Kalman filters or other observers, but the simplest way to do it is by using a lowpass filter. A lowpass filter will allow signals with a frequency below a certain frequency, called the cut-off frequency, to pass. Frequencies above the cut-off frequency are stopped. An ideal lowpass filter is able to eliminate all frequencies above the cut-off frequency. However, a real filter will have a transitional region where the high-frequency signals only are damped, instead of eliminated completely.

Figure 4.5 shows a time series taken from the *MC Lab* towing tank. The black curve represents the force from a force measurement ring, recorded with respect to time, and heavily polluted by high-frequency noise. The red curve represents the signal after it has been filtered by a lowpass filter. As one can see the result is much less noisy, and better for use with the tension controller designed in 5.2.1.

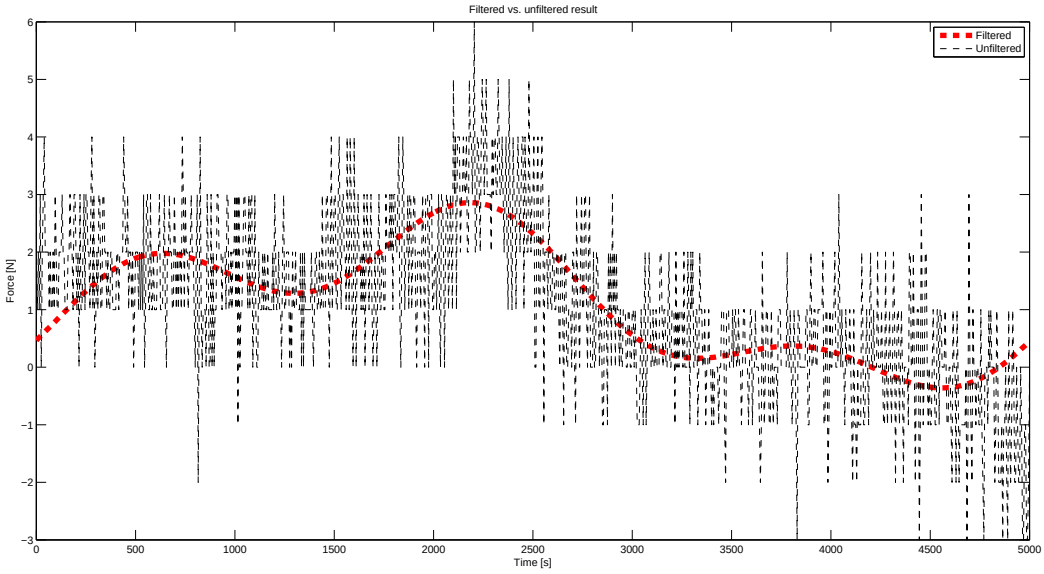

Figure 4.5: Filtered vs unfiltered result of a force measurement series

Lowpass filtering will cause a small phase shift in the signals. The magnitude of the phase shift depends on the filter properties. The filter will therefore have to be tuned in order to balance the effect of the phase shift, and the desired filtering effect of the filter.

A non-ideal lowpass filter can be expressed as

$$n = 1: \quad b(s) = \frac{\omega_c}{s + \omega_c} \tag{4.1a}$$

$$n = 2: \quad b(s) = \frac{\omega_c^2}{s^2 + \sqrt{2}\omega_c s + \omega_c^2} \tag{4.1b}$$

$$n = 3: \quad b(s) = \frac{\omega_c^3}{(s^2 + \omega_c s + \omega_c^2)(s + \omega_c)}, \tag{4.1c}$$

where ω_c is the cut-off frequency and s is the Laplace variable. This is called a n^{th} -order Butterworth filter [Sørensen, 2011]. In Figure 4.5 a cut-off frequency of $\omega_c = 0.007$ Hz was used.

Other filters that can be used are Chebyshev filters, Bessel filters, Legendre-Papoulis filters and Elliptic filters.

4.2.3 Estimated states

Because of the mentioned disturbances, and the fact that the system is not full-state observable, the following states have to be estimated by an observer:

Positions and heading, $\hat{\boldsymbol{\eta}}$	The positions and heading will be estimated to get a wave-filtered result.
Velocities, $\hat{\boldsymbol{\nu}}$	The velocities can be found by taking the time derivative of the position and heading. However, this will result in an extremely noisy signal. The velocities will therefore have to be estimated by the observer.
Bias, $\hat{\boldsymbol{b}}$	The bias is estimated by the observer.
Tension, $\boldsymbol{T}$	If the vessel lacks a tension sensor, the tension has to be estimated by the observer.

Because the model is nonlinear an *Extended Kalman Filter (EKF)* or *Nonlinear passive observer* should be used for position, velocity and bias estimation [Fossen, 2011]. The design of the observers used in this thesis are described in 5.3.

4.3 Common problems during iceberg towing

Some of the key problems in iceberg towing is rupture of the towline, slippage and overturning of icebergs [Eik, 2010]. This chapter describes these problems and how to prevent them from happening.

4.3.1 Rupture of towline

Towline rupture is when the towline breaks because of high tension in the towline. This happens when the towline tension passes the breaking strength of the towline. An example is the vessel *Havila Charisma*, which have been used for towing operations outside the coast of Greenland. Havila Charisma has a bollard pull of 180 tonnes, but the breaking strength of the towline is only 90 tonnes [John McClintock and Brown, 2002, p 51]. The breaking strength is therefore a large limiting factor in the towing operation. A rupture can also cause damage to the ship or personnel when the towline shoots backwards after breaking, similar to ruptures during anchor-handling operations in the North Sea.

If a rupture does happen, the rope trapping procedure will have to be done over again. Caution will have to be paid when designing the control system for towing. Because the tension is usually available for measurement, the control system can easily take this into account by using saturations on the velocity or similar methods. A tension controller can also be used to keep the tension constant.

4.3.2 Slippage

Slippage happens when the towline loses its grip on the iceberg. The main reason for this is low friction between rope and ice. This can be due to a low static friction coefficient, or because the shape of the iceberg makes the tow rope slide upwards until it slips off the iceberg. In such a case, the iceberg can be considered untowable. In the event of an untowable iceberg, another way to guide it away has to be found, but that is outside the scope of this project. A method by using a net instead of a tow rope has been proposed [John McClintock and Brown, 2002].

4.3.3 Overturning

Overturning is when an iceberg flips over due to gravity. An iceberg will seek its points of stability, or equilibrium points, and will therefore turn over if it has a weak metacentric stability. The probability of overturning depends on geometry, gravitational stability and the disintegration history of the iceberg. A tabular iceberg is less likely to overturn, while irregular shapes are more likely. Similarly, icebergs that have started to disintegrate are more likely to overturn due to the creation of an irregular shape over time [Dowdeswell, 1989].

Overturning releases a lot of potential energy into the ocean over a short time. This energy causes horizontal translation, vertical bobbing and rocking of the iceberg [Burton and MacAyeal, 2012].

Fortunately, due to the distance between the vessel and the iceberg, an overturning iceberg will not be very dangerous to the ship or crew in ordinary towing operations [John McClintock and Brown, 2002, p 54]. If the iceberg overturns the vessel crew will have to bring the line back on deck, disconnect it, and do the rope trapping procedure over again. In a worst-case scenario the winch is equipped with a quick-release mechanism that can disconnect the towline.

It is not really possible to prevent an iceberg from overturning when the overturning motion has started. However, it is less likely to happen if the vessel rarely turns or slows down [John McClintock and Brown, 2002, p 46]. Careful management of tension also helps preventing overturning. This is described more thoroughly in 5.2.1.

Chapter 5

Controller and observer design

The main goal of this thesis is to develop guidance systems and controller laws capable of towing an iceberg with a towing vessel. The guidance system is responsible for generating a desired path, while the controller should be capable of following the predefined path, while under the influence of environmental forces such as wind and current. The controller should also take into account the tension in the towline, in order to prevent towline rupture, slippage and overturning. This chapter will go through the design process of the guidance system, and the ancillary control law.

5.1 Configuration space and workspace

Before the guidance and control system is designed, the concept of a underactuated and a fully actuated marine craft will be explained. These concepts are important, because the degree of actuation of a marine craft puts limitation on what control objectives can be satisfied [Fossen, 2011, p 235].

5.1.1 Configuration space

According to Fossen [2011] the configuration space can be defined as:

> *The n-dimensional configuration space is the space of possible positions and orientations that a craft may attain, possibly subject to external contraints.*

The towing vessel operating in three degrees-of-freedom are described by $n_s = 3$ generalized positions and velocities:

$$\boldsymbol{\eta}_s = [x_s, y_s, \psi_s]^\top , \tag{5.1}$$

$$\boldsymbol{\nu}_s = [u_s, v_s, r_s]^\top . \tag{5.2}$$

The order is $2 \cdot 3 = 6$.

This is also true for the iceberg:

$$\boldsymbol{\eta}_i = [x_i, y_i, \psi_i]^\top , \tag{5.3}$$

$$\boldsymbol{\nu}_i = [u_i, v_i, r_i]^\top , \tag{5.4}$$

which means the configuration space for the iceberg is of dimension $n_i = 3$, and the order is 6.

5.1.2 Control inputs

The number of control inputs is denoted r. According to Fossen [2011]:

> *A marine craft is fully actuated if it has equal or more control inputs than generalized coordinates ($r \geq n$),*

and

> *A marine craft is under-actuated if it has less control inputs than generalized coordinates ($r < n$).*

A vessel for towing will usually have a propeller, rudder, bow thruster, and stern thruster. That means it is actuated in all three degrees-of-freedom, and $r_s = 3 = n_s$. CS Enterprise I uses Voith Schneider propellers and is therefore actuated in three degrees-of-freedom. The iceberg does not have its own actuators, but is dependent on the vessel movement and towline. The iceberg itself is therefore under-actuated.

If one looks at the both the vessel and iceberg in the same system, the number of actuators is $r_{s+i} = 3$. The configuration space is now twice as big, due to two different bodies to control, thus $n_{s+i} = 6$. Because $r_{s+i} < n_{s+i}$, the total system is under-actuated.

5.1.3 Workspace

According to Fossen [2011] the workspace is defined as:

> *The workspace is a reduced space of dimension $m < n$ in which the control objective is defined.*

If the control objective is to move the iceberg along a path, then the vessel needs to be actuated in surge and yaw. This can for example be done with a rudder and a propeller. The workspace dimension for the vessel is then $r_s = 2 < n_s = 3$.

Although the iceberg is under-actuated, it can still be moved by the towing vessel. Using the tow rope, the vessel is able to move the iceberg in surge and yaw. The workspace for the iceberg is therefore $r_i = 2 < n_i = 3$. This assumes perfect rigidity between the vessel and the iceberg, such that an actuator on the vessel produces an instant change on the iceberg.

5.2 Controller design

> ***Note on notation:*** *This chapter uses the same notation as used by Skjetne [2005]. Partial differentiation is*

denoted with the differentiation variable as superscript to the function. E.g. the partial derivative of a function $x(t)$, with respect to the variable a, will be written as $x^a(t)$. The time derivative of a function is denoted with a dot above the function name. E.g. the time derivative of $x(t)$ is written as $\dot{x}(t)$.

5.2.1 Using maneuvering control to control the ship along a path

Ship and iceberg model

As described in Chapter 2, the mathematical models for the ship and iceberg can be represented as

$$\begin{aligned} \dot{\boldsymbol{\eta}}_s &= \boldsymbol{R}(\psi_s)\boldsymbol{\nu}_s \\ \dot{\boldsymbol{b}}_s &= -\boldsymbol{T}_{b,s}^{-1}\boldsymbol{b}_s \\ \boldsymbol{M}_s\dot{\boldsymbol{\nu}}_s &= \boldsymbol{\tau}_s - \boldsymbol{R}^\top(\psi_s)\boldsymbol{T} - \boldsymbol{D}_s\boldsymbol{\nu}_s + \boldsymbol{R}^\top(\psi_s)\boldsymbol{b}_s \end{aligned} \tag{5.5}$$

for the ship, and

$$\begin{aligned} \dot{\boldsymbol{\eta}}_i &= \boldsymbol{R}(\psi_i)\boldsymbol{\nu}_i \\ \dot{\boldsymbol{b}}_i &= -\boldsymbol{T}_{b,i}^{-1}\boldsymbol{b}_i \\ \boldsymbol{M}_i\dot{\boldsymbol{\nu}}_i &= \boldsymbol{R}^\top(\psi_i)\boldsymbol{T} - \boldsymbol{D}_i\boldsymbol{\nu}_i + \boldsymbol{R}^\top(\psi_i)\boldsymbol{b}_i \end{aligned} \tag{5.6}$$

for the iceberg. The variables were explained in 2.2.

Problem statement

The controller will be based on the works of Skjetne [2005]. In his PhD thesis he proposes a concept for path tracking and following, which he calls *The maneuvering problem*. The maneuvering problem evolves around two different tasks. The primary task is to converge to and follow a certain continuously parameterized path. The second

task involves satisfying the dynamic behavior along the path [Skjetne, 2005, p 27].

Path parameterization: The path parameterization defines the desired path of the ship, $\boldsymbol{\eta}_d$, with respect to a path variable $\theta(t)$. $\boldsymbol{\eta}_d(\theta)$ can be written as

$$\boldsymbol{\eta}_d(\theta) = \begin{bmatrix} x_d(\theta) \\ y_d(\theta) \\ \psi_d(\theta) \end{bmatrix} \tag{5.7}$$

where $x_d(\theta)$ and $y_d(\theta)$ describes a path in the plane. If the path, for instance, is chosen to be a straight line from South to North, that means $x_d(\theta) = \theta$ and $y_d(\theta) = 0$. $\psi_d(\theta)$ is chosen to be the angle of the tangent vector along the path, expressed as

$$\psi_d(\theta) \equiv \arctan\left(\frac{y_d^\theta(\theta)}{x_d^\theta(\theta)}\right). \tag{5.8}$$

The final expression for $\boldsymbol{\eta}_d(\theta)$, with a northward path, becomes

$$\boldsymbol{\eta}_d(\theta) = \begin{bmatrix} \theta \\ 0 \\ 0 \end{bmatrix} \tag{5.9}$$

Geometric task: The main goal for this controller is to have the ship follow a parameterized path. The position of the ship is given by $\boldsymbol{\eta}_s(t)$ and the desired position is given by $\boldsymbol{\eta}_d(\theta(t))$. The geometric task is concerned with reducing the distance between the position of the ship and desired path over time, thus the task can be expressed as

$$\lim_{t\to\infty} [\boldsymbol{\eta}_s(t) - \boldsymbol{\eta}_d(\theta(t))] = 0 \tag{5.10}$$

Dynamic task: The ship should also follow a given dynamic behavior. Skjetne [2005] mentions three different desired dynamic behaviors:

Time assignment With the time assignment the ship has to be at specific points along the path at specific time instants.

Speed assignment With the speed assignment the ship should try to obtain a specific speed along the path. The desired speed is expressed by the function $v_s(\theta, t)$.

Acceleration assignment With the acceleration assignment the ship should obtain an desired acceleration along the path.

The speed assignment is considered the most suitable dynamic assignment for this task. The dynamic task can therefore be expressed as

$$\lim_{t\to\infty}\left[\dot{\theta}(t) - v_s\left(\theta(t), t\right)\right] = 0 \tag{5.11}$$

where $\dot{\theta}(t)$ is the path speed and $v_s(\theta(t), t)$ is the desired speed. The following identity has to hold [Skjetne, 2005, p 42]

$$|\dot{p}_d| = \sqrt{x_d^\theta(\theta)^2\dot{\theta}^2 + y_d^\theta(\theta)^2\dot{\theta}^2} = \sqrt{x_d^\theta(\theta)^2 + y_d^\theta(\theta)^2}|v_s(\theta, t)| = |U_d(t)|. \tag{5.12}$$

Solving for $v_s(\theta, t)$ yields

$$v_s(\theta, t) = \frac{U_d(t)}{\sqrt{x_d^\theta(\theta)^2 + y_d^\theta(\theta)^2}} \tag{5.13}$$

Differentiating (5.13) with respect to θ yields

$$v_s^\theta(\theta, t) = \frac{-\left[x_d^\theta(\theta)x_d^{\theta^2}(\theta) + y_d^\theta(\theta)y_d^{\theta^2}(\theta)\right]}{\left[x_d^\theta(\theta)^2 + y_d^\theta(\theta)^2\right]^{3/2}}, \tag{5.14}$$

while differentiating (5.13) with respect to time yields

$$v_s^t(\theta, t) = \frac{\dot{U}_d(t)}{\sqrt{x_d^\theta(\theta)^2 + y_d^\theta(\theta)^2}}. \tag{5.15}$$

Backstepping design

A nonlinear design tool called backstepping is used for designing the controller. The goal is to find an expression for the control force, $\boldsymbol{\tau}_s$, that stabilizes the controller.

Step 1: First, the error variables are defined as

$$\boldsymbol{z}_1 \equiv \boldsymbol{R}^\top(\psi_s)(\boldsymbol{\eta}_s - \boldsymbol{\eta}_d) \tag{5.16a}$$
$$\boldsymbol{z}_2 \equiv \boldsymbol{\nu}_s - \boldsymbol{\alpha}_1 \tag{5.16b}$$
$$\omega_s \equiv v_s - \dot{\theta} \tag{5.16c}$$

where $\boldsymbol{\alpha}_1$ is the virtual control to be defined later. The time derivative of (5.16a) is

$$\begin{aligned}
\dot{\boldsymbol{z}}_1 &= \dot{\boldsymbol{R}}^\top(\psi_s)\left[\boldsymbol{\eta}_s - \boldsymbol{\eta}_d\right] + \boldsymbol{R}^\top(\psi_s)\left[\dot{\boldsymbol{\eta}}_s - \boldsymbol{\eta}_d^\theta \dot{\theta}\right] \\
&= r_s \boldsymbol{R}^\top(\psi_s)\boldsymbol{S}\left[\boldsymbol{\eta}_s - \boldsymbol{\eta}_d\right] + \boldsymbol{R}^\top(\psi_s)\dot{\boldsymbol{\eta}}_s - \boldsymbol{R}^\top(\psi_s)\boldsymbol{\eta}_d^\theta \dot{\theta} \\
&= r_s \boldsymbol{R}^\top(\psi_s)\boldsymbol{S}\left[\boldsymbol{\eta}_s - \boldsymbol{\eta}_d\right] + \boldsymbol{R}^\top(\psi_s) \cdot \boldsymbol{R}(\psi_s)\boldsymbol{\nu}_s - \boldsymbol{R}^\top(\psi_s)\boldsymbol{\eta}_d^\theta \dot{\theta} \\
&= -r_s \boldsymbol{S}\boldsymbol{z}_1 + \boldsymbol{\nu}_s - \boldsymbol{R}^\top(\psi_s)\boldsymbol{\eta}_d^\theta \dot{\theta} \\
&= -r_s \boldsymbol{S}\boldsymbol{z}_1 + \boldsymbol{z}_2 + \boldsymbol{\alpha}_1 - \boldsymbol{R}^\top(\psi_s)\boldsymbol{\eta}_d^\theta \dot{\theta}
\end{aligned} \tag{5.17}$$

where $\dot{\boldsymbol{R}}(\psi_s) = r_s \boldsymbol{R}(\psi_s)\boldsymbol{S}$, r_s is the yaw rate of the ship, and $\boldsymbol{S}$ is defined as

$$\boldsymbol{S} = \begin{bmatrix} 0 & -1 & 0 \\ 1 & 0 & 0 \\ 0 & 0 & 0 \end{bmatrix} \tag{5.18}$$

Note that $\boldsymbol{S}$ is skew symmetric: $\boldsymbol{S} = -\boldsymbol{S}^\top$.

The first control Lyapunov function (CLF) can then be defined as

$$V_1 \equiv \frac{1}{2}\boldsymbol{z}_1^\top \boldsymbol{z}_1. \tag{5.19}$$

Differentiating (5.19) with respect to time yields

$$\begin{aligned}
\dot{V}_1 &= \boldsymbol{z}_1^\top \dot{\boldsymbol{z}}_1 \\
&= \boldsymbol{z}_1^\top \left[\cancel{-r_s \boldsymbol{S}\boldsymbol{z}_1} + \boldsymbol{z}_2 + \boldsymbol{\alpha}_1 - \boldsymbol{R}^\top(\psi_s)\boldsymbol{\eta}_d^\theta \dot{\theta} \right] \\
&= \boldsymbol{z}_1^\top \boldsymbol{z}_2 + \boldsymbol{z}_1^\top \left[\boldsymbol{\alpha}_1 - \boldsymbol{R}^\top(\psi_s)\boldsymbol{\eta}_d^\theta \dot{\theta} \right] \\
&= \boldsymbol{z}_1^\top \boldsymbol{z}_2 + \boldsymbol{z}_1^\top \left[\boldsymbol{\alpha}_1 - \boldsymbol{R}^\top(\psi_s)\boldsymbol{\eta}_d^\theta (v_s - \omega_s) \right] \\
&= \boldsymbol{z}_1^\top \boldsymbol{z}_2 + \boldsymbol{z}_1^\top \left[\boldsymbol{\alpha}_1 - \boldsymbol{R}^\top(\psi_s)\boldsymbol{\eta}_d^\theta v_s \right] + \boldsymbol{z}_1^\top \boldsymbol{R}^\top(\psi_s)\boldsymbol{\eta}_d^\theta \omega_s.
\end{aligned} \tag{5.20}$$

The virtual control, $\boldsymbol{\alpha}_1$, is then chosen as

$$\boldsymbol{\alpha}_1 = -\boldsymbol{K}_p \boldsymbol{z}_1 + \boldsymbol{R}^\top(\psi_s)\boldsymbol{\eta}_d^\theta v_s \tag{5.21}$$

where $\boldsymbol{K}_p = \boldsymbol{K}_p^\top > 0$. $\boldsymbol{K}_p$ is a matrix used to tune the controller. Inserting (5.21) into (5.17) yields

$$\begin{aligned}
\dot{\boldsymbol{z}}_1 &= -\boldsymbol{K}_p \boldsymbol{z}_1 + \boldsymbol{R}^\top(\psi_s)\boldsymbol{\eta}_d^\theta v_s + \boldsymbol{z}_2 - r_s \boldsymbol{S}\boldsymbol{z}_1 - \boldsymbol{R}^\top(\psi_s)\boldsymbol{\eta}_d^\theta \dot{\theta} \\
&= -\boldsymbol{K}_p \boldsymbol{z}_1 + \boldsymbol{z}_2 - r_s \boldsymbol{S}\boldsymbol{z}_1 + \boldsymbol{R}^\top(\psi_s)\boldsymbol{\eta}_d^\theta \omega_s,
\end{aligned} \tag{5.22}$$

while inserting (5.21) into (5.20) yields

$$\dot{V}_1 = -\boldsymbol{z}_1^\top \boldsymbol{K}_p \boldsymbol{z}_1 + \boldsymbol{z}_1^\top \boldsymbol{z}_2 + \boldsymbol{z}_1^\top \boldsymbol{R}^\top(\psi_s)\boldsymbol{\eta}_d^\theta \omega_s. \tag{5.23}$$

The next step requires the expression for $\dot{\boldsymbol{\alpha}}_1$, which can be expressed as

$$\dot{\boldsymbol{\alpha}}_1 \equiv \boldsymbol{\sigma}_1 + \boldsymbol{\alpha}_1^\theta \dot{\theta}, \tag{5.24}$$

where

$$\boldsymbol{\sigma}_1 = -\boldsymbol{K}_p(\boldsymbol{\nu}_s - r_s\boldsymbol{S}\boldsymbol{z}_1) - r_s\boldsymbol{S}\boldsymbol{R}^\top(\psi_s)\boldsymbol{\eta}_d^\theta v_s + \boldsymbol{R}^\top(\psi_s)\boldsymbol{\eta}_d^\theta v_s^t, \quad (5.25)$$

and

$$\boldsymbol{\alpha}_1^\theta = \boldsymbol{K}_p\boldsymbol{R}^\top(\psi_s)\boldsymbol{\eta}_d^\theta + \boldsymbol{R}^\top(\psi_s)\left[\boldsymbol{\eta}_d^{\theta^2} v_s + \boldsymbol{\eta}_d^\theta v_s^\theta\right] \quad (5.26)$$

Step 2: The error variable in step 2 is defined as before

$$\boldsymbol{z}_2 \equiv \boldsymbol{\nu}_s - \boldsymbol{\alpha}_1. \quad (5.27)$$

Differentiating with respect to time yields

$$\begin{aligned}\boldsymbol{M}_s\dot{\boldsymbol{z}}_2 &= \boldsymbol{M}_s\dot{\boldsymbol{\nu}}_s - \boldsymbol{M}_s\dot{\boldsymbol{\alpha}}_1 \\ &= \boldsymbol{\tau}_s - \boldsymbol{R}^\top(\psi_s)\boldsymbol{T} - \boldsymbol{D}_s\boldsymbol{\nu}_s + \boldsymbol{R}^\top(\psi_s)\boldsymbol{b}_s - \boldsymbol{M}_s\boldsymbol{\sigma}_1 - \boldsymbol{M}_s\boldsymbol{\alpha}_1^\theta\dot{\theta}.\end{aligned} \quad (5.28)$$

A new control Lyapunov function (CLF) is defined for this step, and can be expressed as

$$V_2 \equiv V_1 + \frac{1}{2}\boldsymbol{z}_2^\top\boldsymbol{M}_s\boldsymbol{z}_2. \quad (5.29)$$

This expression is then differentiated with respect to time, and is expressed as

$$\begin{aligned}\dot{V}_2 &= \dot{V}_1 + \boldsymbol{z}_2^\top\boldsymbol{M}_s\dot{\boldsymbol{z}}_2 \\ &= -\boldsymbol{z}_1^\top\boldsymbol{K}_p\boldsymbol{z}_1 + \boldsymbol{z}_1^\top\boldsymbol{z}_2 + \boldsymbol{z}_1^\top\boldsymbol{R}^\top(\psi_s)\boldsymbol{\eta}_d^\theta\omega_s \\ &\quad + \boldsymbol{z}_2^\top\left[\boldsymbol{\tau_s} - \boldsymbol{R}^\top(\psi_s)\boldsymbol{T} - \boldsymbol{D}_s\boldsymbol{\nu}_s + \boldsymbol{R}^\top(\psi_s)\boldsymbol{b}_s - \boldsymbol{M}_s\boldsymbol{\sigma}_1 - \boldsymbol{M}_s\boldsymbol{\alpha}_1^\theta\dot{\theta}\right].\end{aligned} \quad (5.30)$$

The control-force vector, $\boldsymbol{\tau}_s$, can now be chosen. The following choice is made to cancel the unwanted terms in (5.30)

$$\boldsymbol{\tau}_s = -\boldsymbol{z}_1 - \boldsymbol{K}_d\boldsymbol{z}_2 + \boldsymbol{D}_s\boldsymbol{\nu}_s + \boldsymbol{M}_s\boldsymbol{\sigma}_1 + \boldsymbol{M}_s\boldsymbol{\alpha}_1^{\theta}\dot{\theta} + \boldsymbol{R}^{\top}(\psi_s)\boldsymbol{T} - \boldsymbol{R}^{\top}(\psi_s)\boldsymbol{b}_s, \tag{5.31}$$

where $\boldsymbol{K}_d = \boldsymbol{K}_d^{\top} > 0$ is a matrix used for tuning the controller. The time derivative of the CLF now becomes

$$\dot{V}_2 = -\boldsymbol{z}_1^{\top}\boldsymbol{K}_p\boldsymbol{z}_1 - \boldsymbol{z}_2^{\top}\boldsymbol{K}_d\boldsymbol{z}_2 + \boldsymbol{z}_1^{\top}\boldsymbol{R}^{\top}(\psi_s)\boldsymbol{\eta}_d^{\theta}\omega_s. \tag{5.32}$$

Update law: An update law has to be made in order to close the loop and render the system UGS. The update law is a filtered-gradient update law based on the adaptive system used by Skjetne [2005, p 132]. It can be expressed as

$$\omega_s = \omega, \tag{5.33}$$

and

$$\dot{\omega} = -\lambda\omega - \lambda\mu\left[\boldsymbol{z}_1^{\top}\boldsymbol{R}^{\top}(\psi_s)\boldsymbol{\eta}_d^{\theta} + \boldsymbol{z}_2^{\top}\boldsymbol{M}_s\boldsymbol{\alpha}_1^{\theta}\right] \tag{5.34}$$

Tension control

The tension on the tow rope has to be controlled in order to prevent rupture of the towline, and to prevent undesired iceberg behavior. A typical bollard pull is in the order of 180 tonnes (1765.8 kN) for an AHTS. Moreover, maximum tow force during towing is in the order of 90 tonnes (882.9 kN) [John McClintock and Brown, 2002, p 49].

A proposed way to control the tension is to change the desired velocity, U_d, in (5.13).

$$\begin{aligned} U_d(t) =& K_{scale}\Bigg(K_p\left(T(t) - T_d(t)\right) + K_i\left(\int_0^t \left(T\left(\tau\right) - T_d(\tau)\right)\, d\tau\right) \\ &+ K_d\left(\dot{T}(t) - \dot{T}_d(t)\right)\Bigg) \end{aligned} \tag{5.35}$$

where K_p, K_i, and K_d are gains that tune the behavior of the controller. K_{scale} is a scaling factor between the force and velocity. This assumes there is a known mapping between the tension and the vessel velocity. It also assumes the tension is a function of the vessel velocity. This is assumed true for towing in a straight line in open water.

Choice of path

According to John McClintock and Brown [2002, p 46] the iceberg is very hard to control if the towing path is curved. The following quotes are taken from ship logs, and were found in the mentioned tech report:

> *Some icebergs were drifting on opposite courses to the desired heading. First the captain would try to stop it and then to turn it. Often it appeared the iceberg wanted to tow them. Slowly they could deflect it into the desired course. A key aspect was to keep the tow line as straight as possible: if the towline went over the sides of the vessel there would be a direct loss of towing power. One was not able to turn the iceberg by just turning the vessel. The vessel captains had to keep things straight and slowly force it to another direction. Turning was the hardest thing to do, and sometimes as they turned, the iceberg slowed often just starting to roll and the line came free and they would need to re-deploy. Similarly if the tow speed was slowed, the iceberg might also roll.*

and also

> *The main objective, once under tow was to try to get the iceberg to make some good speed ahead in that direction and take it from there, and as noted the key was to keep the towing in a straight line thereby making it easier to control.*

From reading these quotes, it is evident that the path has to be a straight line. Straight paths can be modeled in several different ways, depending on start and end location. The simplest straight path is a northward or southward path that can be described by

$$\boldsymbol{\eta}_d = \begin{bmatrix} \theta \\ 0 \\ 0 \end{bmatrix}, \tag{5.36}$$

while a generic formula for a straight path can be described by

$$\boldsymbol{\eta}_d = \begin{bmatrix} a_1\theta + b_1 \\ a_2\theta + b_2 \\ \psi_d \end{bmatrix}, \tag{5.37}$$

where a_1, b_1, a_2, and b_2 are constant coefficients that describe the path [Skjetne, 2005, p 3].

5.3 Observer design

An observer is needed to estimate the states in the state-space formulation. This is either done because one or more states are unmeasurable, too expensive to measure or too polluted by noise be used. A wide variety of observers have been used in the marine environment before. These include Extended Kalman Filters (EKFs), Luenberg observers and nonlinear passive observers.

The Extended Kalman Filter is arguably the most used observer for marine vessels. However, it has heavy computational requirements, and is difficult to tune [Fossen, 2011]. This thesis will therefore use the nonlinear passive observer for estimating states.

5.3.1 Nonlinear passive observer for position, velocity and bias estimation

The nonlinear passive observer is motivated from passivity arguments [Fossen and Strand, 1999]. This observer is able to estimate position, velocity and bias. The observer also includes a wave filter.

Additionally, the observer is proven Globally Exponentially Stable (GES), with the conditions stated in Fossen [2011, p 317]. GES is proven through passivation design.

The following vessel model is used to create the observer:

$$\begin{aligned}
\dot{\boldsymbol{\xi}}_s &= \boldsymbol{A}_{s,w}\boldsymbol{\xi}_s \\
\dot{\boldsymbol{\eta}}_s &= \boldsymbol{R}(\psi_s)\boldsymbol{\nu}_s \\
\dot{\boldsymbol{b}}_s &= -\boldsymbol{T}_{s,b}^{-1}\boldsymbol{b}_s \\
\boldsymbol{M}_s\dot{\boldsymbol{\nu}}_s &= -\boldsymbol{D}_s + \boldsymbol{R}^\top(\psi_s)\boldsymbol{b}_s + \boldsymbol{\tau}_s + \boldsymbol{R}^\top(\psi_s)\boldsymbol{T} \\
\boldsymbol{y}_s &= \boldsymbol{\eta}_s + \boldsymbol{C}_{s,w}\boldsymbol{\xi}_s
\end{aligned} \tag{5.38}$$

The observer is made by copying (5.38)

$$
\begin{aligned}
\dot{\hat{\boldsymbol{\xi}}}_s &= \boldsymbol{A}_{s,w}\boldsymbol{\xi}_s + \boldsymbol{K}_{s,1}(\boldsymbol{\omega}_{s,0})\tilde{\boldsymbol{y}}_s \\
\dot{\hat{\boldsymbol{\eta}}}_s &= \boldsymbol{R}(\psi_s)\boldsymbol{\nu}_s + \boldsymbol{K}_{s,2}\tilde{\boldsymbol{y}}_s \\
\dot{\hat{\boldsymbol{b}}}_s &= -\boldsymbol{T}_{s,b}^{-1}\boldsymbol{b}_s + \boldsymbol{K}_{s,3}\tilde{\boldsymbol{y}}_s \\
\boldsymbol{M}_s\dot{\boldsymbol{\nu}}_s &= -\boldsymbol{D}_s + \boldsymbol{R}^\top(\psi_s)\boldsymbol{b}_s + \boldsymbol{\tau}_s + \boldsymbol{R}^\top(\psi_s)\boldsymbol{T} + \boldsymbol{R}^\top(\psi_s)\boldsymbol{K}_{s,4}\tilde{\boldsymbol{y}}_s \\
\boldsymbol{y}_s &= \boldsymbol{\eta}_s + \boldsymbol{C}_{s,w}\boldsymbol{\xi}_s
\end{aligned}
\tag{5.39}
$$

where $\tilde{\boldsymbol{y}}_s = \boldsymbol{y}_s - \hat{\boldsymbol{y}}_s$ is the estimation error. The matrices $\boldsymbol{K}_{s,1} \in \mathbb{R}^{6x3}$ and $\boldsymbol{K}_{s,2;s,3;s,4} \in \mathbb{R}^{3x3}$ are tuning matrices for the observer [Fossen, 2011, p 313]. The hat above the variable implies it is a estimated value. This observer is for the vessel. The observer for the iceberg is made by copying the iceberg model, and then adding the gain parts, similar to 5.39.

5.3.2 Tension observer

An anchor-handling tug supply (AHTS) or similar vessel is required to tow an iceberg. These vessels are equipped with one or more winches, and a readout screen that displays the tension on the tow rope. The tension is therefore available for use by the controller. In the event that the vessel is not equipped with a tension reader, an observer has to be used in order to estimate the tension.

The observer model can be developed by doing a static analysis of a cable segment. First, the following assumptions are made [Sørensen, 2011, p 209]:

- When working with cables we can ignore bending stiffness and torsional stiffness; only the axial stiffness has to be considered.
- Due to small tension compared to material properties, the stress/strain relationship is considered linear.
- The cable is made of an isotropic material: the material properties are independent of direction.

- The cross-sectional area of the cable will not change significantly due to axial deformation.

The cable will be acted upon by the following forces:

- axial forces
- cable self-weight, which causes the cable to act as a catenary
- hydrodynamic drag forces from the water

Two different models can then be made for estimation of tension: a simple model taking only axial and drag forces into consideration, and a more advanced model using catenary equations and drag forces.

Simple model:

This model only takes the axial forces and drag forces into account. The axial stress in the cable can be described by the generalized Hooke's law. In scalar form this can be expressed by

$$\sigma = E\epsilon = \frac{T}{A}, \tag{5.40}$$

where σ is the stress in the cable, E is Young's modulus for the material, ϵ is the strain, A is the cross-sectional area, and T is the tension in the cable. With the assumption that the cross-sectional area of the cable is constant, the axial force in the cable can be considered a constant multiplied with the strain. Moreover, the strain can be considered a function of the cable length, and can be expressed as

$$\epsilon = \epsilon(l, L) = \epsilon(\boldsymbol{\eta}_s, \boldsymbol{\eta}_i, L) \tag{5.41}$$

where l is the current cable length and L is the initial cable length. The current length of the cable depend on the position of the ship, $\boldsymbol{\eta}_s$, and iceberg, $\boldsymbol{\eta}_i$.

On vectorial form this can be written as

$$\boldsymbol{T}_{af} = \begin{bmatrix} X_{af} \\ Y_{af} \\ N_{af} \end{bmatrix} = \boldsymbol{k}_{af} \cdot \epsilon(\boldsymbol{\eta}_s, \boldsymbol{\eta}_i, L) = \begin{bmatrix} k_X & 0 & 0 \\ 0 & k_Y & 0 \\ 0 & 0 & k_N \end{bmatrix} \epsilon(\boldsymbol{\eta}_s, \boldsymbol{\eta}_i, L) \tag{5.42}$$

where $\boldsymbol{k}_{af}$ is a matrix that represents the spring constant (EA) of the cable. In most cases the $\boldsymbol{k}_{af}$ matrix has to be tuned in order to get a decent result.

Discrete behavior of the towline

While the former section describe the towline under tension, the towline model will also have some discrete behavior that have to be modeled by the tension observer. These are:

- When the total distance between the iceberg and the vessel is smaller than the length of the towrope, the towline is considered to have no tension. This is true if the self-weight of the cable is neglected.
- Rupture will occur when the tension in the towline exceeds the yield point of the material it is made of (either in the synthetic rope or the hawser). The rupture will cause the towline to break and the iceberg will no longer be connected to the vessel. Without the rupture mechanism implemented in the tension observer, the estimated tension will increase as long as the vessel is moving forward, if the towline is ruptured.
- If the total distance between vessel and iceberg is larger than the unstretched towline, and the towline has not ruptured, the tension calculations in (5.42) applies.

Figure 5.1 shows how the discrete behavior of the tension observer.

The simple model is finalized when the drag forces, described in 5.3.2, are included. These forces can also be neglected, as they are small compared to the tension forces.

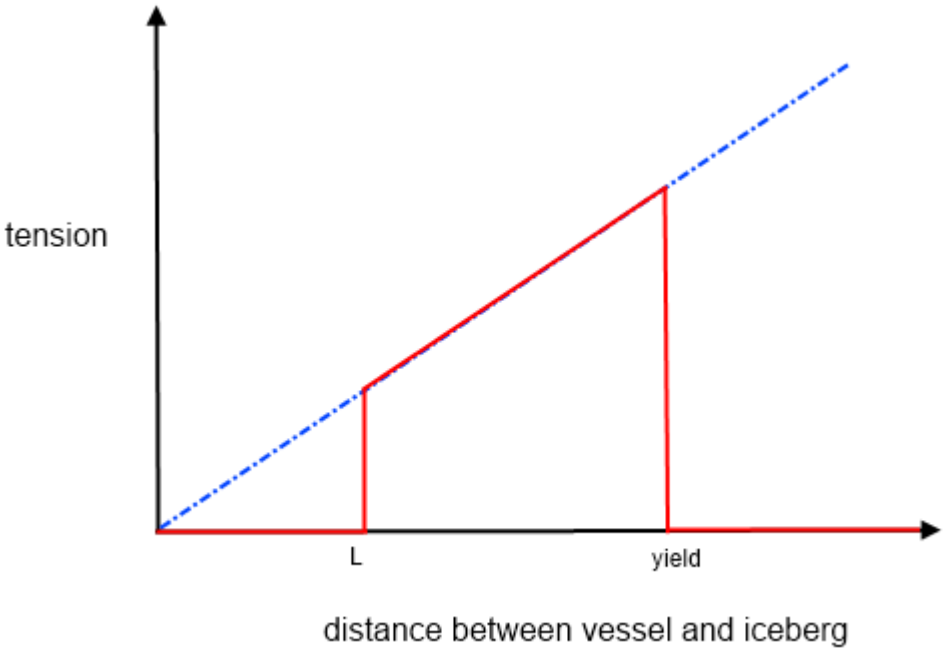

Figure 5.1: Figure of the behavior of the tension observer.

Advanced model:

A more advanced model that captures more of the dynamics in the tow line can be made by using catenary equations. This takes gravity into account, and due to the weight of the cable the curve will look like a catenary. There are several different methods on how to model the effects of the catenary: the finite element method (FEM), catenary equations, and lump-mass-spring formulations (LMS) [Wennersberg, 2009].

The simplest way of finding a catenary model is to use static catenary equations. If the solution of the static catenary equations are converted to polynomials, the result is a quasi-static [Wennersberg, 2009, p 17]. However, that won't be treated in this thesis. Catenary equations can be solved in either two or three dimensions, but only

two dimensions will be treated here. The following formulations of the catenary equations are taken from Sørensen [2011], Wennersberg [2009], and Irvine and Sinclair [1975].

When formulating the problem, we have to look at the geometry of cable, which can be seen in Figure 5.2. The cable length is L, and the cable is attached in $O(0,0)$ and $Q(l,h)$. A Langrangian approach is used to derive the catenary equations. The coordinate s is then used to describe the unstretched Langrangian coordinate, while p represents the stretched Langrangian coordinate. This coordinate system starts in O for both s and p.

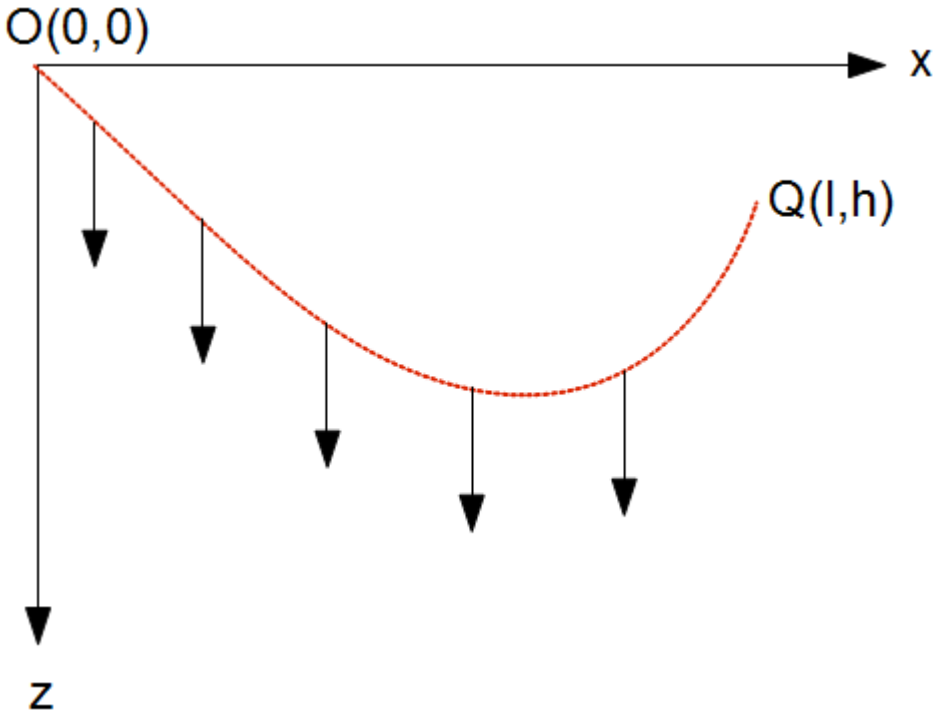

Figure 5.2: General cable configuration.

If one consider a small cable element, i.e. the element illustrated in Figure 5.3, the element will be subjected to three forces: buoyancy

B, self weight W, and tension from adjacent elements T. Buoyancy and self weight will act in the vertical direction, while the tension will act tangentially to the cable element. The buoyancy per unit length can be expressed as

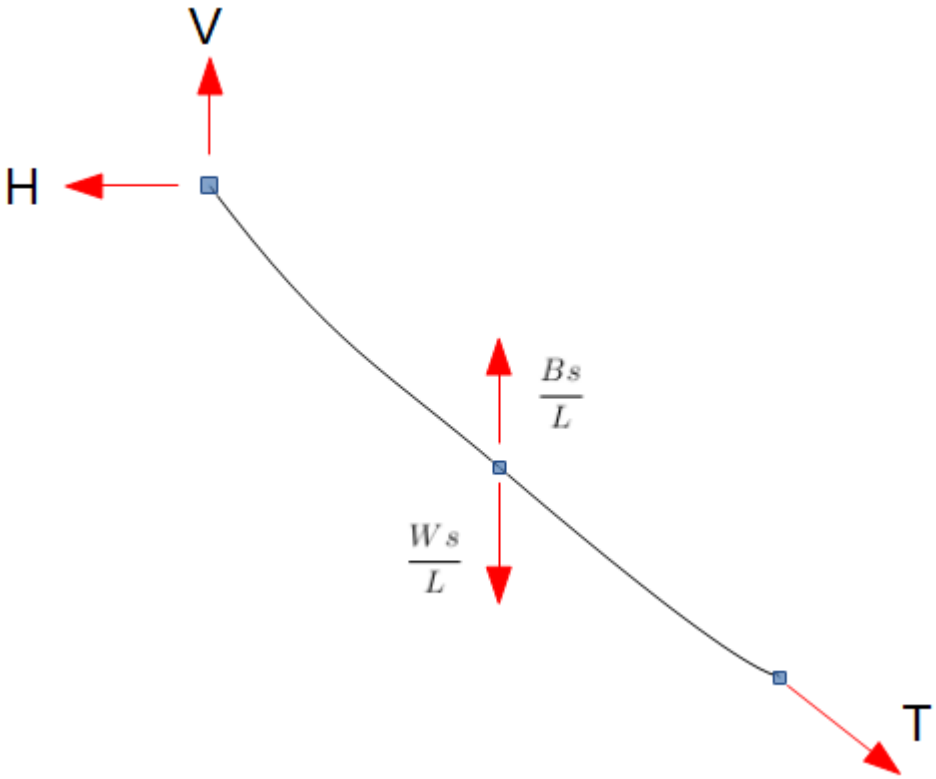

Figure 5.3: Figure of a cable segment with forces acting on it.

$$B = \rho_w g A, \tag{5.43}$$

where ρ_w is the density of water, g the acceleration of gravity, and A is the cross-sectional area of the cable. The weight of the cable is W, while the effective weight is defined as

$$W_e = W - B. \tag{5.44}$$

Finding the catenary equation is then done by balancing the horizontal and vertical forces in the cable segment. The equilibrium in the horizontal direction can be written as

$$T\frac{dx}{dp} = H, \tag{5.45}$$

while the equilibrium equation in the vertical direction is

$$T\frac{dz}{dp} = V - W\frac{s}{L}, \tag{5.46}$$

where T is the tension, H is the horizontal end point force, and V is the vertical end point force. For this cable segment, the generalized Hooke's law can be written as

$$T = EA\left(\frac{dp}{ds} - 1\right), \tag{5.47}$$

where E is Young's modulus (constant). The geometric constraint can be expressed as

$$\left(\frac{dx}{dp}\right)^2 + \left(\frac{dz}{dp}\right)^2 = 1. \tag{5.48}$$

If (5.45) and (5.46) is inserted into (5.48), the cable tension can be written as

$$T(s) = \left\{H^2 + \left(V - W\frac{s}{L}\right)^2\right\}^{1/2}, \tag{5.49}$$

which is a function of the Lagrangian variable s. The functions $x(s)$ and $z(s)$ are found as follows:

$$\frac{dx}{ds} = \frac{dx}{dp}\frac{dp}{ds} = \frac{H}{EA} + \frac{H}{[H^2 + (V - Ws/L)^2]^{1/2}} \tag{5.50}$$

$$\frac{dz}{ds} = \frac{dz}{dp}\frac{dp}{ds} = \frac{1}{EA}\left(V - \frac{Ws}{L}\right) + \frac{V - Ws/L}{[H^2 + (V - Ws/L)^2]^{1/2}}. \tag{5.51}$$

The following boundary conditions are used when integrating:

$$x = 0, \qquad z = 0, \qquad p = 0 \qquad \text{at} \qquad s = 0 \tag{5.52}$$

$$x = l, \qquad z = h, \qquad p = L_s \qquad \text{at} \qquad s = L \tag{5.53}$$

By integrating (5.50) from $s = 0$ to s gives the following solution for $x(s)$:

$$x(s) = \frac{Hs}{EA} + \frac{HL}{W}\left[\operatorname{asinh}\left(\frac{V}{H}\right) - \operatorname{asinh}\left(\frac{V - Ws/L}{H}\right)\right]. \tag{5.54}$$

Integrating (5.51) from $s = 0$ to s yields the following solution for $z(s)$:

$$z(s) = \frac{Ws}{EA}\left(\frac{V}{W} - \frac{s}{2L}\right) + \frac{HL}{W}\left[\left\{1 + \left(\frac{V}{H}\right)^2\right\}^{1/2} - \left\{1 + \left(\frac{V - Ws/L}{H}\right)^2\right\}^{1/2}\right]. \tag{5.55}$$

By applying the boundary condition (5.53), a solution of H and V becomes

$$l = \frac{HL}{EA} + \frac{HL}{W}\left[\operatorname{asinh}\left(\frac{V}{H}\right) - \operatorname{asinh}\left(\frac{V - W}{H}\right)\right], \tag{5.56}$$

and

$$h = \frac{WL}{EA}\left(\frac{V}{W} - \frac{1}{2}\right) + \frac{HL}{W}\left[\left\{1 + \left(\frac{V}{H}\right)^2\right\}^{1/2} - \left\{1 + \left(\frac{V-W}{H}\right)^2\right\}^{1/2}\right]. \tag{5.57}$$

This is a set of equations that have to be solved together in order to find H and V. The catenary equation can be reduced further by assuming that both ends of the cable are attached at the same horizontal level. This is not completely true for iceberg towing, as the cable is connected at the below the surface level for the iceberg, and slightly above surface level for the vessel. However, this distance is very small compared to the cable sag, and the connection points will therefore be treated as if they were on the same level.

This makes the cable configuration symmetric about an imaginary vertical axis (the z axis in Figure 5.4), and the new coordinate system is placed there. The new origin coincides with the lowest point on the cable.

The equations (5.56) and (5.57) are now solved with $h = 0$. The equations are therefore reduced to

$$\sinh\left(\frac{Wl}{2HL} - \frac{W}{2EA}\right) = \frac{W}{2H}, \tag{5.58}$$

and

$$V = \frac{W}{2}. \tag{5.59}$$

(5.58) can be solved numerically, using software such as Matlab. In Matlab this equation is solved using the *solve()* function. This is much more computationally heavy than the simple model, because the equation has to be solved for every time step, whereas the simple model is just a linear expression.

Another problem with this model is the fact that the tow line consists of two different segments: the synthetic tow rope and the steel hawser, as seen in Figure 1.3. (5.58) is mainly a expression to

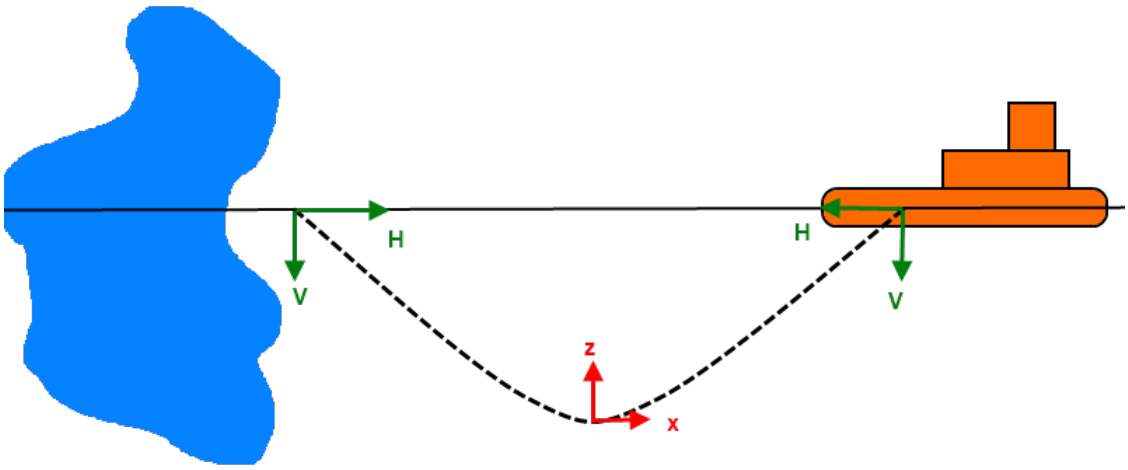

Figure 5.4: Figure of a the cable connected to ship and iceberg.

be used with a single material. However, if one assume the hawser is much longer and lighter than the synthetic tow rope, the synthetic tow rope can be neglected and the cable can be considered equal to the hawser. (5.58) and (5.59) can also be modified to be used with two different towline segments, but this thesis will not go further into that topic.

It should be noted that only the horizontal forces are important for the controller, as the controller only controls the vessel in the horizontal plane.

Hydrodynamic drag forces:

According to Sørensen [2011, p 222], hydrodynamic drag forces on mooring lines are usually modeled with the cross-flow principle. This implies that the flow separates due to the cross-flow past the cable. An infinitesimal cable element with length dp, described by Figure 5.5, is acted upon by a current. The current does not have to be a literal current. When the vessel moves through the water, the cable will have a velocity relative to the water that produces the same effect as an actual current.

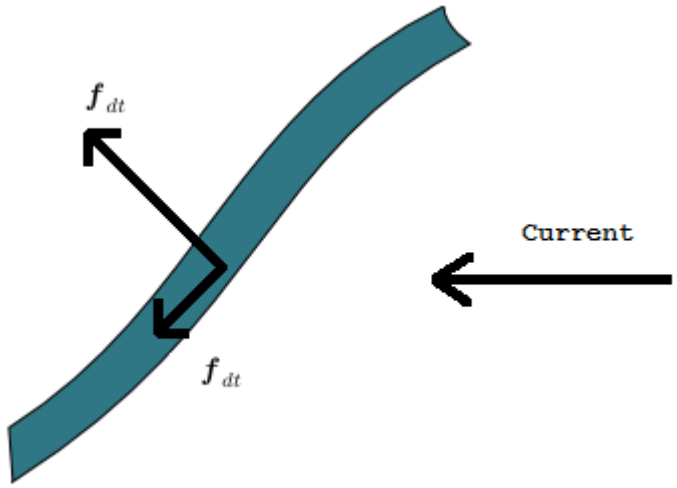

Figure 5.5: Figure of a cable element in current.

The drag forces from the water can then be modeled by Morison's equation. Morison's equation is expressed as

$$d\boldsymbol{f}_{dt} = -\frac{1}{2} C_{DT} \rho_w d \cdot dp |\boldsymbol{v}_t| \boldsymbol{v}_t \tag{5.60}$$

in the tangential direction, and

$$d\boldsymbol{f}_{dn} = -\frac{1}{2} C_{DN} \rho_w d \cdot dp |\boldsymbol{v}_n| \boldsymbol{v}_n \tag{5.61}$$

in the normal direction of the cable. C_{DT} and C_{DN} are the tangential and normal drag coefficients. ρ_w is the density of water, while d is the diameter of the cable. $\boldsymbol{v}_t$ and $\boldsymbol{v}_n$ are the tangential velocity and normal velocity of the current, on component form. The length of the cable segment is dp [Sørensen, 2011]. Integrating (5.60) and (5.61) along the entire cable length gives the total drag force acting on the cable.

The drag on the towline is assumed very small compared to the axial forces. They are therefore neglected in further on.

Chapter 6

Simulation

The model was tested and verified in a simulated environment. This chapter describes the setup and results of these simulations.

6.1 Setup

The simulations were run in Matlab 2009b/2012b and Simulink [MathWorks, 2012]. For simplicity the MSS toolbox [MSS, 2010] was used in several parts of the model. This includes the rotation matrix blocks, and the models for the vessel and iceberg (later modified, however). The old Simulink models made in the master thesis of Skåtun [2011], and later modified by Nam Dinh Tran, were used as template. The Simulink diagrams themselves are illustrated in Appendix B.

Simulink is also able to interact with LabView using the Simulation Interface Toolkit. The user interface shown in Figure A.1 can then be used to control the vessel. However, the controllers, observers, vessel models and so on are still implemented in Simulink.

A problem with the simulation was that the tension measurements were lacking, due to the fact that both the vessel and iceberg were simulated. The tension observer was therefore used instead. Tuning a tension observer in such a way that the estimated values are sensible, is a huge task. Whether the estimated values are anywhere close to

the real values is difficult to say. However, the qualitative dynamics should still be caught by the observer.

6.2 Result

The first goal was to get the vessel to follow the desired path, which was set to $\boldsymbol{\eta}_d = [\theta + 10, \theta + 10, 0]^\top$ in all the simulations. The vessel and iceberg starts in the origin, to see if the vessel is tracking or not.

The ability to follow the path in a smooth manner was largely influenced by the tuning parameters for the update law, as can be seen in the figures 6.1a, 6.1b, 6.2a and 6.2b. The two tuning parameters are μ and λ, as can be seen in (5.34). The vessel has no problem following the path, as long as the tuning parameters are set somewhat correctly. The best results were found when these values were very small, as in Figure 6.1a. When either μ or λ were increased, the path of the ship would get sudden deviations along the path, as seen in the figures 6.1b, 6.2a, and 6.2b. From the figures 6.3b, 6.4a, and 6.4b one can also see a sudden jump in the heading, ψ, when either μ or λ is increased.

Further on one can look at the velocity, $\boldsymbol{\nu}_s$, and the desired velocity function, v_s. Figure 6.5a shows the desired velocity function. This is dependent on the tension controller and will have a transient behavior while the tension in the cable is zero (assuming the simple tension estimation method is used). It then slowly falls until it reaches a constant value. Figure 6.5b shows similar transient behavior for all the elements of $\boldsymbol{\nu}_s$. Because the vessel is only moving in the surge direction after a while, the velocity in surge, u, will settle at a constant value after a certain time. The other elements will be zero, or have a rather small value, depending on current strength.

Figure 6.6 is a plot of the U_d, which is set by the tension controller. The speed is initially rising until the towline has tension, and then decrease until it reaches a constant velocity.

The a plot of the towline forces can be seen in Figure 6.7. The

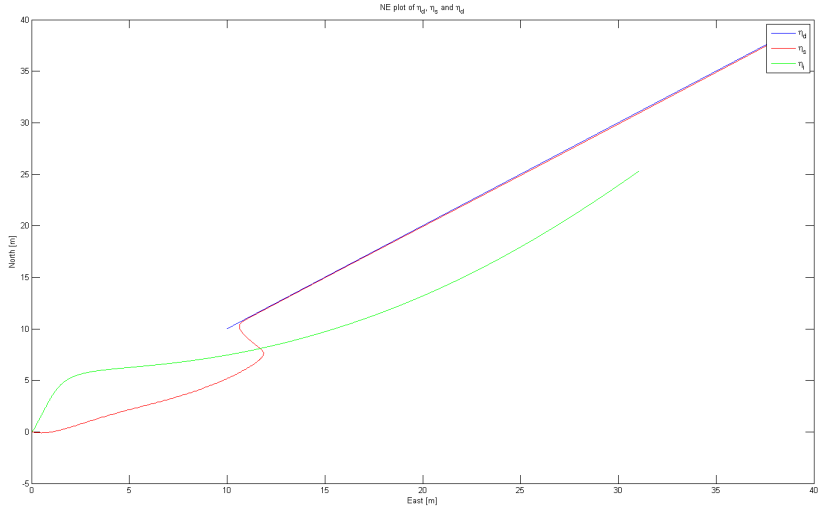

(a) $\mu = 0.0000000000001$, $\lambda = 0.001$

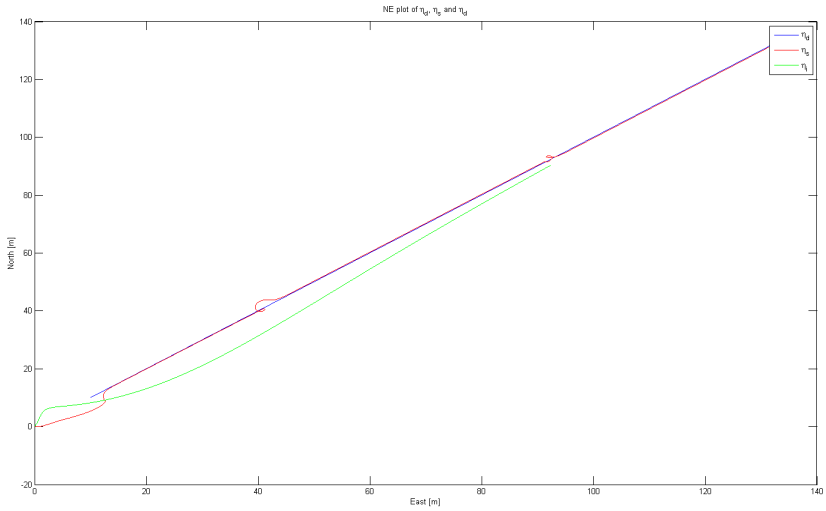

(b) $\mu = 0.0000000001$, $\lambda = 0.01$

Figure 6.1: Figure of North-East plots

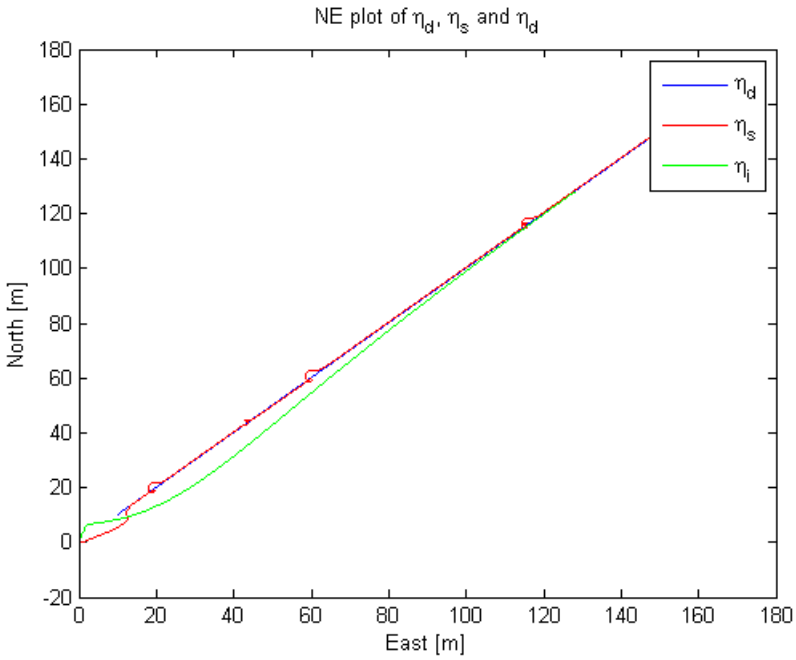

(a) $\mu = 0.0000000001$, $\lambda = 0.1$

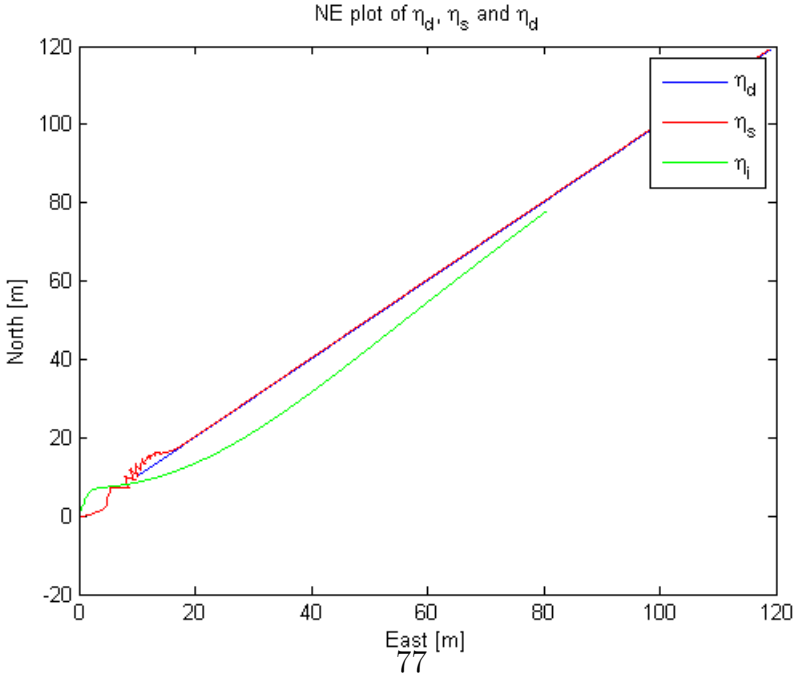

(b) $\mu = 0.01$, $\lambda = 0.001$

Figure 6.2: Figure of North-East plots

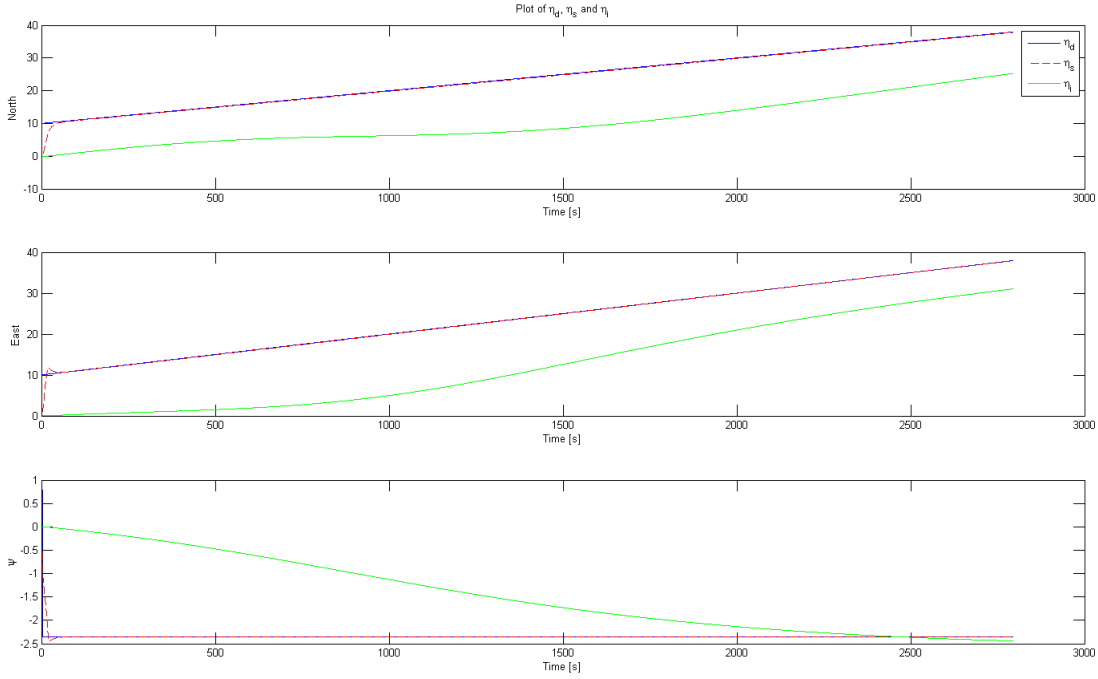

(a) $\mu = 0.0000000000001$, $\lambda = 0.001$

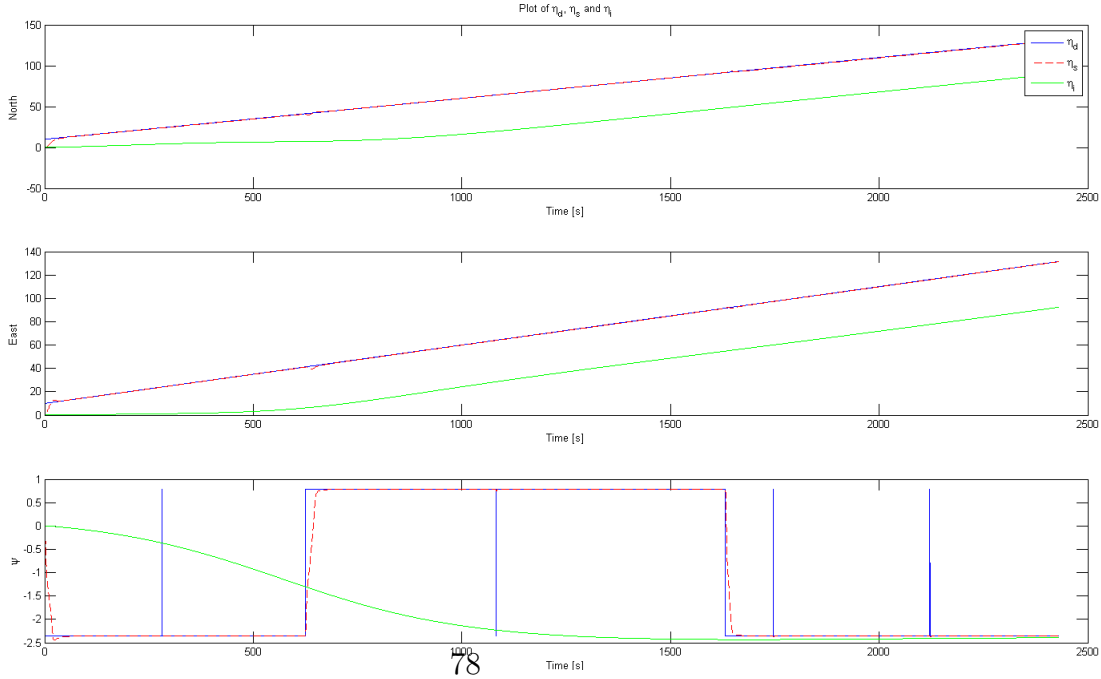

(b) $\mu = 0.0000000001$, $\lambda = 0.01$

Figure 6.3: Figure of a subplot with η_d, η_s, and η_i

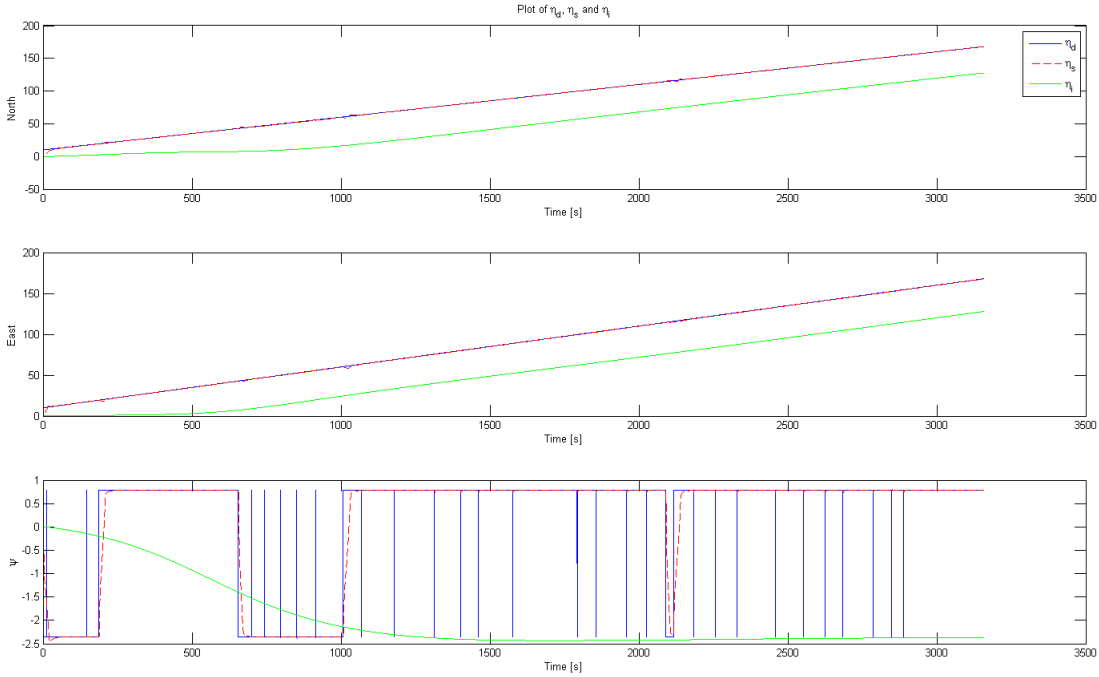

(a) $\mu = 0.0000000001$, $\lambda = 0.1$

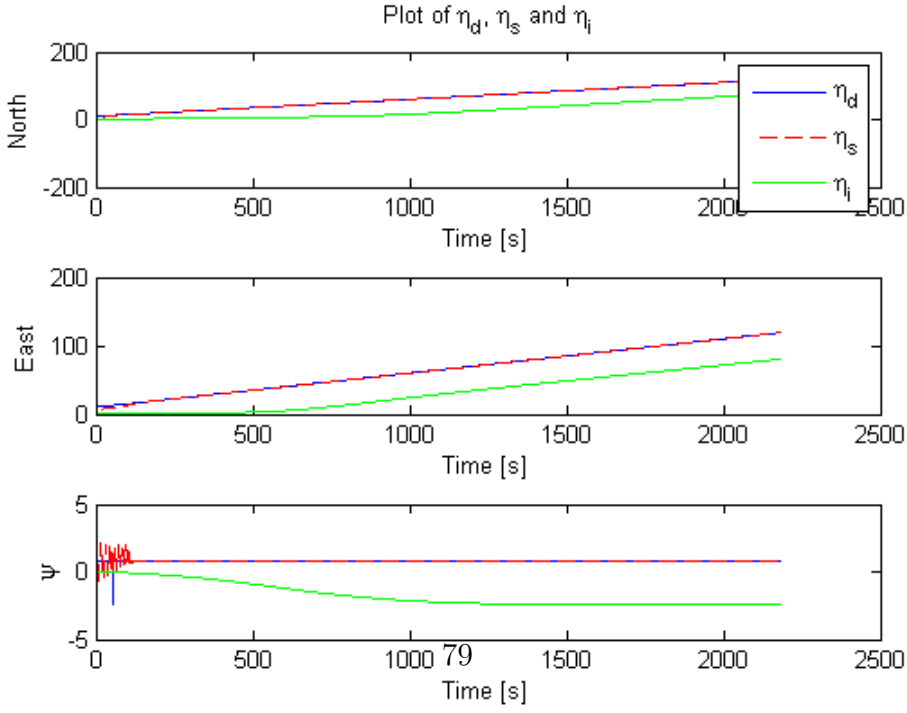

(b) $\mu = 0.01$, $\lambda = 0.001$

Figure 6.4: Figure of a subplot with η_d, η_s, and η_i

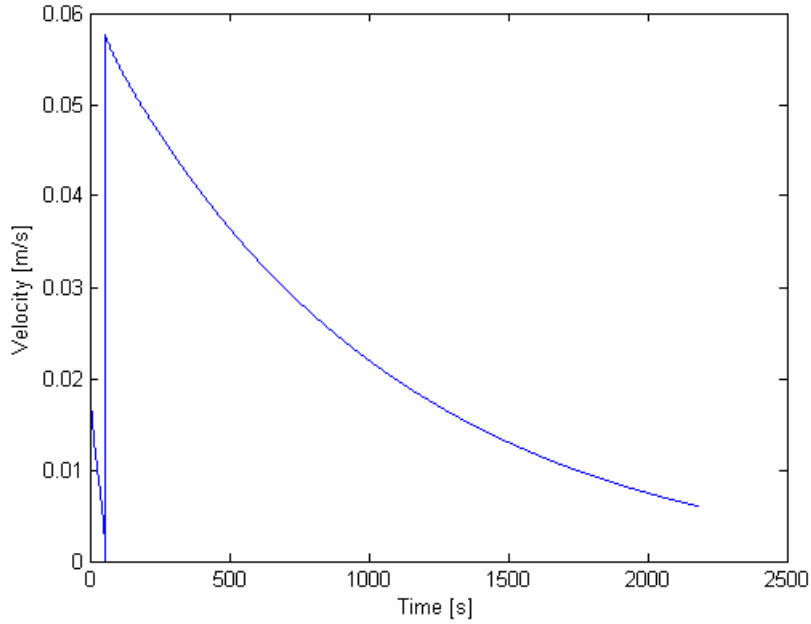

(a) The desired velocity function

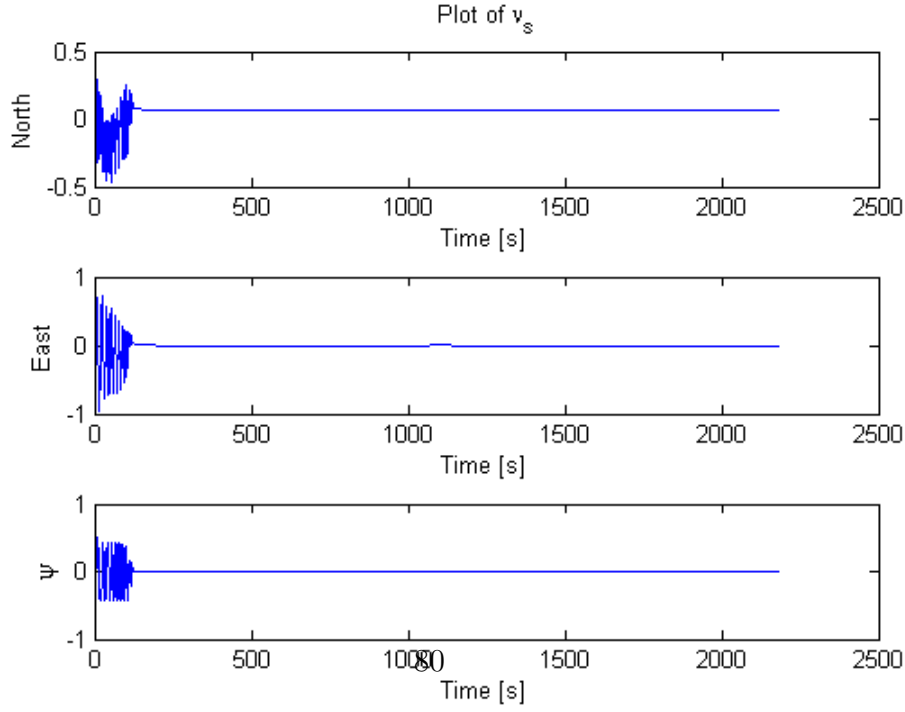

(b) The velocity vector, $\boldsymbol{\nu}_s$

Figure 6.5: Figure of a v_s and ν_s plot

same effect as in velocity can be observed: the towline increases until the towline has tension. It then stays somewhat constant. N_{tow} is set equal to zero, because it is assumed the towline is unable to create a moment about the z axis on the iceberg.

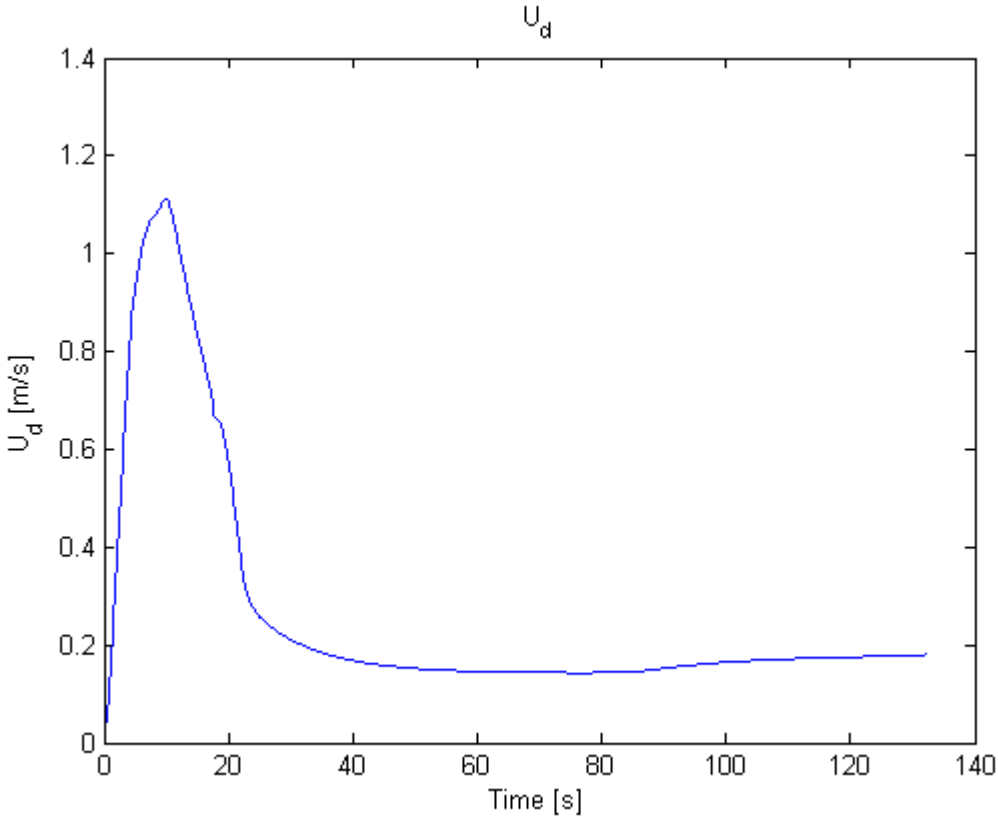

Figure 6.6: Plot of U_d.

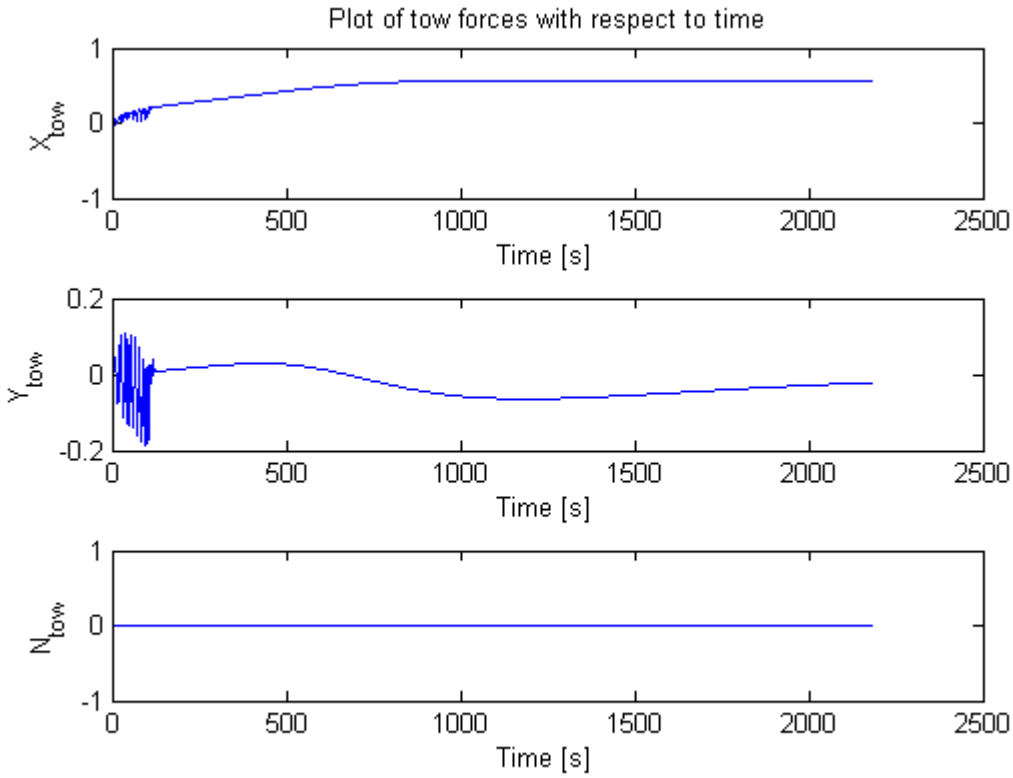

Figure 6.7: Plot of the towline forces, T.

Chapter 7

Model-tank experiments

One of the goals of the thesis was to implement and test the proposed guidance and control system in the *MC Lab*, using the model ship *CS Enterprise I*. The model ship was going to tow an emulated iceberg, preferably in wind/current. This chapter describes the process and results of the towing tank experiments.

7.1 Towing tank

The experiment was performed in the Marine Cybernetics Laboratory (MC Lab) at NTNU [MC Lab, 2012]. This is a small tank formerly used for storing model vessels. The tank is rectangular and its dimensions are $L \cdot B \cdot D = 40\ m \cdot 6.45\ m \cdot 1.5\ m$. It is equipped with a carriage and a positioning system that can measure 6 degrees-of-freedom in real-time. The carriage itself can move in 5 degrees-of-freedom.

The laboratory is capable of making regular waves with a height up to $H < 0.25\ m$ and with a wave period between $T = 0.3 - 3\ s$. It can make irregular waves with a significant wave height up to $H_s < 0.15\ m$ and a wave period between $T = 0.6 - 1.5\ m$. The laboratory is unfortunately incapable of generating current or wind, but plans for installing current and wind generators exist [Skåtun, 2011].

Typical scaling ratios vary between $\lambda = 50 - 150$ [MC Lab, 2012].

7.2 Model vessel

The model vessel used in this experiment is *CS Enterprise I*, which has a scale of 1:50. The hull is based on the anchor-handling tug *Aziz* [Model Slipway, 2012], and is depicted in Figure 7.1.

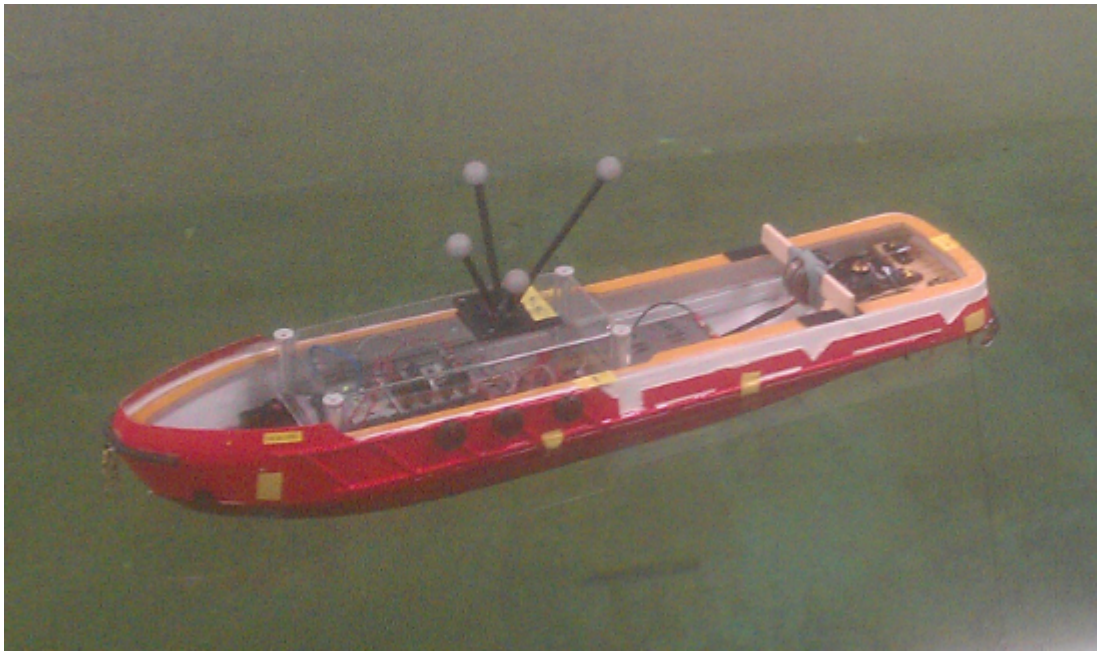

Figure 7.1: Figure of the model vessel.

The vessel is equipped with two Voith-Schneider propeller units (VSPs) that can generate thrust in three degrees-of-freedom (x, y, and ψ). The VSP combines both steering and propulsion in one unit. The magnitude is determined by rotational speed and direction of thrust is determined by blade angle [Voith, 2012].

7.2.1 Dimensions

The length of *CS Enterprise I* is $L_s = 1.105\ m$, while the beam is $B_s = 0.248\ m$ [Model Slipway, 2012].

As described in 3.1.1, using system identification methods, Skåtun [2011] tried to find sensible values for damping and added mass for *CS Enterprise I*. Unfortunately this didn't work and values from another, similar, model vessel have to be used instead. The substitute values chosen are from the model vessel *Cybership II*, which was system identified by Skjetne [2005]. The mass matrix can then be expressed as

$$\boldsymbol{M}_s = \begin{bmatrix} 25.8 & 0 & 0 \\ 0 & 33.8 & 1.0115 \\ 0 & 1.0115 & 2.76 \end{bmatrix}, \tag{7.1}$$

while the damping can be expressed by

$$\boldsymbol{D}_s = \begin{bmatrix} 2 & 0 & 0 \\ 0 & 7 & 0.1 \\ 0 & 0.1 & 0.5 \end{bmatrix}. \tag{7.2}$$

More proper values are to be found by Nam Dinh Tran, in his thesis. However, these values were not available during the experiment.

7.2.2 Measurement of position and tension

The MC Lab uses software and hardware from Qualisys [2012]. This includes Oqus cameras and the Qualisys Track Manager (QTM). The Oqus cameras are high-speed cameras that uses infrared (IR) sensors to track various IR markers places on the model vessel and model iceberg. This can be seen in the figures 7.1 and 7.2. Both the model vessel and the iceberg are equipped with four IR markers, while the towing carriage is equipped with three Oqus cameras [Skåtun, 2011].

QTM is a software that handles motion capture from the cameras and can calculate in 3D and 6 degrees-of-freedom. QTM is responsible for calculating the position and orientation of the vessel [Skåtun,

2011]. The control of the vessel itself happens on a dedicated computer running the LabView software package. The LabView implementation running on the MC Lab computer has an add-on called *Simulation Interface Toolkit (SIT)*, that creates an interface between Matlab/Simulink and LabView. That makes it possible to control the vessel using Simulink models.

There were great expectations about the tension measurement system in the lab before the experiment was done. Measurement of tension in the tow rope is important in a control system for iceberg maneuvering. Unfortunately, the MC Lab only supports offline measurements of tension. This is done with a force measurement ring that is placed between the vessel and tow rope. An electrical wire is connected between the force measurement ring and a PC. Due to the fact that the measurements happens offline, they can't be used in the control system. The wire also limits the vessel from moving more than a couple of meters in the tank.

Because of these limitations, the force measurement rings were not used in the experiments. The tension observer, described in 5.3.2, was used instead. This places severe limits on the implementation, due to the fact that the observer is very difficult to tune.

7.3 Creation of an emulated iceberg

The model vessel has a scale of 1:50. An optimal iceberg should therefore be in the same scale, which means it should have a mass between 4 kg and $40,000$ kg. Anything above 100 kg is too unpractical to handle in the towing tank, and therefore the iceberg will be very small compared to an actual iceberg, even in model scale.

An ideal model iceberg should also be made of ice and have the same hydrodynamic properties as a real iceberg. Because this thesis is concerned with the control of icebergs, not simulation, the model iceberg will instead be very simple. The emulated iceberg's task is to create a certain amount of inertia and drag on the system.

A mason bucket was therefore chosen to emulate the iceberg. The mason bucket has a volume of 100 liters, a radius of $r_{i,b} = 0.255\ m$ at the bottom, and a height of $h_i = 0.43\ m$. It has a fairly circular cross-section and will be considered a circular cylinder for the rest of this thesis.

Figure 7.2 shows a picture of the emulated iceberg floating in the water of the towing tank. The four poles are reflectors that are used to find the position and velocity of the iceberg during the testing.

Figure 7.2: Figure of the emulated iceberg.

Metal weights are inserted into the bucket to make it heavier. These weights are distributed evenly along the bottom to make weight distribution somewhat symmetric, and to make the bucket float straight

in the water. It was also tried using water as weight, but due to the large effect of free surface, this idea was soon abandoned.

7.3.1 Dimensions

The dimensions of the emulated iceberg can be seen in Figure 7.3.

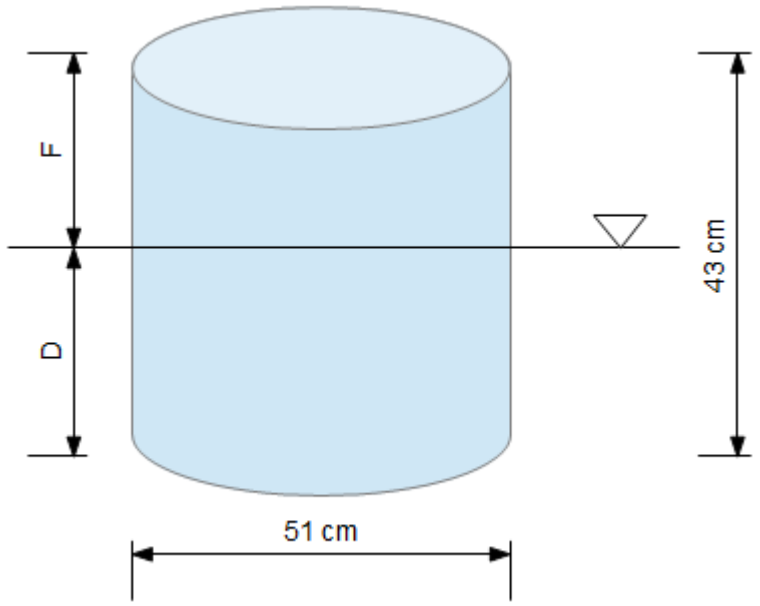

Figure 7.3: Figure of the dimensions of the mason bucket.

The rigid-body mass matrix can be written as

$$\boldsymbol{M}_{RB,i} = \begin{bmatrix} m & 0 & 0 \\ 0 & m & mx_g \\ 0 & mx_g & I_z \end{bmatrix} \tag{7.3}$$

where m is the mass, I_z is the moment of inertia about the z axis, and x_g is the distance from center-of-origin (CO) to center-of-gravity (CG) in the x direction. According to Archimedes' principle, the mass of a floating body can be expressed as

$$m = \rho_w \nabla \tag{7.4}$$

where ρ_w is the density of water and ∇ is the volume of the water the mason bucket displaces. That is the same as the volume of the mason bucket under water. This volume can be expressed as

$$\begin{aligned} \nabla = \pi r^2 D = \pi r^2 (0,43\ m - F) = 1000\ kg/m^3 \cdot \pi\ (0.255\ m)^2 (0.43\ m - F) \\ = 204.28\ kg/m \cdot (0.43\ m - F) \end{aligned} \tag{7.5}$$

where r is the radius, and F is the freeboard of the mason bucket. If the origin is placed in the center of the bucket, and the bucket is symmetric along the xz and xy plane, $mx_g = 0$, because $x_g = 0$.

I_z can be found with the following relation for moment of inertia for a thin-walled circular cylinder:

$$\begin{aligned} I_z = mr^2 = 204.28\ \text{kg/m}\ (0.43\ m - F) \cdot (0.255\ m)^2 \\ \approx 13.28\ \text{kgm}(0.43\ m - F) \end{aligned} \tag{7.6}$$

The final rigid-body matrix is then

$$\boldsymbol{M}_{RB,i} = \begin{bmatrix} 204.28(0.43 - F) & 0 & 0 \\ 0 & 204.28(0.43 - F) & 0 \\ 0 & 0 & 13.28(0.43 - F) \end{bmatrix}. \tag{7.7}$$

So if, for instance, the freeboard is 20 cm, the mass matrix becomes

$$\boldsymbol{M}_{RB,i} = \begin{bmatrix} 47 & 0 & 0 \\ 0 & 47 & 0 \\ 0 & 0 & 3.05 \end{bmatrix}. \tag{7.8}$$

The added-mass matrix is expressed as

$$\boldsymbol{M}_{A,i} = \begin{bmatrix} -X_{\dot{u}} & 0 & 0 \\ 0 & -Y_{\dot{v}} & -Y_{\dot{r}} \\ 0 & -Y_{\dot{r}} & -N_{\dot{r}} \end{bmatrix}, \tag{7.9}$$

where the elements of the matrix are written in SNAME notation [SNAME, 1950]. For simplicity, the added-mass matrix can be considered equal to the mass matrix. That means $\boldsymbol{M}_i = \boldsymbol{M}_{RB,i} + \boldsymbol{M}_{RB,i} = 2 \cdot \boldsymbol{M}_{RB,i}$.

The damping matrix can be expressed by

$$\boldsymbol{D}_i = \begin{bmatrix} -X_u & 0 & 0 \\ 0 & -Y_v & -Y_r \\ 0 & -N_v & -N_r \end{bmatrix}, \tag{7.10}$$

which also follows SNAME notation for the elements. The damping in surge is found by using the same principles as in (2.3) and 3.2.2.

7.3.2 Disturbances from wind and current

A real iceberg is subjected to wind, wave, current and ice forces. Out of these four forces, the current contributes most to the motion of the iceberg. Unfortunately, the towing tank is only able to generate waves.

In order to simulate current, a wind maker could be used. This will not generate a current itself, but it will generate a slowly varying environmental force acting on the iceberg. Both wind and current can be written using the current coefficients defined by Fossen [2011, p 189]:

$$\begin{aligned} X_{wind} &= qC_X(\gamma_w)A_{Fw} \\ Y_{wind} &= qC_Y(\gamma_w)A_{Lw} \\ N_{wind} &= qC_N(\gamma_w)A_{Lw}L_{oa}, \end{aligned} \tag{7.11}$$

where A_{Fw} is the frontal projected areas, A_{Lw} is the lateral projected areas, and

$$\gamma_w = \psi - \beta_w - \pi, \tag{7.12}$$

where β_w is the wind direction in NED and ψ is the heading angle. The dynamic pressure of apparent wind is:

$$q = \frac{1}{2}\rho_a V_w^2, \tag{7.13}$$

where ρ_a is air density and V_w is the wind velocity.

Any eventual wind flow will have to be created by fans. A problem with the fans could be too low pressure induced on the iceberg, due to weak fans. To increase the forces acting on the iceberg one could increase the projected area by attaching vertical plates on top of the iceberg. This will also create a moment about the longitudinal axis (roll), but this moment is assumed to be so small compared to the transversal force that it can be neglected.

Due to problems with the experimental setup, and the lack of a proper current generator, the experiments were run without environmental disturbances.

7.4 Computer interface

The application used for controlling the vessel is written in LabView.

Figure A.1 in the appendix shows a screenshot of the interface that is used for iceberg control. The original interface was created by Skåtun [2011], in cooperation with Øivind Kåre Kjerstad. The new interface includes the iceberg in the 3D visualization, with added support for the iceberg in Qualisys.

7.5 Execution of the experiment

The experiment was executed by setting up the vessel and iceberg as shown in Figure 7.4. The vessel is pointing in the North direction in the local NED reference frame, while the iceberg is almost directly behind it. The desired path is northwards and the towing carriage is stationary.

All the experiments were executed as follows:

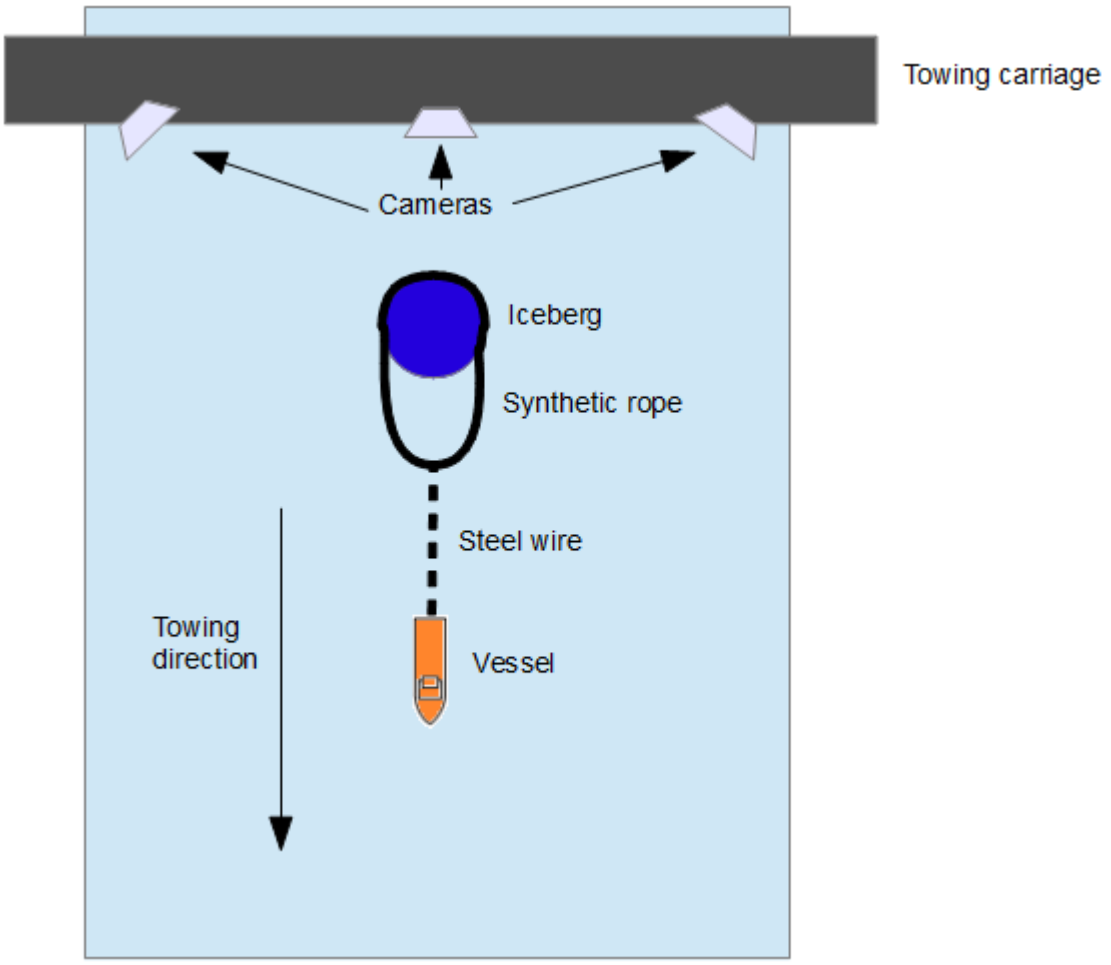

Figure 7.4: Figure of the emulated iceberg and the vessel in the towing tank.

- The vessel and emulated iceberg were set up as in Figure 7.4. The vessel was about 1.5 meters in front of the iceberg, while the towline is acting like a catenary. The tow rope is looped around the emulated iceberg and connected to the hawser (the steel wire). Unfortunately, the chosen tow rope is not buoyant

like it would be in a real world application. Therefore the rope is forced to stay on the surface by taping it to the iceberg. The tape only restricts the rope in the heave direction, and not in yaw.

- The desired path is set to $\boldsymbol{\eta}_d(\theta) = [\theta, 0, 0]^\top$, which is a straight line northwards. This path was used in all the experiments.

- The vessel is then turned on. The Qualisys positioning system is turned on, and one can control if it gives correct values on the computer in lab. Iceberg-towing mode is turned on if the software transfer between computer and vessel microcontroller is successful, and the Qualisys system is sending correct values to LabView (the user interface and controller application).

- The vessel starts moving and its behavior is observed.

7.6 Results

Due to the lack of recording abilities, the results are mostly qualitative data from watching the vessel and iceberg in the tank.

The first few runs experienced a lot of problems with the lab setup, see 7.6.1. Constant disconnects from the vessel computer made the experiment hard to perform, but a few runs were made anyhow.

The vessel seemed to follow the path to an acceptable standard. However, the motion and behavior of the vessel was not as smooth as wanted and this had to be improved by tuning the parameters of the system. These parameters are mainly $\boldsymbol{K}_p$ and $\boldsymbol{K}_d$ for the controller, and μ and λ for the guidance system (update law to be specific). There was also problems with the update law, which was looked into first.

Choice of update law

When the experiment initially began, the update law in the control system was based on the gradient update law from Skjetne [2005], which can be expressed as

$$\omega_s = -\mu \left[\boldsymbol{z}_1^\top \boldsymbol{R}(\psi_s)^\top \boldsymbol{\eta}_d^\theta \boldsymbol{z}_2^\top \boldsymbol{M}_s \boldsymbol{\alpha}_1^\theta \right]. \tag{7.14}$$

Unfortunately, this gave poor results. Often the Simulink implementation would not run at all, and when it did it gave poor results in the path following. Almost as a coincidence, the update law was changed to

$$\omega_s = \omega, \tag{7.15}$$

and

$$\dot{\omega} = -\lambda\omega - \lambda\mu \left[\boldsymbol{z}_1^\top \boldsymbol{R}^\top(\psi_s) \boldsymbol{\eta}_d^\theta + \boldsymbol{z}_2^\top \boldsymbol{M}_s \boldsymbol{\alpha}_1^\theta \right], \tag{7.16}$$

which is also written in 5.2.1. This is the filtered-gradient update law, also described by Skjetne [2005]. The result was a much more stable controller, and the Simulink implementation stopped crashing due to update law errors. It is likely that the filtered-gradient update law works better because it doesn't have a sudden initial jump in the beginning of the experiment or simulation, which the gradient update law sometimes get.

Improving the motion of the vessel

Later on, the vessel motion had to be improved. The vessel experienced rapid motions when towing, which caused oscillations along the path. The vessel would also move sideways while towing at maximum tension. These problems were mainly due to three reasons:

- The vessel had powerful actuators. For such a small hull (about 110 cm in length), the model VSPs could produce much higher thrust than full-scale VSPs could produce on a real-sized vessel.

This problem was solved by saturating the outputs from the thrust allocator to the VSPs.

- The controller gain matrices were untuned. These matrices are tuned by trial-and-error, which takes several runs with the towing system. However, the constant crashing of the vessel computer made this a slow process.

- The vessel used the tension observer instead of actual tension measurements. Due to the difficulties of tuning this observer (mainly finding reasonable values for the gains), the result was somewhat unsatisfactory in terms of estimated tension compared to a realistic tension.

7.6.1 Problems with the lab setup

Unfortunately, a lot of problems were experienced during the experiment. The main problems were:

- The Qualisys positioning system was often lagging, which means the system experienced a huge time delay between on the position and velocity measurements. The system would not work until the lag was gone.

- The Qualisys positioning system would often not work at all, meaning the system would often not send the positions of the vessel and iceberg to the control computer. This could either be because the vessel/iceberg was out of sight, or due to internal failure in the Qualisys system. It would usually start working again after half an hour.

- The wireless network was very unstable and would often stop working. When this happened, the vessel would have to be pulled two the edge of the tank, opened, and then reset. After the reset the software would have to be reuploaded to the vessel computer. This was very time consuming in general.

- The LabView software on the control computer was also very unstable, and several crashes per run was the standard.

These problems made it hard to perform the experiment. About 50 minutes of failseeking was necessary for every 10 minutes of experiments.

7.7 Final discussion

The final system worked fine, but nowhere near perfect. The system followed the path in a decent way as long as it started along the path. It is hard to say if it worked properly when it started somewhere else, e.g. two meters East of the path. This is due to the short range of motion available: the towing tank only had an effective length of $10\ m - 15\ m$, because of limitations with the Oqus cameras.

There were huge problems with the laboratory setup, as pointed out in 7.6.1. Until these problems are improved, I would not recommend using the towing tank. Most of the time in the tank was used to fix these problems.

Chapter 8

Conclusion

In this thesis, a model for open water iceberg towing has been presented. A few different concepts in iceberg towing was first introduced. This includes towing methods, connection methods and towline choice.

A mathematical model for the vessel, iceberg and towing rope was then set up. This model was based on the work of Marchenko and Eik [2011], which is a scalar model for surge motion. The model for the vessel and iceberg was expanded to three degrees-of-freedom using the Fossen-style of notation. Mass and damping estimation of the vessel and iceberg was then performed using former data on vessels and icebergs.

A chapter on the ability to control icebergs was written. This includes topics such as controllable degrees-of-freedom; sensors, measurements and disturbances; and finally a few problems regarding iceberg towing were explained. This includes rupture of the towline, slippage, and overturning.

A controller was designed using *maneuvering theory*. The goal of the controller is to control the ship along a path, with the iceberg trailing behind it. A nonlinear control method called *backstepping* was used in the design of the controller. A PID controller was designed to control the tension in the towline. Moreover, two different

observers were designed. Two nonlinear passive observers are going to be used for estimating position, velocity, and bias for the vessel and iceberg. An observer is also designed for estimating tension in the towline, in the event that tension measurements are unavailable at the towing vessel. This observer can either estimate using a simple mathematical model based on Hooke's Law, or a more advanced mathematical model based on catenary equations.

Closed-loop simulations have been run to test the behavior of the system, and how they compare to the expected behavior. The model seems to hold for the simulations that were run. The ship follows the designated path, while holding the tension within an acceptable limit.

Finally, model experiments were performed. These experiments were done in the *MC Lab* at NTNU. The experiments gave important data regarding towing of emulated icebergs. These data were mainly qualitative, as technical difficulties (lack of computer power) made it difficult to save the numerical data found in the experiment. Overall, the experiment was hard to perform due to huge problems in the laboratory setup in the MC Lab.

8.1 Further work

The controller that was designed has path following of the ship as main objective. However, in the real world the main objective is to deflect the iceberg away from an undesired path, which usually is towards an offshore installation or similar. A better controller should therefore be designed on the principle of path following for the iceberg, using the vessel as an actuating force the iceberg. This concept is illustrated in Figure 8.1.

The main goal of the ship is now to steer the iceberg along its predefined path, not to follow its own path. Due to the complexity of such a design, the controller in this thesis was made simpler.

A more sophisticated approach to modeling the vessel and iceberg

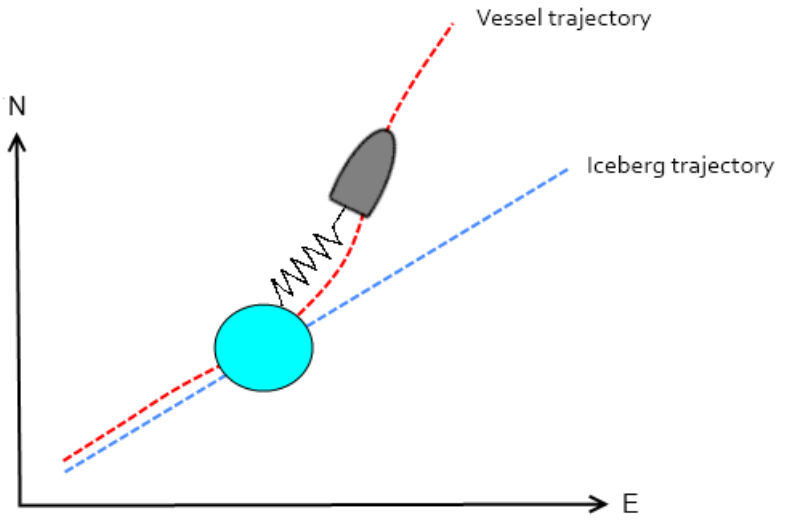

Figure 8.1: Figure of the behavior of a controller where the iceberg follows the path.

can also be made. At the moment only linear damping is included in the model, and the Coriolis effect is completely neglected. By adding a nonlinear damping matrix, $\boldsymbol{D}_{nl}(\boldsymbol{\nu})$, and the Coriolis matrices, $\boldsymbol{C}(\boldsymbol{\nu})$ and $\boldsymbol{C}_A(\boldsymbol{\nu})$, more dynamics can be captured by the model. This is also true for the modeling of environmental disturbances. At the moment, this dynamic is captured by bias estimation, which is a method not based on first principles. A more realistic model can be made using e.g. relative velocity, as in the original 6 DOF Fossen-model.

Appendix A

Large figures

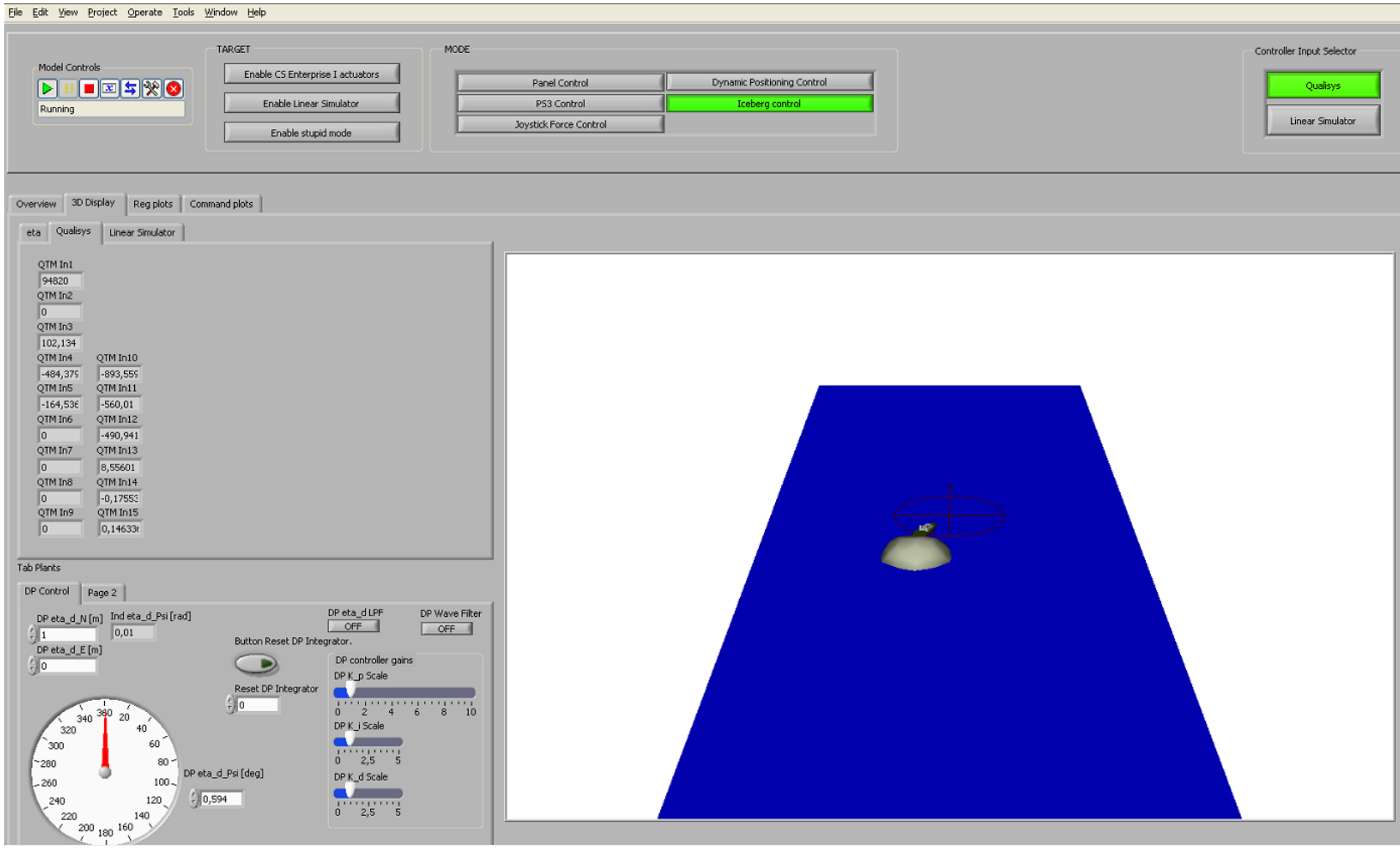
File Edit View Project Operate Tools Window Help
Model Controls
Running
TARGET
Enable CS Enterprise I actuators
Enable Linear Simulator
Enable stupid mode
MODE
Panel Control
Dynamic Positioning Control
PS3 Control
Iceberg control
Joystick Force Control
Controller Input Selector
Qualisys
Linear Simulator
Overview
3D Display
Reg plots
Command plots
eta
Qualisys
Linear Simulator
QTM In1
94820
QTM In2
0
QTM In3
102,134
QTM In4
-484,37
QTM In5
-164,53
QTM In6
0
QTM In7
0
QTM In8
0
QTM In9
0
QTM In10
-893,55
QTM In11
-560,01
QTM In12
-490,941
QTM In13
8,55601
QTM In14
-0,1755
QTM In15
0,14633
Tab Plants
DP Control
Page 2
DP eta_d_N [m]
1
DP eta_d_E [m]
0
Ind eta_d_Psi [rad]
0,01
DP eta_d LPF
OFF
DP Wave Filter
OFF
Button Reset DP Integrator.
Reset DP Integrator
0
DP controller gains
DP K_p Scale
0 2 4 6 8 10
DP K_i Scale
0 2,5 5
DP K_d Scale
0 2,5 5
DP eta_d_Psi [deg]
0,594

Appendix B

Simulink diagrams

The following figures are screenshots taken from the Simulink implementation of the iceberg towing application.

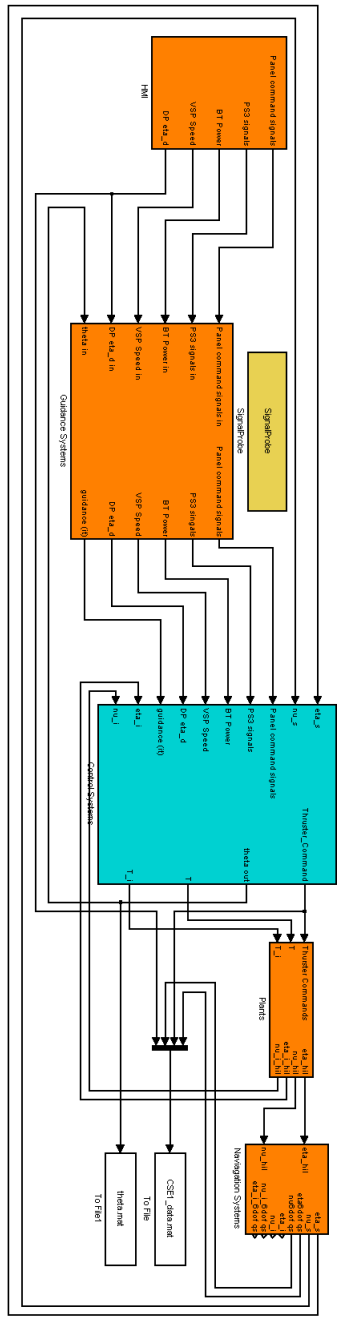

Figure B.1: Figure of the main Simulink diagram.

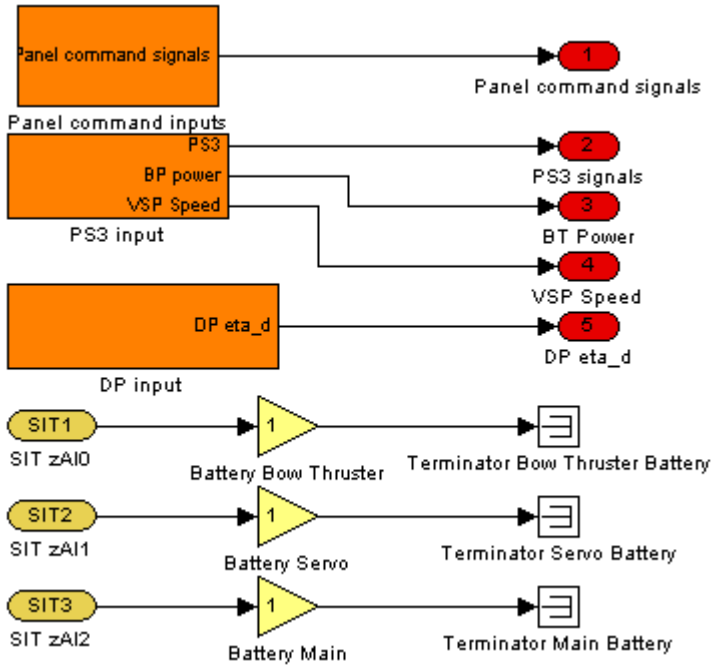

Figure B.2: Figure of the HMI (Human Interface) diagram.

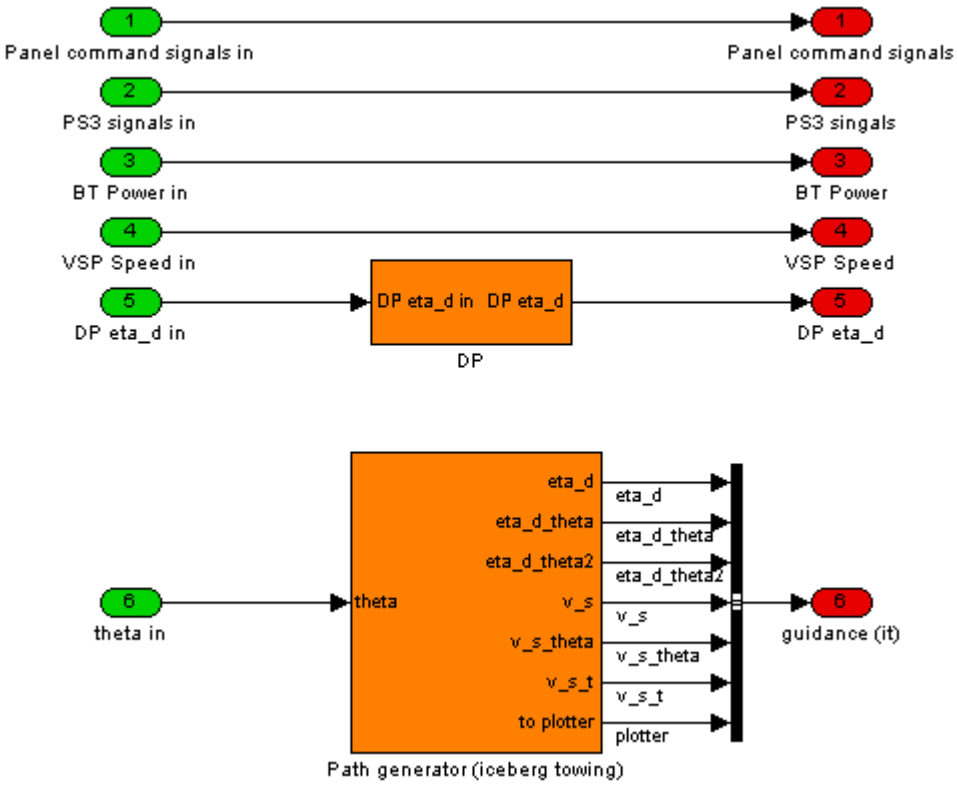

Figure B.3: Figure of the guidance system diagram.

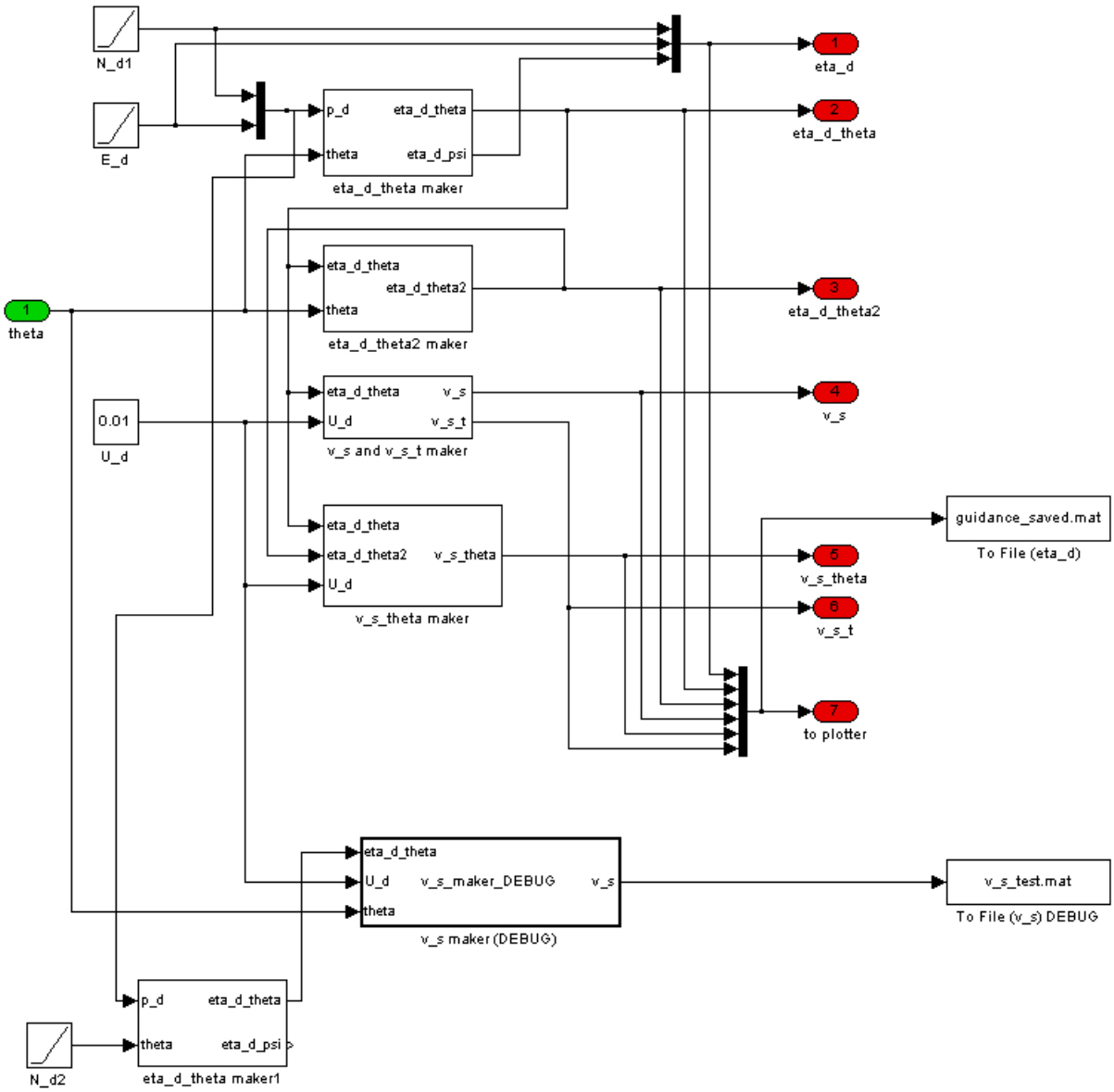

Figure B.4: Figure of the path generator diagram.

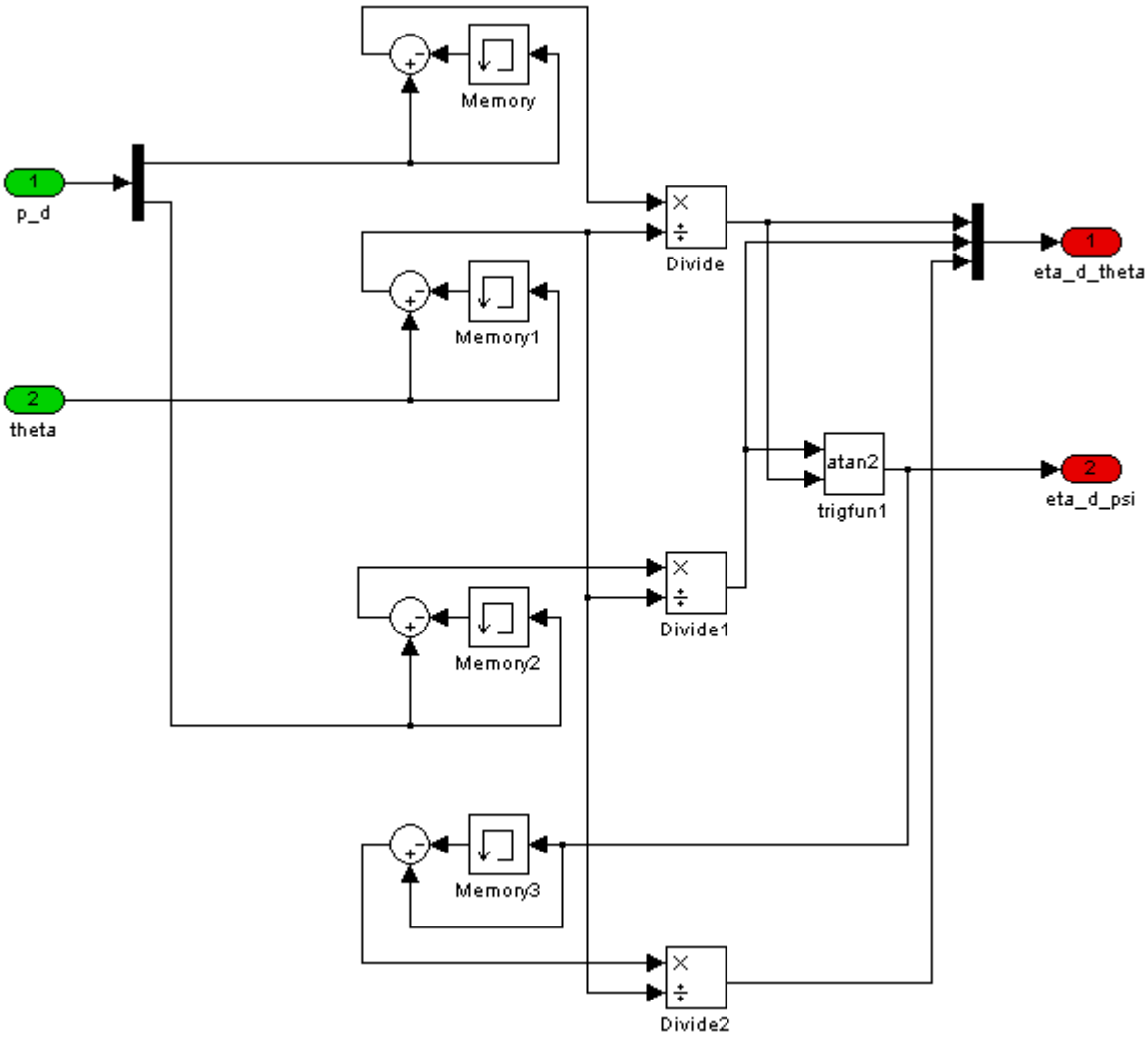

Figure B.5: Figure of the eta_d_theta maker diagram.

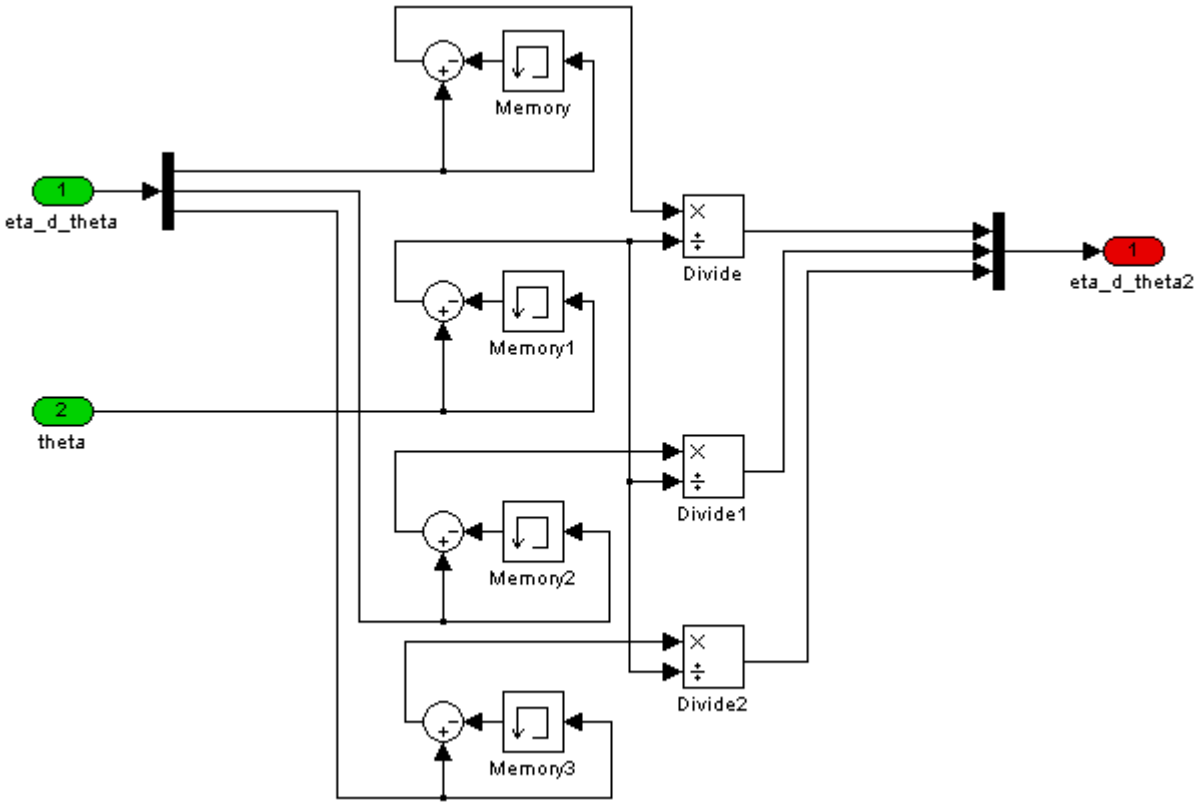

Figure B.6: Figure of the eta_d_theta2 maker diagram.

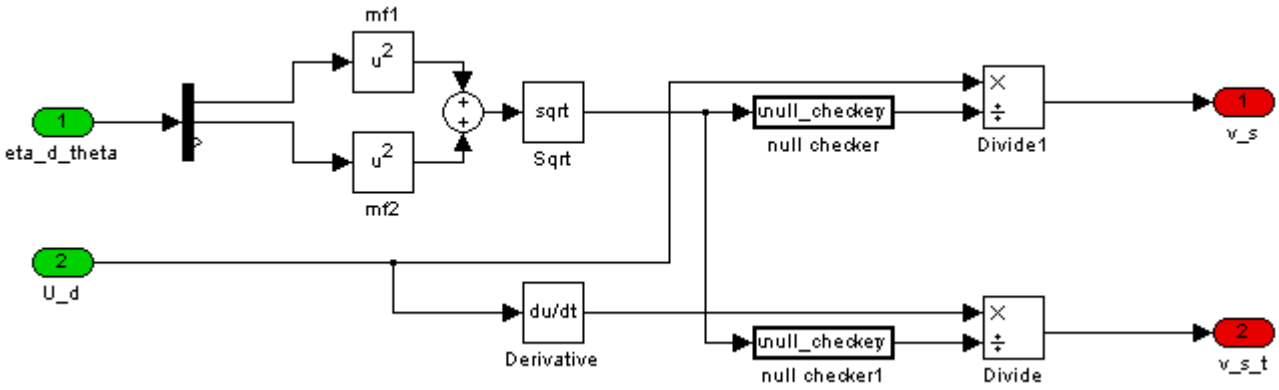

Figure B.7: Figure of the v_s and v_s_t maker diagram.

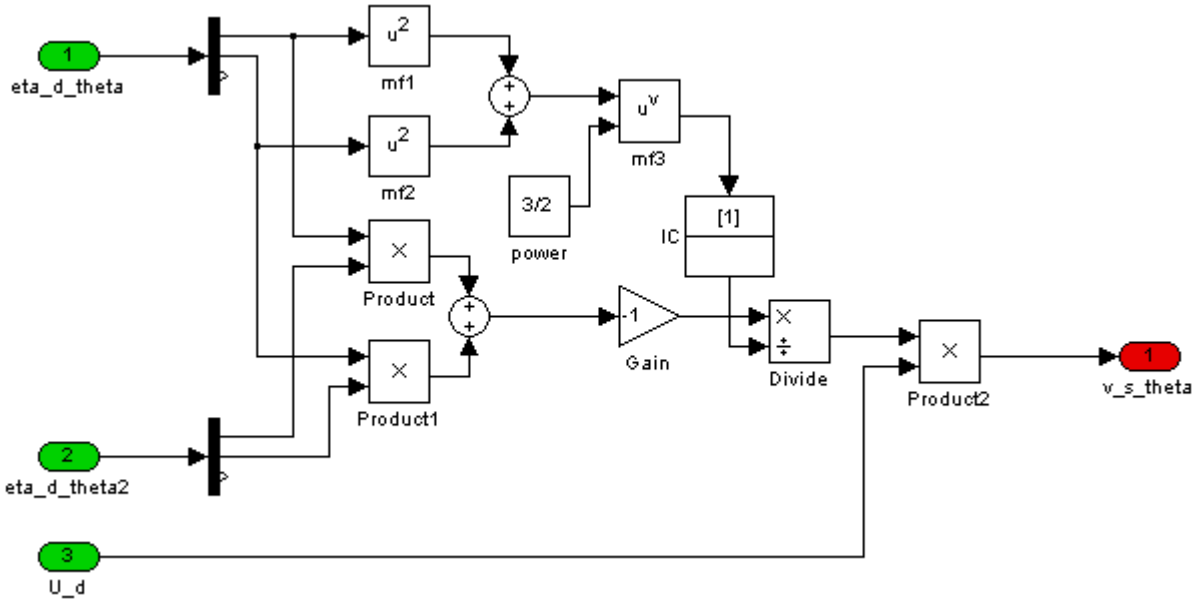

Figure B.8: Figure of the v_s_theta maker diagram.

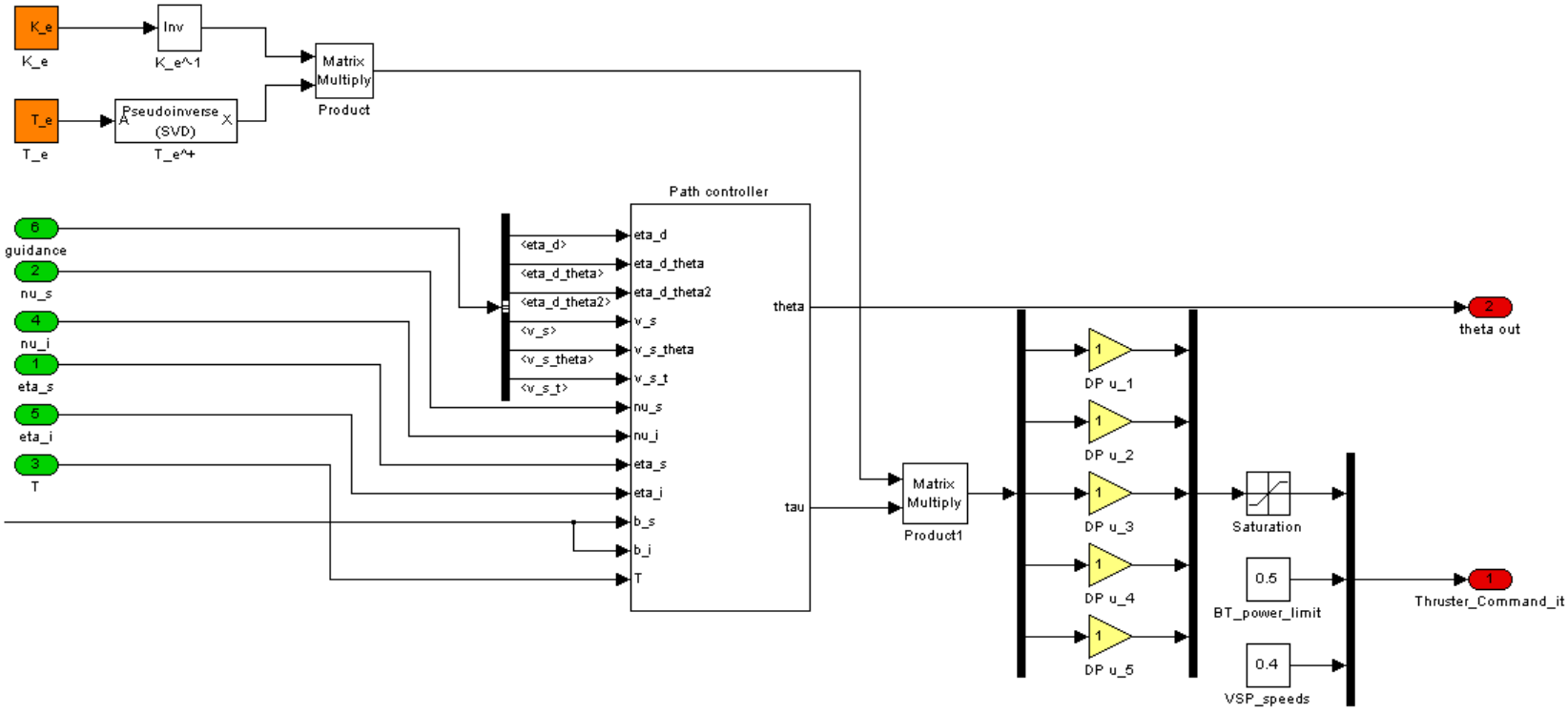
K_e
K_e
Inv
K_e^-1
Matrix Multiply
Product
T_e
T_e
Pseudoinverse (SVD)
A
X
T_e^+
Path controller
6
guidance
2
nu_s
4
nu_i
1
eta_s
5
eta_i
3
T
<eta_d>
<eta_d_theta>
<eta_d_theta2>
<v_s>
<v_s_theta>
<v_s_t>
eta_d
eta_d_theta
eta_d_theta2
v_s
v_s_theta
v_s_t
nu_s
nu_i
eta_s
eta_i
b_s
b_i
T
theta
tau
Matrix Multiply
Product1
1
DP u_1
1
DP u_2
1
DP u_3
1
DP u_4
1
DP u_5
Saturation
0.5
BT_power_limit
0.4
VSP_speeds
2
theta out
1
Thruster_Command_it

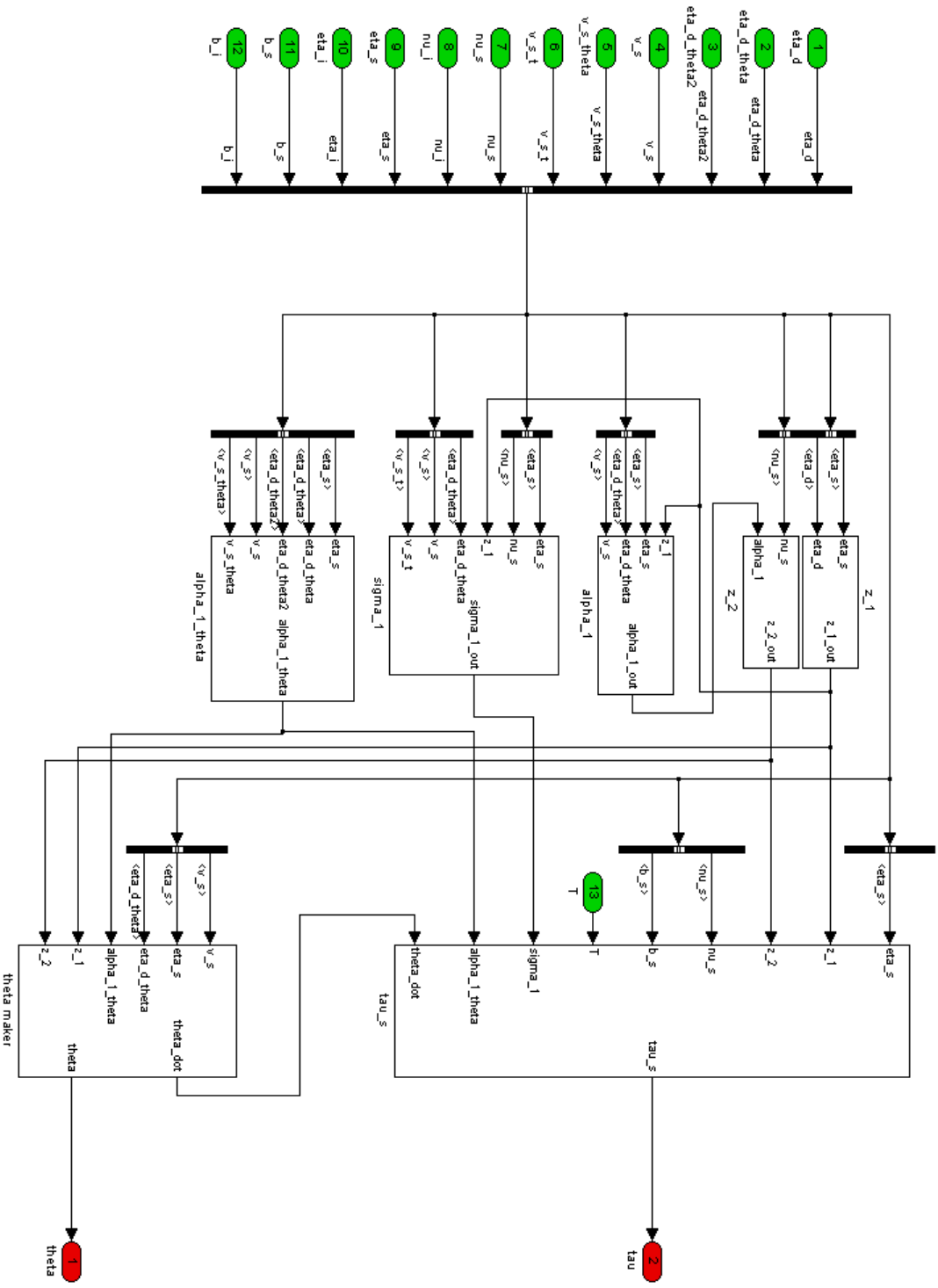

Figure B.10: Figure of the maneuvering controller diagram.

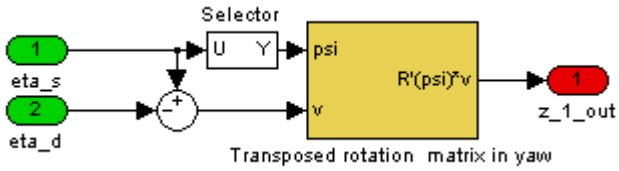

Figure B.11: Figure of the z_1 diagram.

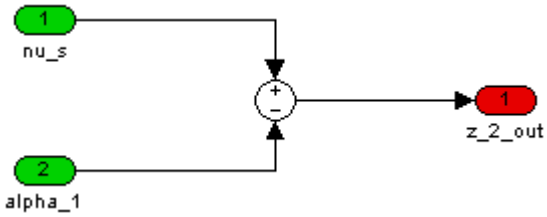

Figure B.12: Figure of the z_2 diagram.

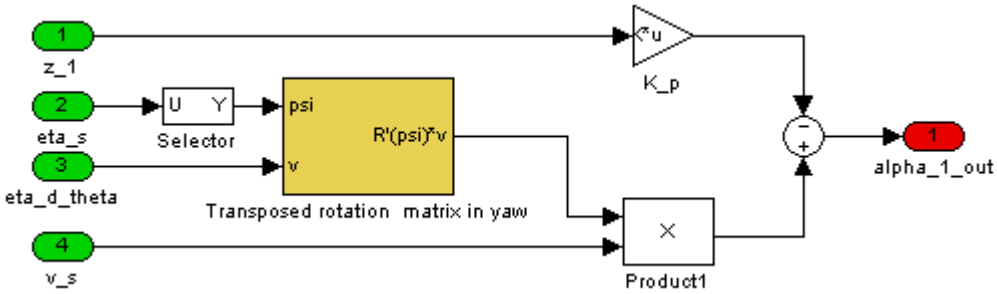

Figure B.13: Figure of the alpha_1 diagram.

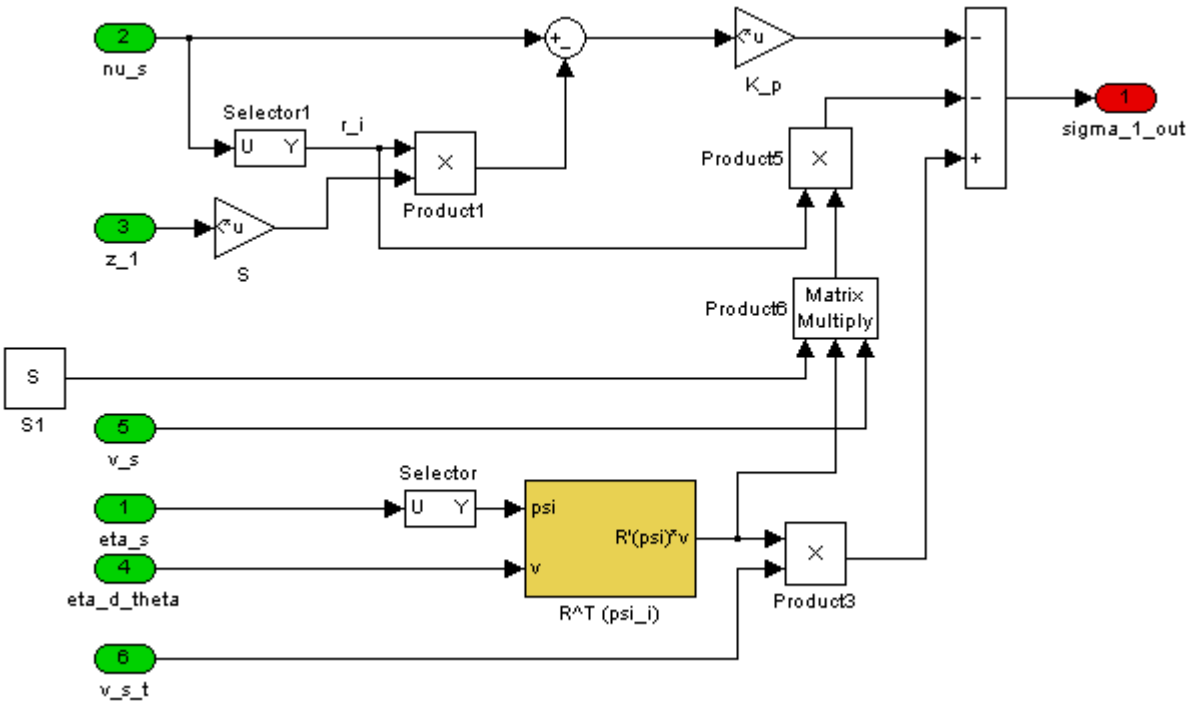

Figure B.14: Figure of the sigma_1 diagram.

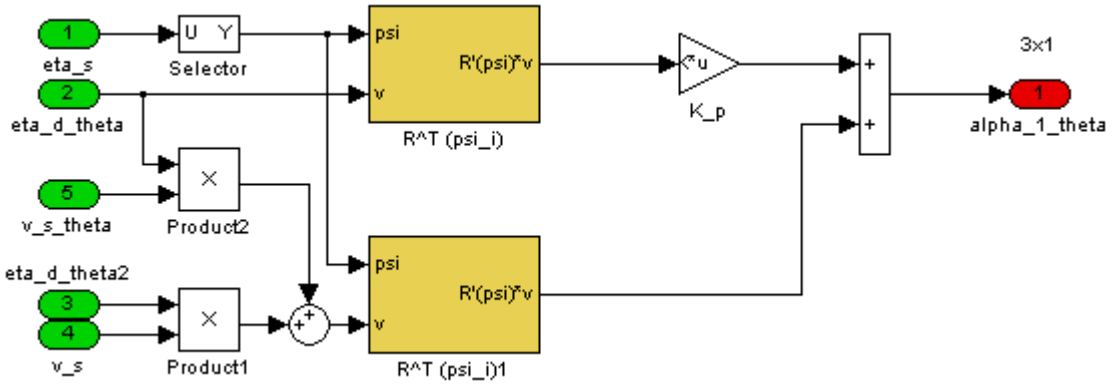

Figure B.15: Figure of the alpha_1_theta diagram.

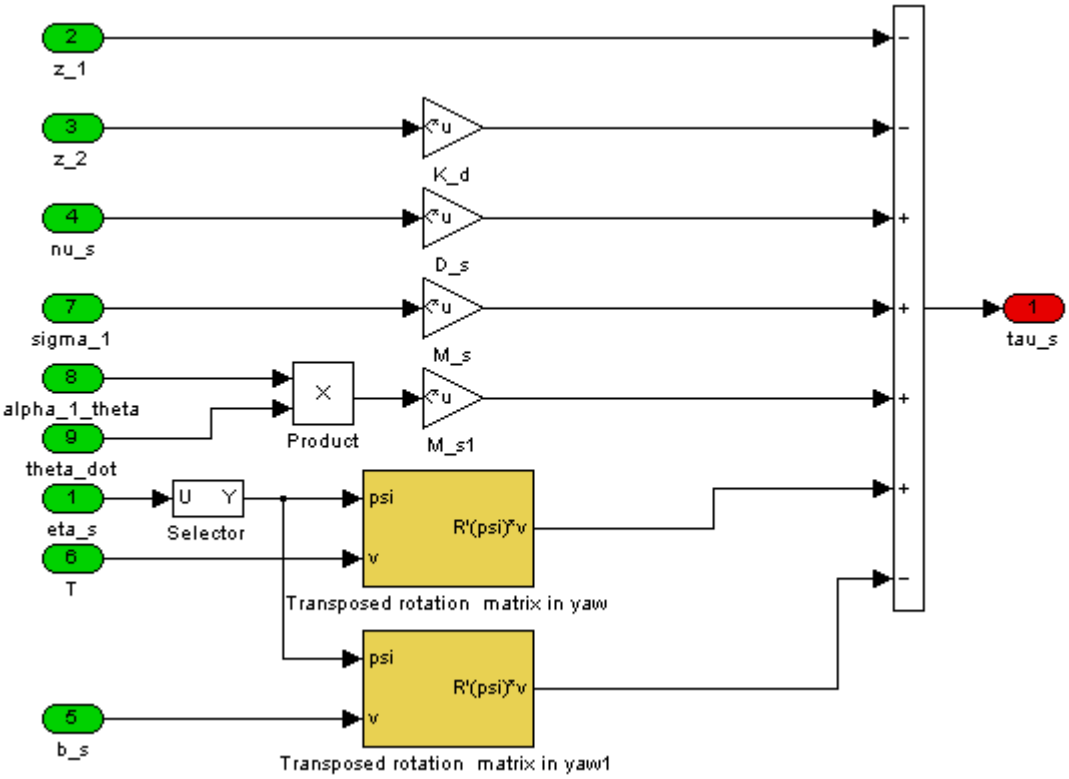

Figure B.16: Figure of the tau_s diagram.

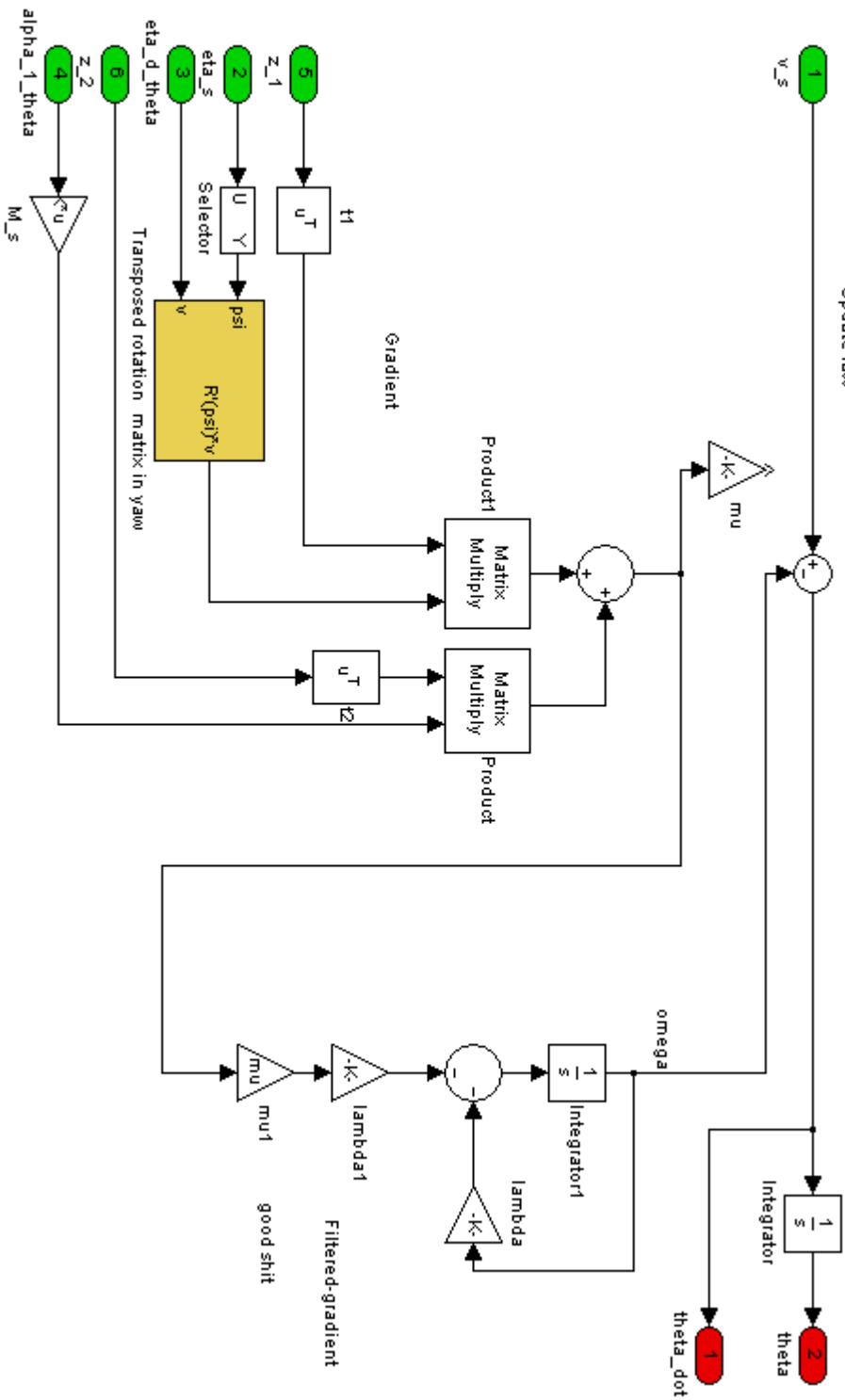

Figure B.17: Figure of the theta maker diagram.

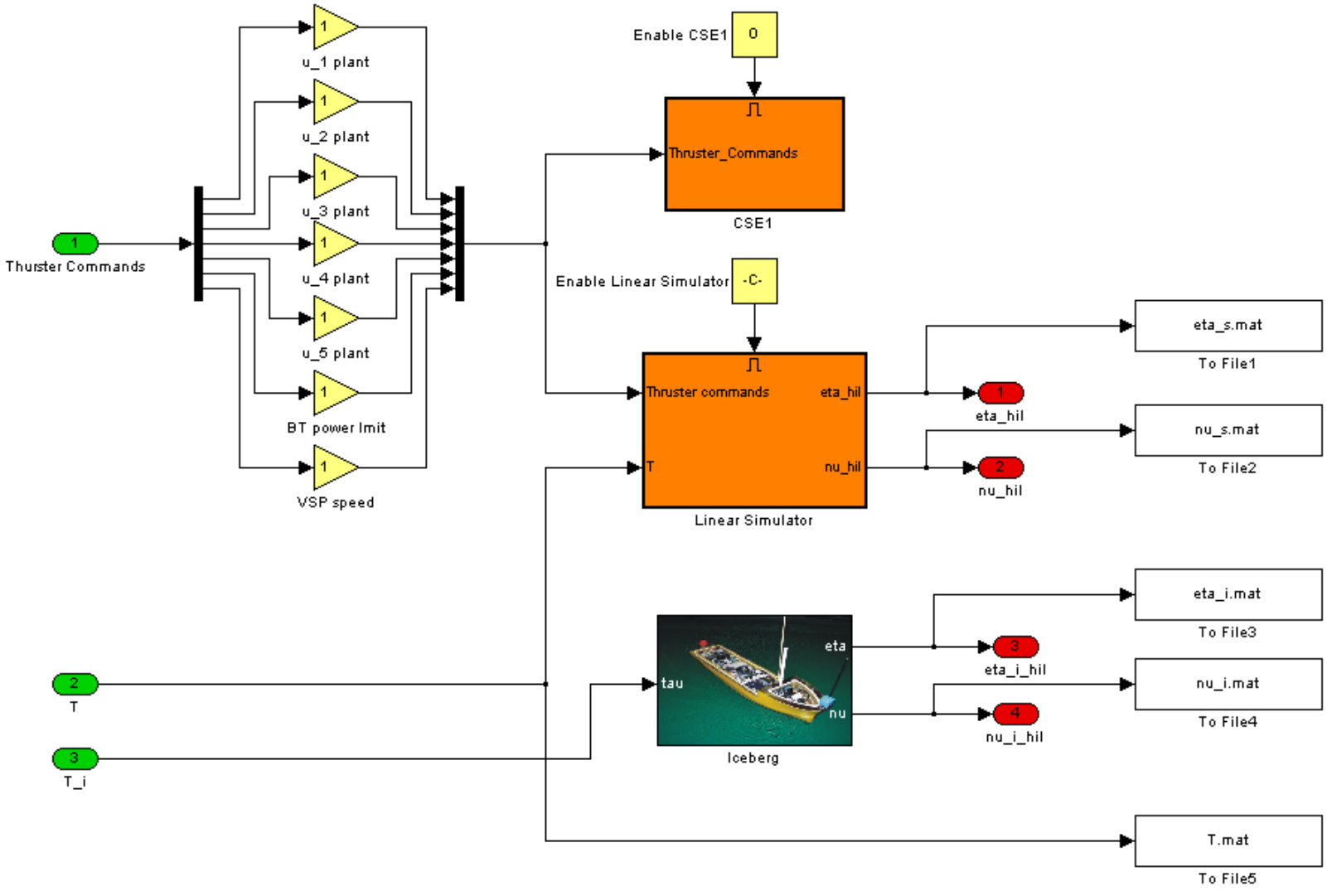

Figure B.18: Figure of the plants diagram.

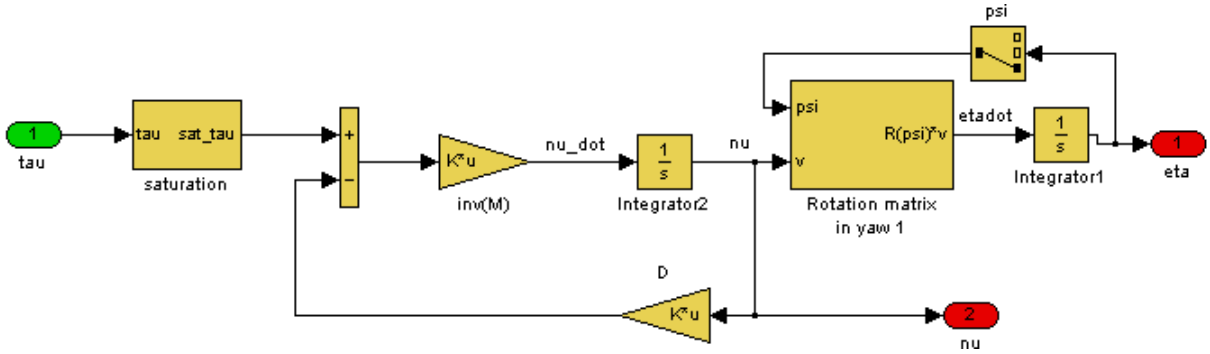

Figure B.19: Figure of the iceberg diagram.

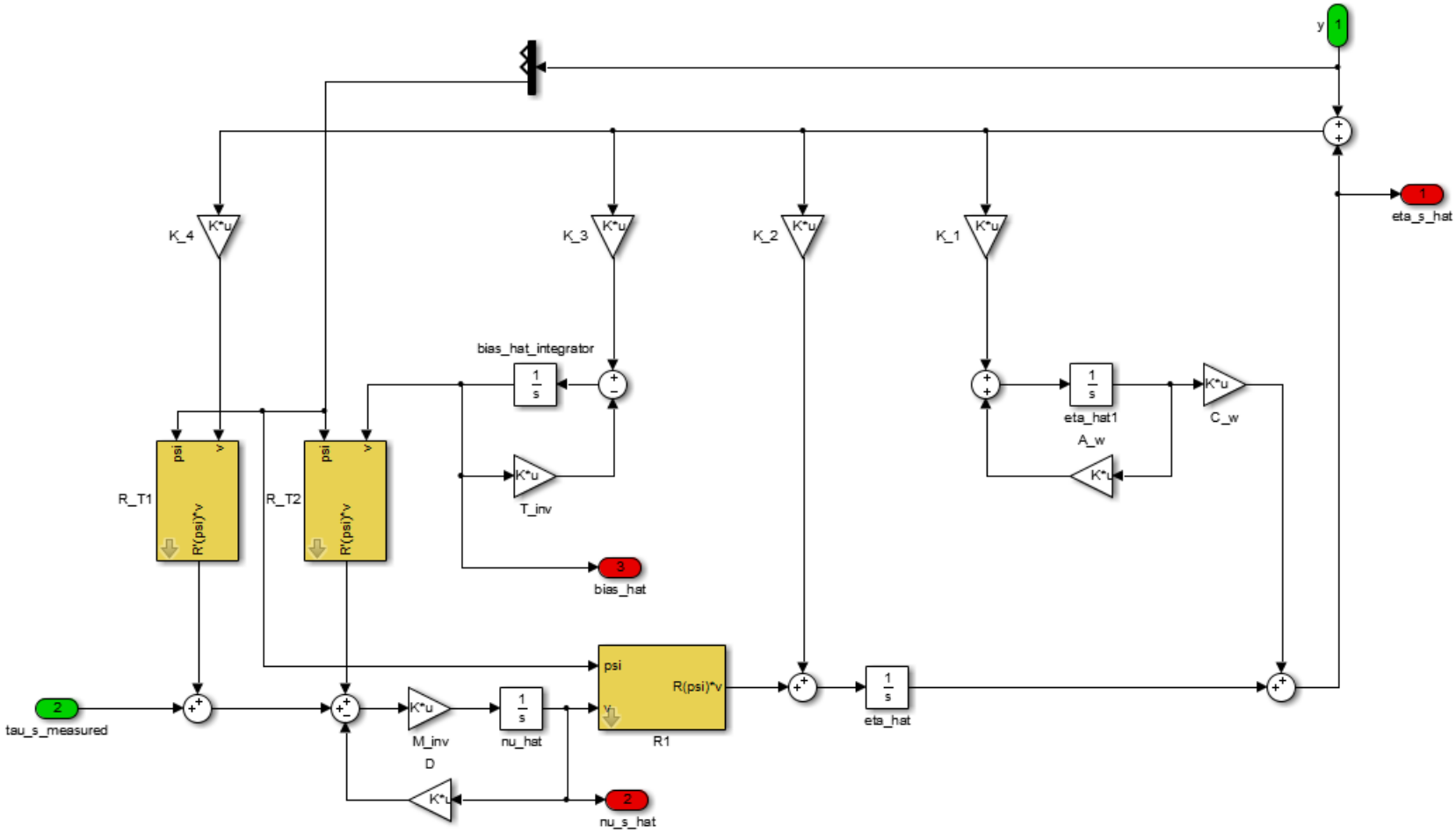
y
1
eta_s_hat
K_4
K_3
K_2
K_1
K*u
bias_hat_integrator
1/s
T_inv
bias_hat
3
R_T1
R_T2
psi
v
R'(psi)*v
eta_hat1
A_w
C_w
tau_s_measured
2
M_inv
D
nu_hat
R1
R(psi)*v
eta_hat
nu_s_hat

Bibliography

J. M. Amundson D. S. Abbot A. Boghosian L. M. Cathles S. Correa-Legisos K. N. Darnell N. Guttenberg D. M. Holland Burton, J. C. and D. R. MacAyeal. Laboratory investigations of iceberg capsize dynamics, energy dissipation and tsunamigenesis. *Journal of Geophysical Research*, 117:1–13, 2012.

U.S. Coast Guard Navigation Center. NDGPS General Information. Webpage, 2012. http://www.navcen.uscg.gov/?pageName=dgpsMain.

Alexander S. Desroches. Calculations of extreme towline tension during open ocean towing. Master's thesis, Massachusetts Institute of Technology, 1997.

Julian A. Dowdeswell. On the nature of Svalbard icebergs. *Journal of Glaciology*, 35:224–234, 1989.

Kenneth Eik and Aleksey Marchenko. Model tests of iceberg towing. *Cold Regions Science and Technology*, 61:13–28, 2009.

Kenneth Johannesen Eik. *Ice Management in Arctic Offshore Operations and Field Developments*. PhD thesis, Norwegian University of Science and Technology, Department of Civil and Transport Engineering, 2010.

T. I. Fossen. *Handbook of Marine Craft Hydrodynamics and Motion Control*. John Wiley & Sons Ltd, 2011.

T. I. Fossen and J. P. Strand. Passive nonlinear observer for ships using lyapunov methods: full-scale experiments with a supply vessel. *Automatica*, 35:3–16, 1999.

H. M. Irvine and G. B. Sinclair. The suspended elastic cable under the action of concentrated vertical loads. *Solid Structures*, 12:309–317, 1975.

Richard McKenna Freeman Ralph John McClintock, Terry Bullock and Rob Brown. Greenland iceberg management: Implications for Grand Banks management systems. Technical Report 20-65, AMEC and C-CORE, March 2002.

Aleksey Marchenko and Kenneth Eik. Iceberg towing: Analysis of field experiments and numerical simulations. *Coastal Technology Workshop*, pages 235–246, 2008.

Aleksey Marchenko and Kenneth Eik. Iceberg towing in open water: Mathematical modeling and analysis of model tests. *Cold Regions Science and Technology*, 73:12–31, 2011.

MathWorks. MATLAB. Webpage, 2012. http://www.mathworks.se/products/matlab/.

NTNU MC Lab. Marine Cybernetics Laboratory (MC LAB). Webpage, 2012. http://www.ntnu.no/imt/lab/kybernetikk.

Model Slipway. Anchor handling tug aziz / arif. Webpage, viewed 04.12.2012., 2012. http://www.modelslipway.com/aziz.htm.

Alan S. Morris. *Measurements & Instrumentation Principles*. Butterworth-Heinemann, 2001.

MSS. MSS. Marine Systems Simulator. Webpage, viewed 03.11.2012., 2010. http://www.marinecontrol.org.

Qualisys. Qualisys, motio capture systems. Webpage, viewed 04.12.2012., 2012. http://www.qualisys.com/products/.

Roger Skjetne. *The Maneuvering Problem*. PhD thesis, Norwegian University of Science and Technology, Department of Marine Technology, 2005.

Håkon Skåtun. Development of a DP system for CS Enterprise I with Voith Schneider thrusters. Master's thesis, Norwegian University of Science and Technology, 2011.

SNAME. Nomenclature for treating the motion of a submerged body through a fluid. *Technical and Research Bulletin*, 1-5, 1950.

A. J. Sørensen. *Marine control systems - Propulsion and Motion Control of Ships and Ocean Structures*. Department of Marine Technology, NTNU, 2011.

Eduardo A. Tannuri, Tiago T. Bravin, and Celso P. Pesce. Dynamic positioning systems: Comparison between wave filtering algorithms and their influence on performance. *ASME Conference Proceedings*, 2003(36819): 109–117, 2003. doi: 10.1115/OMAE2003-37067. URL `http://link.aip.org/link/abstract/ASMECP/v2003/i36819/p109/s1`.

Garry Timco. Grand Banks iceberg management. Technical Report 20-84, National Research Council Canada, May 2007.

Voith. Voith Schenider Propeller. Webpage, 2012. http://www.voith.com/en/products-services/power-transmission/voith-schneider-propeller-10002.html.

Wamit. Wamit. Webpage, viewed 13.12.2012., 2012. http://www.wamit.com/.

Lars Andreas Lien Wennersberg. Modeling and simulation of anchor handling vessels. Master's thesis, Norwegian University of Science and Technology, 2009.